



Building stone quarries: resource evaluation by block modelling and unmanned aerial photogrammetric surveys

Maxim Bogdanowitsch¹ · Luís Sousa^{2,3} · Siegfried Siegesmund¹

Received: 27 February 2021 / Accepted: 3 October 2021 / Published online: 18 December 2021
© The Author(s) 2021

Abstract

The production of building stones shown an exponential growth in last decades as consequences of the demand and developments in the extraction and processing techniques. From the several conditioning factors affecting this industry, the geological constrains at quarry scale stands out as one of most important. Globalization and increasing competition in the building stone market require large raw material blocks to keep further processing as cost-effective as possible. Therefore, the potential extraction volume of in-situ stone blocks plays an important role in the yield of a dimensional stone quarry. The full characterization of the fracturing in the quarries comes up as fundamental in the assessment of the in-situ blocks volume/shape and potential extracted raw blocks. Identify the joint sets present, their spacing and the differences across the quarry demands a continuous assess during the quarry live span. Information from unmanned aerial vehicles helps in the field survey, namely trough digital surface models, orthophotos, and three-dimensional models. Also, the fracturing modelling by specific software programs is crucial to improve the block size assessment and the increase the quarry yield. In this research fracturing of twenty-one quarries of granite, limestone, marble, and slate from Portugal were assessed by combining field surveys with new techniques. From the studied quarries several cases were selected and presented to highlight the importance of this combined methodology in the fracturing assessment and how they can be helpful in the maximization of the resources and quarry management.

Keywords Building stones · Quarries · Exploitation · Fracturing modelling · UAV technique · 3D BlockExpert · Photogrammetry

Introduction

Most of historic buildings and structures have been constructed from natural stones (Siegesmund and Török 2014). Today designers are rediscovering the beauty of natural stone materials for structural applications especially in the

building sector and furnishing accessories. The market of the dimension stones will keep the exponential growing in the next decades (Fig. 1). This great demand led to major improvements in the extraction and processing of natural building stones. Therefore, the potential extraction volume of in-situ blocks plays an important role in the profitability of a dimensional stone deposit, considering a market which is worth over 21 billion dollars in 2017 (Montani 2018). According to Montani (2019), the raw production in 2018 increased slightly to 153 million tons. The amount of the quarrying (160 Mt) and processing waste (62.75 Mt) of the quarries reaches more than 71%, leaving less than 29% for the final products in the year 2018 (Montani 2019) (Fig. 1). These ratios have not changed in the last 2 decades and around 51% of the extracted material is dumped already in the quarry, while 20% is lost during processing in the factories.

An essential progress is necessary, to reduce waste production and increasing the volume of raw blocks. To realize

This article is part of a Topical Collection in Environmental Earth Sciences on “Building Stones and Geomaterials through History and Environments—from Quarry to Heritage. Insights of the Conditioning Factors”, guest edited by Siegfried Siegesmund, Luís Manuel Oliveira Sousa, and Rubén Alfonso López-Doncel.

✉ Maxim Bogdanowitsch
bogdanowitsch.maxim@googlemail.com

- ¹ Geoscience Centre, University of Göttingen, Goldschmidtstrasse 3, 37077 Göttingen, Germany
- ² Department of Geology, University of Trás-os-Montes e Alto Douro, Quinta de Prados, 5000-801 Vila Real, Portugal
- ³ CGeo Research Centre, Vila Real, Portugal

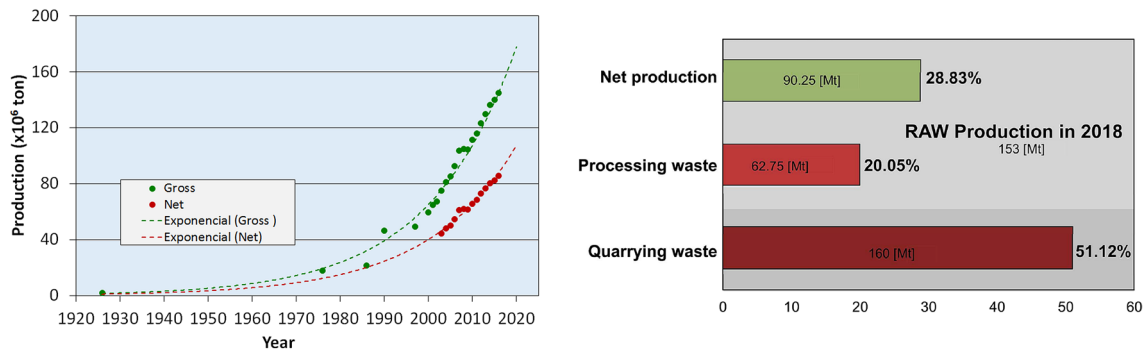


Fig. 1 The production of dimension stone shown an exponential growth (left; data from Montani 2017). Less than one-third of the extracted resource goes into the global trade as a finished product (right; data from Montani 2019)

this critical point, it is crucial to concentrate more on geological conditions in the deposits, to optimize a sustainable extraction of resources (Siegesmund and Török 2014). There are several conditioning factors of the exploitation and utilization of the building stones, some related with material itself like the physico-mechanical properties and others with geological constraints at outcrop scale (Carvalho et al. 2013; Yarahmadi et al. 2015, 2019a, 2019b; Mustafa et al. 2016; Sousa et al. 2017, 2018; Siegesmund et al. 2018; Sousa 2019).

One of the key information required by the owners of the dimension stone quarries is the amount of extractable and profitable stone blocks, i.e. the quarry yield. Especially joint systems play an important role to give reliable information about quantity and quality of in-situ blocks (Mosch 2008). The extraction of stone blocks is limited by fracturing pattern, the density and spacing of the fractures, and the thickness of the bedding planes (in case of stratified deposits). During exploration, evaluating fractures play a major role and will define the productivity of a dimension stone reserve (Mosch et al. 2011; Nikolayev et al. 2007; Yarahmadi et al. 2018). Therefore, it is necessary to perform measurements and analysis of the discontinuity distribution, to predict the sizes and shapes of the extracted blocks (Sousa et al. 2017; Figarska-Warchoł and Stańczak 2019). The final block size and quality of the blocks are influenced by several factors like microcracks, fissures, bedding planes, joints, and faults (Palmström 2001; Yarahmadi et al. 2017) (Fig. 2), despite of some of them only are identified during the processing stage when the slabs breaks under high pressure (Yarahmadi et al. 2019b).

The orientation of fractures identified in a quarry is normally related with regional fault zones nearby (Sousa et al. 2016; Santos et al. 2018). These first-order fractures mostly occur together with lower-order fractures oriented orthogonally to those of the first-order. Nevertheless, it should be noted that fractures may occur irregularly, vary widely from quarry to quarry and may not always be related to regional

fault zones (Ehlen 1999; Sousa 2010), affecting the shape and the volume of the in-situ blocks (Mosch et al. 2011). For these reasons, not only large-scale surveys are important for the development of a deposit, also detailed small-scale surveys in the quarries are required (Santos et al. 2018). It also important assess how fracturing pattern and density changes within the quarry as the depth and the proximity to the faults have noticeable influence (Sousa et al. 2017).

One aspect usually neglected during the analyses of the joint spacing is the distribution of the data, which usually follows a lognormal distribution (Priest 1993; Sousa 2010; Annavarapu et al. 2012; Sousa et al. 2016; Carvalho et al. 2018; Santos et al. 2018; Ferrari et al. 2019; Bruzzi et al. 2020). Consequently, the mean value is not the best measure of the “average” distance or block volume, being preferable a more realistic value as the median value (Sousa 2010; Morales Demarco et al. 2013). Using median values, the results of the block size and quarry yield will be more conservative (Morales Demarco et al. 2013) and closer to the reality.

During processing, quartz or calcite filled veins can open and should also be considered as discontinuities (Yarahmadi et al. 2019b). The occurrence of fractures in the rock mass can have a negative effect on the coloration, as it is the case with some of the weathered granites in northern Portugal (Sousa et al. 2016, 2017). The commercial value of a granite quarry depends on the occurrence of large granite volumes and a homogeneous color, which is depending on the occurrence of natural fractures (Santos et al. 2018). The color variation (Fig. 3) in the weathered granite is caused by weathering processes and the heterogeneous coloration of the granites can be perceived by the customers as negative. The same is true for other rock types, like the marbles showing spots and veins with different colors associated to dolerite dikes (Menningen et al. 2018). Such information needs to be also considered during the resource evaluation.

New techniques and equipment can help in field survey, like the use of unmanned aerial vehicles (UAV). In fact, this

Fig. 2 The discontinuities affect the dimension stones at all scales with different magnitude. **(a)** Intragranular fissure in a feldspar; **(b)** intragranular and transgranular fissures in a granite; **(c)** open, closed and filled joints in a granite; **(d)** fault in a granite quarry; **(e)** fracturing in an underground marble quarry; **(f)** joints and bedding planes in a limestone quarry; **(g)** karstification in limestone; **(h)** joint set in a slate quarry

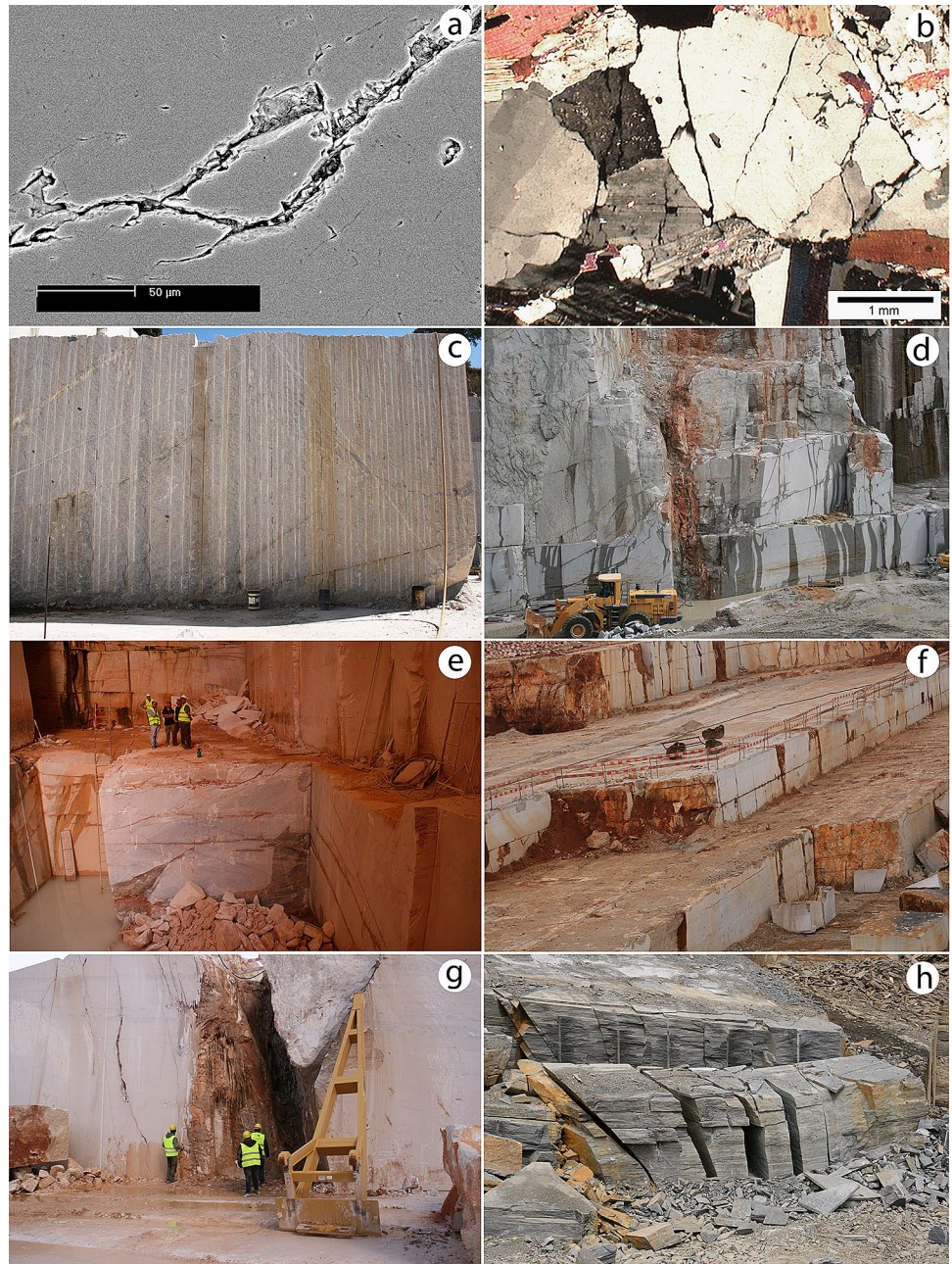


Fig. 3 Color variations along joints diminishes the quarry yield



equipment is now popularized, are friendly used and accessible to everyone. Taking images by UAVs is not only a safe method, to obtain images of hard accessible slopes in quarries; it is also a fast technique to study and monitor quarrying areas (Salvini et al. 2017). UAVs can be used to map visible discontinuities, regardless of their position, attitude or height above ground (Sousa et al. 2019; Török et al. 2020). The acquired images allow processing of detailed digital surface models (DSMs), orthophotos, and three-dimensional (3D) models (Egels and Kasser 2001). These data can be used in commercial terms to calculate the yield, volume of waste and for analysis of stability, and stress distribution, among other applications (Wang et al. 2019a, b; Török et al. 2020; Pagano et al. 2020; Duarte et al. 2020; Akara et al. 2020). The utilization in practical applications to daily problems in mining industry is nowadays very common (Török et al. 2020; Duarte et al. 2020; Lazar et al. 2020).

Quarrying activities intends to maximize the extraction volume of final blocks and minimize cost for investors by reducing the amount of waste. To determine the potential volume of blocks that could be exploited or expected in a rock massif, modelling of natural fracture patterns will be needed (Rasmussen 2020). This fracturing modelling is crucial to improve the block size assessment in the quarries, and is accomplished by considering the number of joint sets and joint spacing (Nefeslioglu et al. 2006; Sousa 2010). Small variations in the fracturing pattern has major impact on the size of the quarried blocks and in some case make the exploration impossible (Sousa et al. 2017). To optimize the production and especially the size of commercial block in dimension stone quarries, the evaluation of in-situ block geometry requires consideration of density and condition of joints, obtained by fieldwork and airborne photogrammetric surveys. These surveys avoid errors related with geological heterogeneities and can be used in small or large areas (Bogdanowitsch 2020). 3D applications like 3D-BlockExpert and photogrammetric surveys can help to identify and recognize the shape and volume of in-situ blocks in all rock types (Mosch et al. 2011; Morales Demarco 2012; Sousa et al. 2017; Yarahmadi et al. 2018). Furthermore, the modelling of the fractures allows the maximization the volume of the final blocks by changing the cut distances and/or cut strikes (Sousa et al. 2017; Yarahmadi et al. 2018).

In this work, several case studies will be discussed, outlining the main rock groups from igneous (granite) and sedimentary (limestone) to metamorphic (marble and slate) rocks. During two-field investigations, in the years of 2016 and 2018, data were collected in 22 well-known granite, limestone, marble, and slate quarries around Portugal for discontinuity mapping using a low cost commercial drone, alongside the conventional field work methods which were mentioned in Sousa et al. (2017). From the studied quarries several cases were selected and presented to highlight the

importance of these combined techniques in the fracturing assessment and quarry management. Natural constraints, specially the geological ones, defines the scope of the methodology applicable in each quarry. Therefore, the selected cases belong to the four of rock types studied. By the first time, the combination of field and airborne survey was systematically applied in the characterization of building stones quarries. The results highlight the importance of these new techniques to improve the quarry yield and maximize the available resources.

Materials and methods

Materials

Mainland Portugal has a great rock diversity, which is reflected in the distribution of quarry clusters (Fig. 4). The geological diversity, excellent physical–mechanical properties together with technological advances in quarrying and processing make Portugal one of the leading countries in this sector (Carvalho et al. 2018). The location of the clusters besides the fracturing is controlled by the texture, color, and location of the processing chain. Investors tend to explore the processing plants near the quarries of important stones.

In the following, a brief description of the main Portuguese stones is made with a special reference to the clusters where studies were conducted.

In northern Portugal, outcrops of granitic bodies of Variscan age predominate, showing distinct mineral compositions and textures. The most common are the two-micas syn-tectonic granites, while the post-tectonic, the most favourable in terms in fracturing, are scarce but important (Casal Moura 2000; Sousa 2007b; Carvalho et al. 2018). As can be seen in Fig. 4, in the north of Portugal the clusters of ornamental granite dominate, particularly the light or grey colored ones, such as those located in Pedras Salgadas (number 5 in Fig. 4) and Alpendorada (number 11 in Fig. 4) (Sousa et al. 2020). In the last decades, the weathered granites, yellowish colored, are more and more extracted as the clusters of Ponte de Lima (number 2 in Fig. 4), Mondim de Basto (number 4 in Fig. 4), and Serra da Falperra (number 7 in Fig. 4) (Sousa et al. 2020).

The Estremoz Anticline (numbers 44–53 in Fig. 4) is the most active marble mining area in Portugal, dating back to the Roman period (Taelman et al. 2013). Nowadays about 40 active quarries extracting dimension stones in this region (Lopes et al. 2015), but the total number reaches 150 (Carvalho et al. 2018). The Estremoz Anticline is a 40 to 45 km NW–SE striking variscan structure in central Alentejo with a maximum width of 10 km at the City of Estremoz (Lopes et al. 2015). The Paleozoic calcite marbles belong to the geological Ossa-Morena Zone, which is a southern branch

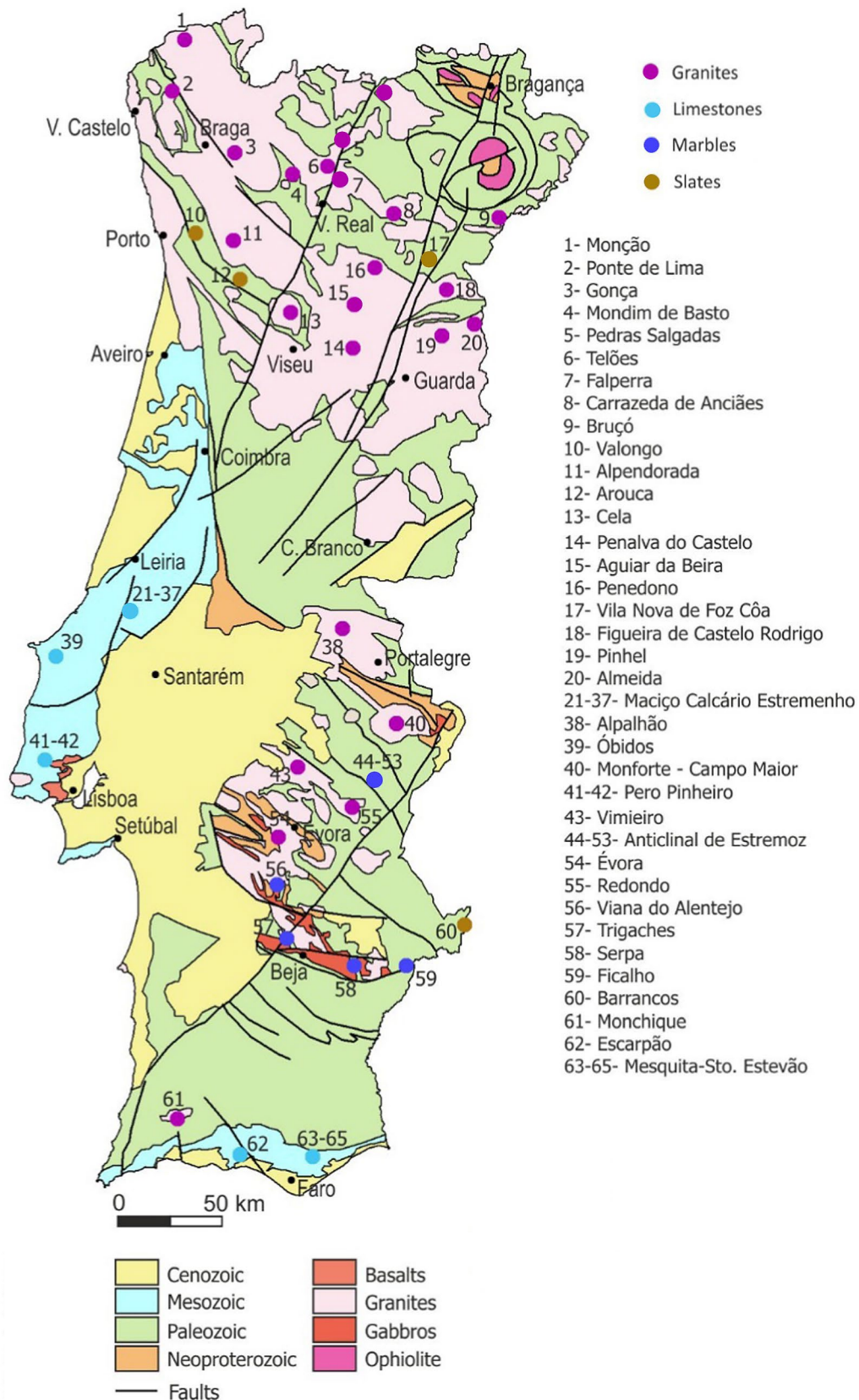


Fig. 4 Distribution of the foremost quarry clusters in Portugal (adapted from Carvalho et al. 2018)

of the European Variscides in Portugal (Lopes et al. 2015). The stratigraphic sequence of the Estremoz Anticline consists in the core of the Precambrian Mares Formation, which includes Ediacaran greywackes, shales, and black cherts. Followed by fine grained Cambrian metadolomites, acid metavolcanics, and metaconglomerate at the base of the Dolomitic Formation. On top of the dolomitic limestones, a quartz and iron-rich horizon up to 50 m thick forms the base of the Volcanic-Sedimentary Complex (VSC) of Estremoz, followed by metadolomites. The VSC includes different colored marbles, varying from white to grey and pink. The Estremoz Anticline is surrounded by metavolcanic rocks, aged Silurian to Devonian (Pereira et al. 2012; Taelman et al. 2013; Lopes and Martins 2015). The quarry yield of large sized blocks is about 20% (Carvalho et al. 2018), as consequence of the important constraints to exploration. The main constrains are the folding and shearing related to Variscan orogeny, the volcano sedimentary–sedimentary inter-fingering, and the weathering (Carvalho et al. 2008; Lopes and Silva 2006).

The areas appropriate for limestone exploration are in the west and south borders of Portugal mainland (Kullberg et al. 2013). In the main mining district (numbers 21–37 in Fig. 4), located at Maciço Calcário Estremenho (MCE), several ornamental varieties are exploited. The MCE is an intracratonic rift basin, that developed under extensional tectonic during the opening of the North Atlantic Ocean (Alves et al. 2003; Carvalho et al. 2018). During the late Miocene, the MCE was also influenced by Alpine compressive tectonics. The exploitation occurs mainly in strata of coarse-grained calciclastic sparitic rocks of some horizons of Middle Jurassic age (Carvalho and Lisboa 2018) formed at a carbonate ramp depositional system (Azerêdo 1998, 2007). Cream colored fine- to coarse-grained calcarenites showing several types of sedimentary laminations can be found. These laminations are very important to define the texture of the stone, since from the same facies different textural patterns can be found according to the cutting direction (Carvalho and Lisboa 2018). The Upper Jurassic limestones are exploited in two sites where a grey calciclastic micritic limestone is found (Carvalho and Lisboa 2018). The thickness of the exploitable limestones ranging from 40 to 150 m and 50 quarries are currently spread in main six clusters (Carvalho and Lisboa, 2018; Carvalho et al. 2018).

Despite the large areas of slate-bearing unities outcropping in Portugal there are only four feasibly economic explorations. The most important ones located in the north of Portugal: Valongo (number 10 in Fig. 4), Arouca (number 12 in Fig. 4), and Vila Nova de Foz Côa (number 17 in Fig. 4). Valongo and Arouca quarries exploit Ordovician stratigraphic horizons with slaty-cleavage composed by high quality, whilst in Vila Nova de Foz Côa siliceous slates are extracted in Cambrian levels.

In Vila Nova de Foz Côa cluster the conjugation of the schistosity (primary and secondary) with the jointing turns possible to obtain geometric blocks in some areas of the folded sequence (Lourenço et al. 2012). The quarrying starts more than 200 years ago to supply vineyards support-masts nowadays spread along the Douro valley wine producer region (Búrcio 2004; Lourenço et al. 2012; Sousa et al. 2015). In the present, this stone is used worldwide in different applications after technical improvements in the extraction and processing stages.

In this research, 22 quarries were studied (Table 1), named as following: 7 in granites: Branco Micaela, C&G, Granitos Ribeiro, Irmãos Queirós, Mármore Central Tansmontana (MCT), Oliveira Rodrigues and Transgranitos; 7 in marbles: António Galego, Bentel, Cochicho, Geopedra, Granoguli, Marmetal JPL and Mármore Galvão; 5 in limestones: Cheira Pia do Zé Gomes, Codorneiro, Portela 8, Vale da Louceira and Vale da Moita; 3 in slates: Cupastone, Solicel and Solicel upper quarry. The location of the quarries can be seen in Fig. 4. More information about the stones extracted will be presented later.

Table 1 Location of the studied quarries

Rock type	Quarry name	Location—cluster number (see Fig. 4)
Granite	Branco Micaela	15
	C&G	5
	Granitos Ribeiro	7
	Irmãos Queirós	5
	Mármore Central Tansmontana (MCT)	30 km NE from cluster 5
	Oliveira Rodrigues	5
	Transgranitos	7
Marble	António Galego	44–53
	Bentel	44–53
	Cochicho	44–53
	Geopedra	44–53
	Granoguli	44–53
	Marmetal JPL	44–53
	Mármore Galvão	44–53
Limestone	Cheira Pia do Zé Gomes	21–37
	Codorneiro	21–37
	Portela 8	21–37
	Vale da Louceira	21–37
	Vale da Moita	21–37
Slate	Cupastone	17
	Solicel	17
	Solicel upper quarry	17

Methods

Field mapping (conventional mapping techniques)

In this research, the scan line sampling technique or window sampling was used to identify different joint sets on vertical quarry walls (see ISRM 1978). To minimize the disadvantages of this technique (see Shang et al. 2018) orthogonal scan lines must be used. The orientation of natural discontinuity planes was measured by compass and their dip direction and dip angle were recorded. Afterwards, the joint data were processed with the StereoNet software (Allmendinger et al 2011), version 10.2.9, to generate a rose and Schmidt contour diagram (Fig. 5).

The joint spacing was measured along the same scan lines, perpendicular to the fracture surfaces. Since the mean

joint spacing is more susceptible to outliers, Sousa 2010 does not recommend using this parameter to characterize the joint spacing distribution, but rather the median joint spacing. A histogram offers the possibility of analysing and representing the joint spacing distribution for different orientated joint sets. With the help of the median joint spacing an average block volume can be calculated (Singewald 1992).

For fracture mapping, the “P” system was adopted, which was introduced by Dershowitz and Einstein (1988), to define density (P10 and P20) and intensity (P21) in the Cochicho case study (Salvini et al. 2017). This method is used to define fracture density and intensity parameters by mapping line traces on 2D survey windows (Salvini et al. 2017). This approach offers a convenient framework to move in between different scales and dimension. The parameters can be calculated as follows (Salvini et al. 2017):

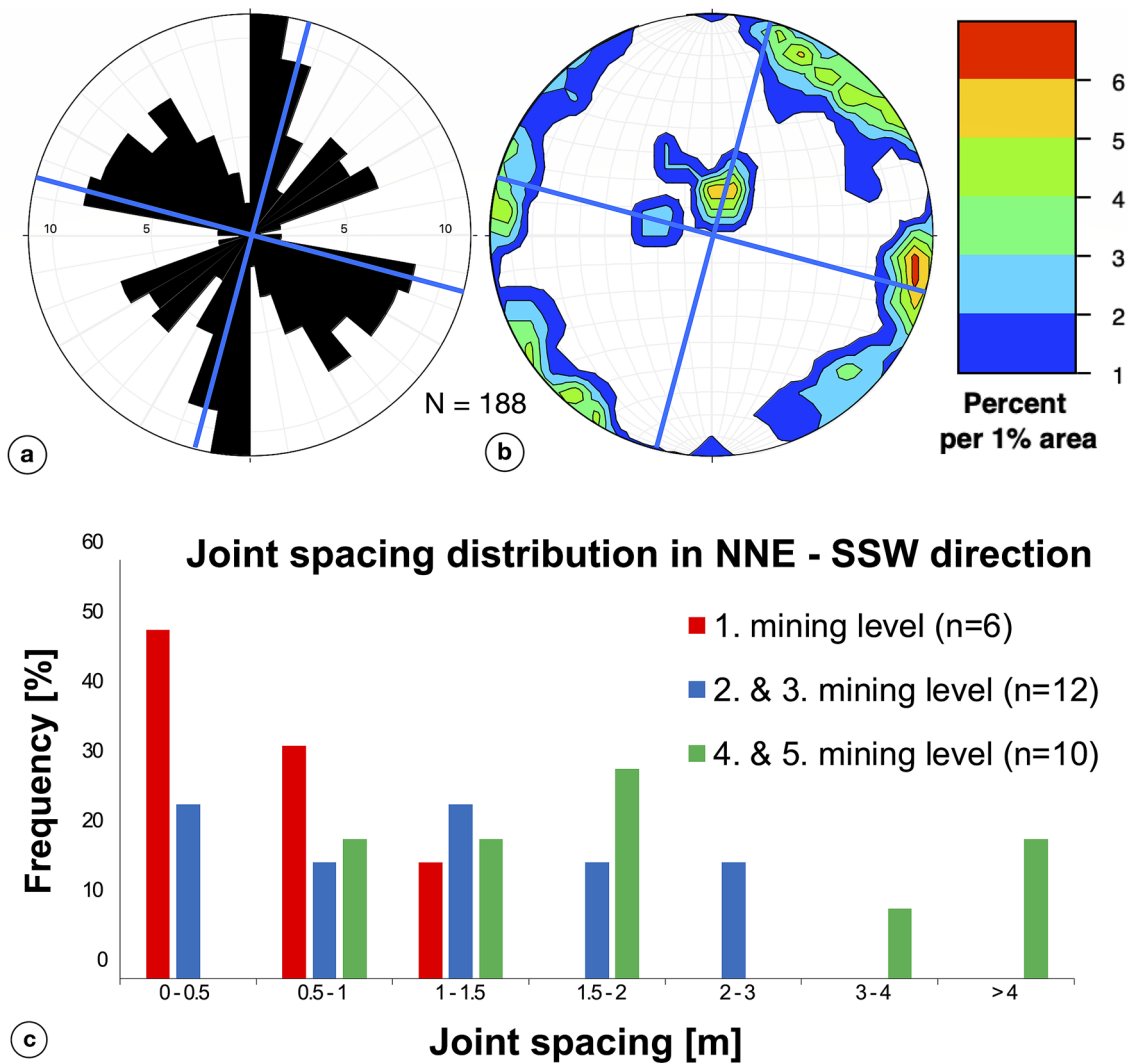


Fig. 5 Example of data in a granite quarry: (a) Strike direction of joint sets in a rose diagram. (b) Stereographic projection of the density distribution of pole points in a Schmidt contour diagram (lower

hemispherical equal-area). (c) Presentation of the joint spacing distribution in a histogram

$P10 (m^{-1}) =$ number of fractures/lengths of scan line,

$P20 (m^{-2}) =$ number of fractures/areas of exposure,

$P21 (m/m^{-2}) =$ length of fracture traces/area of exposure.

Due to the simplicity of the method and the availability of high spatial resolution orthophotos and 3D information, it was possible to extract the needed data by a detailed cartographic approach within a geographic information system (GIS) (Salvini et al. 2017).

A main problem of this technique is the termination behaviour of the joints. The observed direction of a joint on a quarrying wall can end, change or even shift with increasing depth (Schneider 2009). In this case, errors can occur during the evaluation of the in-situ blocks. Therefore, it is important to clean the surfaces of the rock bodies as far as possible, to track and measure the trend and orientation of the joint surfaces. However, the surfaces of the exploited areas are often covered by sedimentary cover or waste material, so that under such conditions, no statements can be made about the trend of the joint surfaces (Mosch 2008). This problem also occurred during the mapping of joints with the help of the aerial photography's and 3D models, which made it sometimes impossible to draw valid conclusions.

3D fracture modelling (3D-BlockExpert)

To visualize the orientation of joint surfaces in a raw block, the program 3D-BlockExpert was developed (Nikolayev et al. 2007; Mosch et al. 2011) and used in this research. With this method, it is possible to model the trend of joint surfaces within a raw block and to calculate the shape, potential volume, and distribution of the in-situ blocks. It is assumed that a joint surface is equal to a plane (Mosch et al.

2011), which can be defined with three points (X, Y, Z) in a coordinate system (Fig. 6). This method can be applied directly to the quarry wall, even in the stage of exploration (Mosch et al. 2011) by following the scan line sampling technique or window sampling (ISRM 1978; 1981). In this approach, the joint surfaces can only be modeled as continuous separating surfaces intersecting the entire raw block. Consequently, inaccurate prognosis of the block sizes in stratified sedimentary rock can occur, where the vertical joints often terminate at layer parallel discontinuities (Schneider 2009; Schneider et al. 2022).

Using the mathematical models from 3D-BlockExpert, two-dimensional sections can be generated parallel to each surface of a block. The generated surfaces are perpendicular to the outer walls and can be chosen freely. If put together, a 3D model and a first impression of the orientation of joint surfaces can be obtained. From the 3D-BlockExpert model, information about block sizes, block geometry, and position of mineable in-situ blocks can be extracted (Fig. 7). The identified vertical to sub-vertical joints can be used for modelling the deeper and future quarry levels and a possible yield can be calculated (Sousa et al. 2017).

A powerful function of the 3D-BlockExpert software is the differential view of two parallel cutting sections, which allows the simulation and spatial construction of a potential slab (Mosch et al. 2011). The black areas in the differential view are representing fracture surfaces, which cannot be used for the extraction of dimensional stones and will be considered as waste material. With the help of the function "optimization", final blocks customized in size can be displayed to predict potential block volumes (Schneider 2009).

For details, mathematical background information on the detailed operation of the software is available in Mosch et al. (2011).

Fig. 6 Example of data acquisition by three points (each point with an X-, Y-, and Z-coordinate) for describing a joint plan in a coordinate system (modified after Mosch 2008)

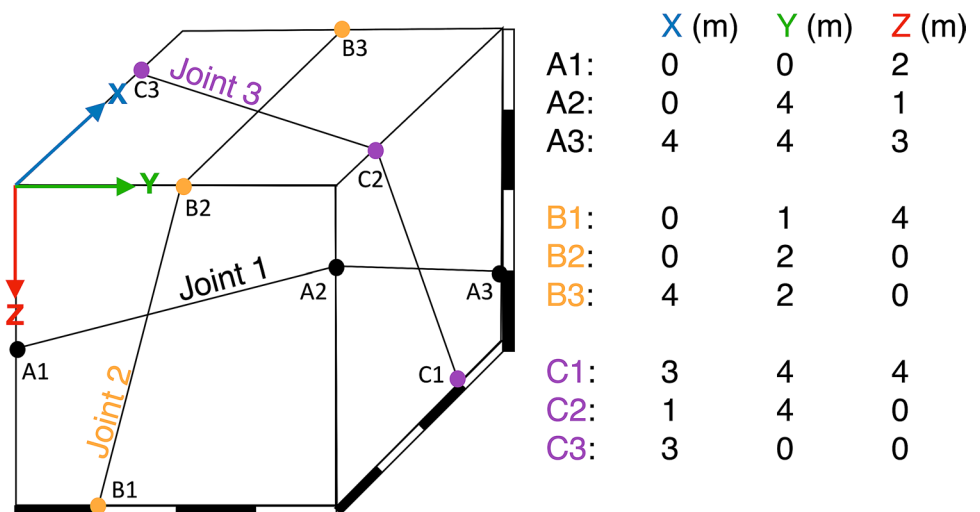
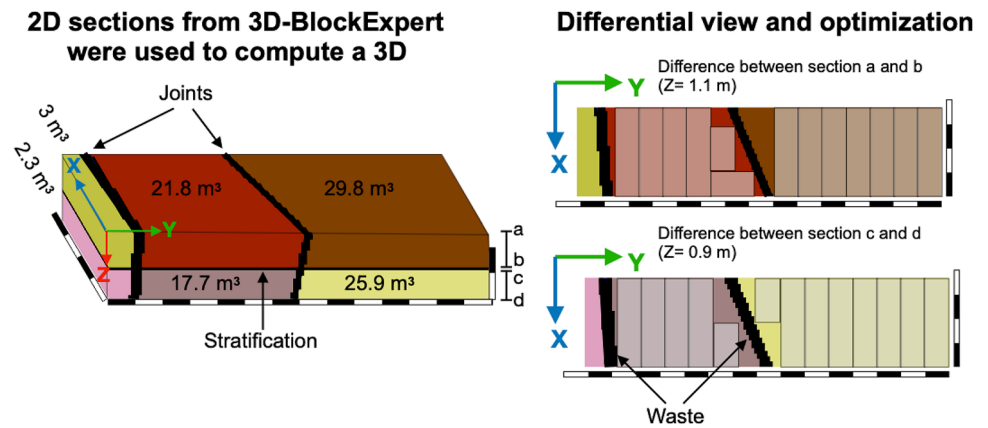


Fig. 7 Procedure to optimize in-situ block extraction with the help of the 3D-BlockExpert software. On the left the computed joints and the stratification dividing the raw block into smaller blocks. The software gives information about the volumes of the blocks defined by the natural discontinuities



Volume/shape of the blocks (calculation of the quantity of in-situ blocks)

According to Singewald (1992), extracted blocks with a minimum volume of 0.4 m³ ($V_{\text{minimum}} = 0,4 \times 1 \times 1 \text{ m}$) are required for further processing. However, a granite block with this dimension is considered as waste and that value is depending on the rock type. To evaluate the quantity of in-situ blocks, joint spacing values as measure of fracture density will be taken into account (Figarska-Warchoł and Stańczak 2019).

On the basis of the median joint spacing values, the volume of a median block can be calculated after following equation (Singewald 1992):

$$V_{\text{median block}} [m^3] = X_{\text{median}} [m] \times Y_{\text{median}} [m] \times Z_{\text{median}} [m]. \quad (1)$$

In the case of a uniform and orthogonal fracture system, this approach is a first possibility for estimating the average block sizes in a dimensional stone deposit. In many situations a non-orthogonal joint system is observed in the studied quarries and the extracted blocks have irregular shapes (Fig. 8), which causes waste (Figarska-Warchoł and Stańczak 2019).

The minimum block volume depends on the joint orientation and the dihedral angles between average planes of the discontinuity sets (see Figarska-Warchoł and Stańczak 2019).

Airborne photogrammetry and modelling

The method of photogrammetry describes the process of using 2D images to create a 3D model, which can be used for surveying in remote sensing and generating data for Geographic Information Systems (GIS) (Egels et al. 2001).

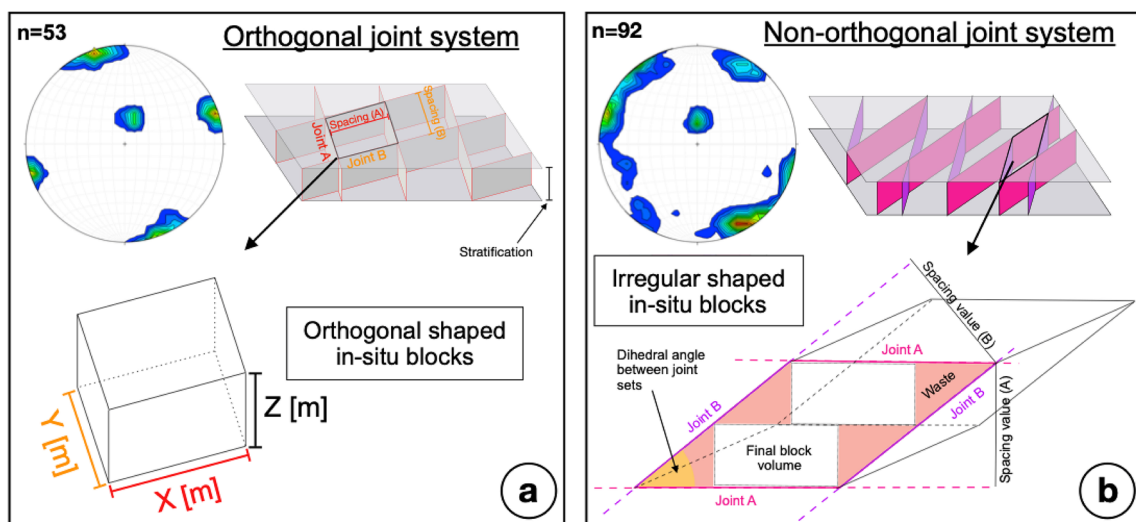


Fig. 8 Density distribution diagrams represent orientation of joints controlling different shapes of in-situ blocks in case of (a) an orthogonal joint system and (b) a non-orthogonal joint system

The enormous popularity of the unmanned aerial vehicles (UAVs) in the field of mapping and photogrammetric surveys is a result of the rapid development of computer software, hardware technologies, and improvements in the digital camera technology (Wang et al. 2019a, b). Today all-in-one solutions are available on the market, that allow even pilots with small experience in aerial photography, to take detailed pictures and produce high resolution and affordable 3D models.

A DJI Phantom 4 was used as a UAV system for data acquisition in the quarries (see Fig. 9). It is a small quadcopter with a fixed 12-megapixel camera and a maximal flight time of approximately 20 min. With the help of the built-in GPS, georeferenced images can be taken to compute point clouds.

Aerial photographs from two-field surveys in Portugal from 2016 and 2018 were processed photogrammetrically using the Pix4D software. This widely used software package computes a 3D point cloud using 2D feature matches (triangulations), automatic calculation of camera positions and structure from motion (Mills et al. 2019; Szeliski 2011). A summary of the point cloud data for 21 quarries from Portugal can be found in Table 2. This table includes the mapped area (total: 2.3 km²), number of images used for the photogrammetry reconstruction (total: 4175), the ground sampling distance (GSD) with a mean of 3.97 cm/pixel and

the year of the survey for each quarry. The GSD describes the ground distance covered within a pixel (Medinac 2019).

The surveys from 2016 show a smaller number of images. At that time no planned missions were performed and the obtained images by an UAV were only used for perspective reasons. Still the number of images were enough to compute 3D models for further structural analysis. The surveys from 2018 were performed more systematically, using autonomous flight missions for accurate flight routes.

Once the point cloud is processed, the data can be exported as a georeferenced point cloud, which comprises a digital outcrop model (DOM), digital surface model (DSM) for ground elevation and orthophotos, which can be used for mapping the orientation and spacings from discontinuities (Wang et al. 2019a, b). Some of the DOMs were further processed in a specialized point cloud program called Cloud-Compare (see Fig. 10).

The quality of the aerial images is depending on multiple parameters which have a significant impact on the results of the photogrammetry: camera resolution, distance from the target area, lighting conditions, flight height, overlap between photos and weather conditions (Medinac 2019). Some of the parameters cannot be controlled by the operator, such as the weather and lighting conditions (Medinac 2019).

The orientation and spacing of discontinuities are normally measured in the outcrop, which can be hazardous and

Table 2 Summary of the point cloud data set for each quarry

Location/quarry	Area (km ²)	Images (number)	GSD (cm/pixel)	Survey (year)
António Galego	0.064	196	3.74	2018
Bentel/Geopedra*	0.107	218	3.04	2018
Branco Micaela	0.076	39	4.84	2016
C&G	0.069	27	3.00	2016
Cheira Pia do Zé Gomes	0.048	122	2.10	2018
Cochicho	0.076	136	3.68	2018
Codorneiro	0.068	195	2.89	2018
Cupastone	0.173	259	3.69	2018
Granitos Ribeiro	0.176	49	4.89	2016
Granoguli	0.130	271	2.43	2018
Irmaos Queirós	0.085	28	6.25	2016
Marmetal JPL	0.219	349	3.29	2018
Mármore Central Tansmontana	0.138	33	11.93	2016
Mármore Galvão	0.090	358	3.11	2018
Oliveira Rodrigues	0.064	19	6.67	2016
Portela 8	0.0022	47	2.12	2018
SoliceL	0.422	906	6.25	2018
SoliceL upper quarry	0.021	102	1.60	2018
Transgranitos	0.116	376	2.82	2018
Vale da Louceira	0.068	258	2.35	2018
Vale da Moita	0.071	187	3.28	2018

*Quarries located side by side



Fig. 9 Data collection by (a) traditional joint survey, using a geological compass and measuring tape. (b) All-in-one UAV: DJI Phantom 4 with remote control. (c) UAV during photogrammetric survey



Fig. 10 Point clouds were used to identify the orientation of joints and the joint spacing. In this case, joint traces are visible after rain wetting

sometimes impossible at slopes or higher outcrops (Dewez et al. 2016). The aim was to map the traces and spacings of joints on the horizontal quarry surfaces. Afterwards the orthophotos were used in ArcGIS to map the joint orientation, stratification, cutting pattern of the quarry, and to measure the spacing of the different joint sets. It was assumed that the joints have a vertical orientation (90°), which was confirmed by previous field observations. The detailed 3D model also helped to identify and measure joint spacings (Fig. 10). In some cases, the horizontal quarry surfaces were covered by waste or sediment and active mining made the mapping nearly impossible. A better situation was found

after a rain shower when the joints are more visible on the surfaces.

Since processing 3D point clouds is not a challenging task anymore, the question is, how to evaluate the collected data. One of the most important properties already discussed in this research, the 2D plane, corresponding to joints, faults and fractures within a quarry.

A so called “virtual geological 3D-outcrop” can help to distinguish fracture networks, when using the information from the 3D point clouds correctly. Measuring dip and dip direction is a time consuming process, requires expertise and is done by hand with a compass in the quarries (Dewez et al. 2016). To help in this situation and to compare the data with the conventional methods, a helpful plugin was used in CloudCompare (open-source software), to perform planar facet extraction. FACETS is a user friendly and well-integrated structural geology plugin in CloudCompare. This plugin was designed to extract planes from unstructured 3D point clouds and was used to identify and calculate the dip and dip direction of stratification and joint sets (Dewez et al. 2016). Another useful aspect is the integrated interactive stereogram-rendering tool to produce structural geology diagnostics. In a final stage, it is possible to export facet polygons as 3D polygon shapefile towards third party software like ArcGIS (for more details see Dewez et al. 2016; Millis et al. 2019).

General methodology

The application of the above-mentioned methods in the studied quarries allows to maximize the fracturing assessment. Field observation and the information gathered from UAVs

enhance the characterization of the fracturing at each quarry site. A better resource evaluation is achieved when multiple sources of information are used. In this manuscript rather than explain the complete fracturing evaluation performed at each quarry, special cases are presented where combined methods improve the resources evaluation. Therefore, some examples are explained for each type of stone.

Results and discussion

This chapter is subdivided according to the rock types studied. For each rock type, i.e. granite, marble, limestone, and slate a general characterization is presented.

Granite quarries

The orientation and spacing of natural fractures were measured in seven granite quarries in NE Portugal (Fig. 11). Two important regional faults, the Vila Real Fault and the Vilarça Fault are located near the studied granites, therefore, the fracturing patterns observed in the quarries of the north-east of Portugal are dominated by the NNE–SSW jointing (Lourenço et al. 2002; Sousa 2000). Other important fault sets in the region are the N40°– 50°W and N60°– 80°E (Sousa 2007a, 2007b). The link between jointing and regional faults is not always clear because the secondary faults located near the quarries can have a great influence in the local jointing (Sousa et al. 2016). Generally, the fracture sets identified in studied quarries coincide with the main regional fracturing pattern and corroborate the results obtained by others researches in the region (Sousa 2000; Lourenço et al. 2002; Morais 2003; Santos et al. 2017; Sousa et al. 2016; Sousa et al. 2017).

The histograms of joint spacing values measured in quarry show the prevail lower spacing classes and a log-normal distribution, as is common in fracturing evaluation in granitic building stones (Sousa 2007a, 2010; Morales Demarco et al. 2012). The mean/median joint spacing value is very low, usually ranging between 1 and 5 m, in accordance with previous research in these granites (Sousa 2000, 2007a; Santos et al. 2016; Sousa et al. 2016, 2017, 2018).

Case study: Granitos Ribeiro quarry

The natural fracture patterns and the resulting in-situ block geometry of the yellowish granite called Amarelo Real, in the region of Vila Pouca de Aguiar, located in the north part of Portugal, were studied. The stone is a two-mica, medium-grained, hypidiomorphic granular granite with a slight porphyritic tendency (Fig. 12). According to Sousa

et al. (2005), the mineralogical composition of Amarelo Real granite is as follows: quartz (35.8%), K-feldspar (23.6%), plagioclase (29.3%), biotite (3.3%), muscovite (7.9%), and apatite (0.1%). The intense fracturing by the sub-vertical joints is notorious in the quarries by the low volume of the extracted blocks and low quarry yield (Sousa et al. 2017).

Besides the Granitos Ribeiro quarry another quarry, Transgranitos, located nearby was also studied to compare the fracturing pattern. Both quarries are located approximately 10 km south of Vila Pouca de Aguiar, on top of the mountain range Serra da Falperra. The companies Granitos Ribeiro and Transgranitos (Fig. 13) operate the near-surface extraction of the weathered and highly fractured granite (Sousa et al. 2017).

To determine the geometry of the in-situ blocks and the influence of the discontinuity pattern, several joint surveys were performed, following four scanlines in the upper and lower parts of the Granitos Ribeiro quarry. The obtained joint data were processed with the StereoNet software to stereographic projections for further analysis. Additionally, the 3D-BlockExpert was applied for modelling the fracture network of two selected areas in the lower part of the same quarry. With the help of a drone, a detailed 3D-Model, DSM and an orthophoto was generated to identify large-scale fracture system through the quarry.

In total, three main joints were identified across the Granitos Ribeiro quarry. The main joint sets have an NNE–SSW orientation, followed by an NW–SE and another set orthogonal to the previous with an NE–SW orientation (Fig. 14). The sub-horizontal to horizontal joints are dipping to the south.

Only 1-kilometer SE of the Granitos Ribeiro quarry, separated by the highway A24, the Transgranitos quarry is located. Two dominant joint sets can be recognized, one which is striking in NW–SE and the second one in NE–SW direction. Several previous studies in these granite quarries indicating two to three main joint sets, which are parallel to the Vila Real Fault (NNE–SSW) and also orientated to the WNW–ESE and NE–SW faults (Sousa 2007b, 2010, 2014; Santos 2017; Santos et al 2018). In general, the measured joints are sub-vertical to vertical and are compatible to regional fracturing, which was shaped by NNE–SSW structures of tectonic origin (Lourenço et al. 2002). One of the most important regional faults in NE Portugal is the Vila Real Fault, which is located near the investigated area (Sousa 2007a). Figure 13 shows the differences in jointing in these quarries as a result of regional faults. In Transgranitos quarries, the NNE–SSW regional faults are absent and the same is true for the joints observed in the quarry. In contrast, in the Granitos Ribeiro quarry, the NNE–SSW joints are very important. This relationship between regional faults and jointing in these quarries was also mention by Santos et al. (2018).

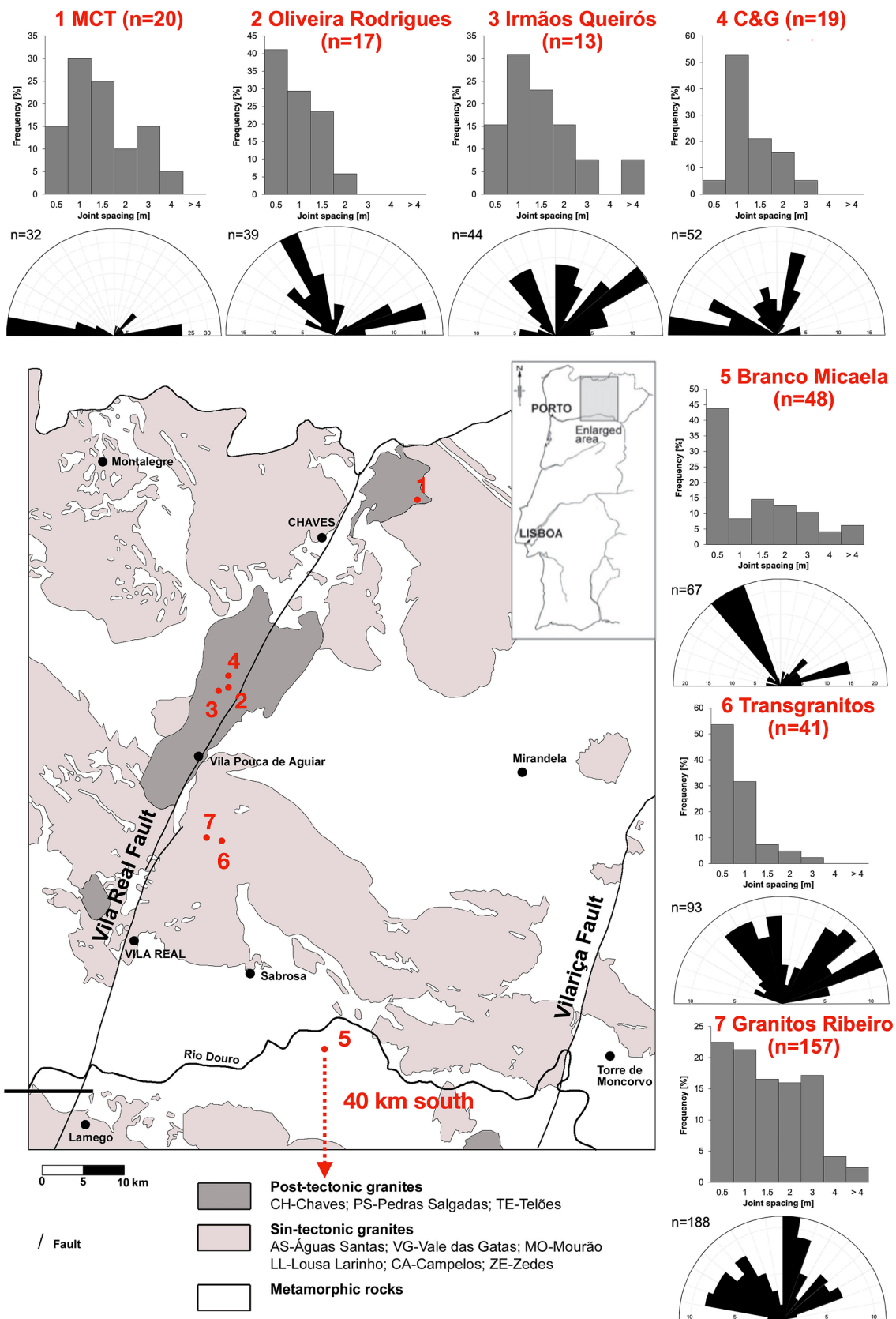


Fig. 11 Location of the studied quarries with rose diagram and joint spacing (map modified from Sousa 2007a)

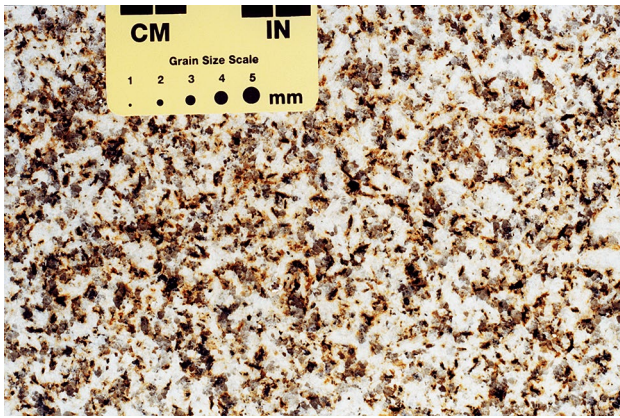


Fig. 12 Typical yellowish tone of Amarelo Real granite

The measured joints differ across the Granitos Ribeiro quarry in direction of strike. Following the first scan line (scan line 1, Fig. 15), which is parallel to the NNE–SSW

fault and passing mining levels two to four, all three main joint sets can be recognized. Nevertheless, the two orthogonal joint sets are more dominant than the NNE–SSW striking joint set. A similar situation can be found within the second scan line, which is located at the bottom of mining level four. The dominant joint set shows a NW–SE direction, and another set orthogonal to the dominant direction. The third scan line is in the first and second mining level and is more influenced by horizontal joint sets. The two dominant joint sets are showing an NNE–SSW and NE–SW direction. The last scan line is in the first mining level and is almost orthogonal to the previous scan lines. Two directions of strike, one N–S and one ESE–WNW direction can be recognized. Mining levels one and two are stronger influenced by horizontal joints.

Horizontal joints are related to the stress relaxation in the granite complex (Sousa et al. 2017). In the first extraction level, following scan line four, the median horizontal joint spacing is about 0.95 m (Table 3) and varies between

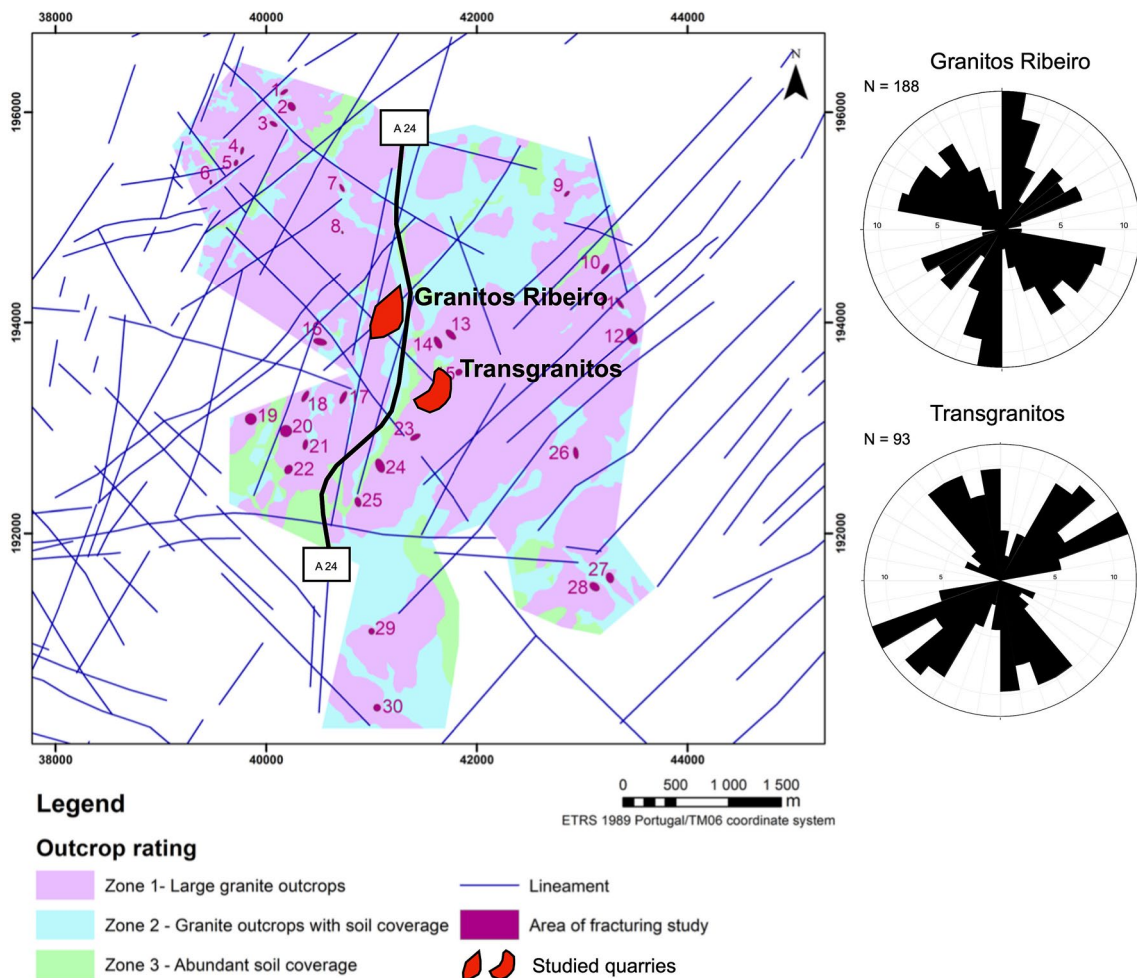


Fig. 13 Detailed fracturing surveys in marked quarries with regional lineaments, identified in aerial photography. Rose diagrams for measured joints in the Granitos Ribeiro and Transgranitos quarry (the map was modified from Santos et al. 2018)

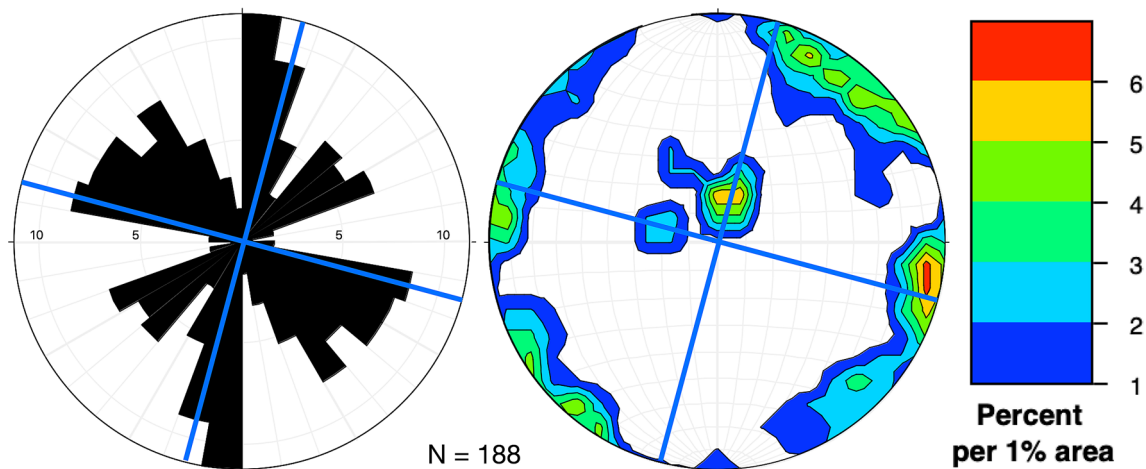


Fig. 14 Rose diagram of three identified fracture directions (left) and stereographic projection of the density distribution of pole points (right) for measured joints in the Granitos Ribeiro quarry. Blue lines indicate strike direction of sawed quarry faces (Schmidt net, lower hemisphere)

0.4 m and 2.5 m. In mining levels two and three, the maximum joint spacing is 3 m and indicating an increasing median spacing of 1.4 m. Joints of mining levels four and five reaching a maximum of 4.5 m and the mean horizontal joint spacing increases to 1.8 m. The sub-horizontal to horizontal joint spacing is increasing with the depth (Fig. 16) of and within individual mining levels (Sousa et al. 2015).

A similar trend can be observed with the sub-vertical to vertical joint spacing throughout the mining levels. In the first mining level, the median spacing of the NNE–SSW and the NE–SW is 0.5 m, reaching a maximum of 1 m and indicating the nearby presence of the main faults. The joint spacing of the NW–SE joint set, which is orthogonal to the NE–SW varies from 0.1 m to 2.8 m and is showing a median joint spacing of 1 m. In general, all joint sets are showing a high-joint spacing distribution in the range 0.1–0.5 m and as an exceptional case only the NW–SE striking joints are showing spacings higher than 1.5 m (Fig. 17). The median vertical joint spacing in the second and third mining level keep increasing and varying between 1.1 m and 1.6 m. The spacings of the NNE–SSW (1.13 m) and NE–SW (1.1 m) joint sets have doubled while the median of the NW–SE joint spacing increased by 0.65 m, compared to the first mining level.

The highest spacings of the vertical joint sets were reached in the fourth and fifth excavation level. The spacing of all joint sets varying between 0.8 m (NE–SW joint set) and 5.8 m (NNE–SSW joint set). The median spacing of the NW–SE joint set nearly doubled (3 m), compared to the previous mining levels. The median spacing of the NNE–SSW (2 m) and NE–SW (1.75 m) joint set keep increasing. In Fig. 18, the planes of the three main joint sets were colored

in a 3D model, to identify the frequency and orientation of the joint sets.

The investigated spacings of the vertical joint sets and the horizontal spacings were used to compute median block volumes. The vertical NE–SW and NW–SE joint sets are approximately orthogonal, the angle between the NNE–SSW and NE–SW joint set is 40° and the angle between NNE–SSW and NW–SE joint set is 50° .

In the following sketch (Fig. 19), four blocks and their maximum volume were modeled, resulting from the joint set orientation and median edge lengths of the joint spacings from mining level one (L_1). In all following cases, the horizontal joints have a median spacing of 0.95 m. The first block (VB_1) is defined by the NNE–SSW and NW–SE striking joint sets and has a volume of 0.39 m^3 ($VB_1L_1 = 0.82 \times 0.5 \times 0.95 \text{ m}$). In this case, 0.2 m^3 are lost, which is 33.83% of the total volume, caused by the joint spacing and the angle of 50° . Block two (VB_2) and three (VB_3) have a volume of 0.09 m^3 ($VB_{2/3}L_1 = 0.18 \times 0.5 \times 0.95 \text{ m}$) considering that the volume of block two is mainly influenced by the smallest spacings of the NE–SW (0.5 m) and NNE–SSW (0.5 m) joint sets, as it is the case of block number 3. The loss of 75% of the total volume is higher than the first block, which is a result of the geometry of the parallelogram with a narrow angle of 40° and the two smallest joint spacings. The fourth (VB_4) and biggest block has a maximum volume of 0.45 m^3 ($VB_4L_1 = 0.5 \times 0.95 \times 0.95 \text{ m}$), leaving no waste, due to the orthogonal joint sets (Table 4).

The final block volumes were also calculated for the lower mining levels with respect to the increased joint spacing values of the studied joint sets. Already a big difference in the final block volume is noticeable in mining levels two and three ($L_{2/3}$). The volume of the final

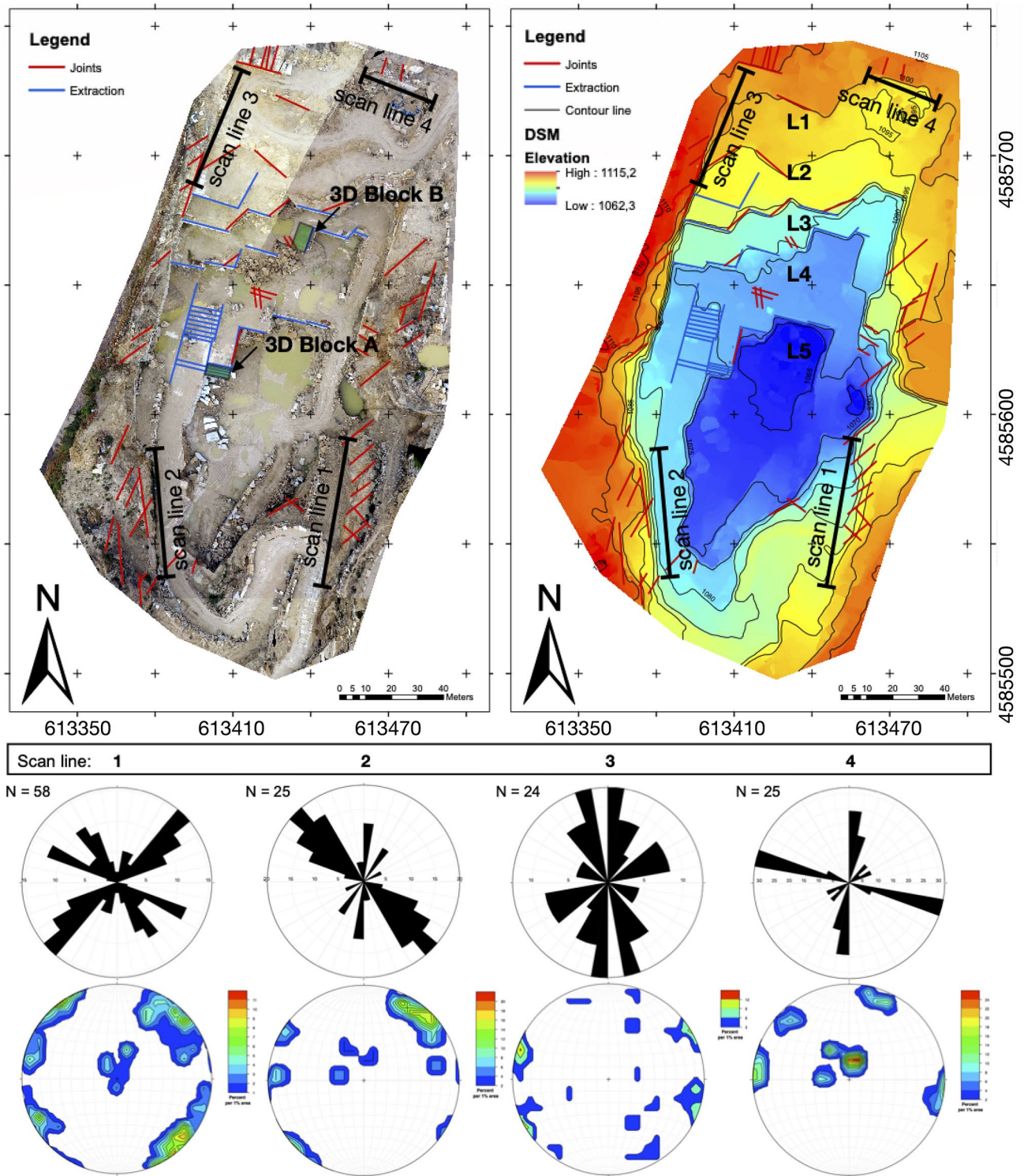


Fig. 15 Orthophoto and digital surface model (DSM), with location of the four scan lines and 3D-BlockExpert models of the Granitos Ribeiro quarry. Rose diagram of the identified fracture directions and

stereographic projection of the density distribution of pole points for measured joints corresponding to the four scan lines (Schmidt net, lower hemisphere)

Table 3 Median and mean joint spacing of the investigated joint sets divided into the different mining levels of Granitos Ribeiro quarry

Joint set	1. mining level				2. & 3. mining levels				4. & 5. mining levels			
	NNE-SSW	NE-SW	NW-SE	Horizontal	NNE-SSW	NE-SW	NW-SE	Horizontal	NNE-SSW	NE-SW	NW-SE	Horizontal
Median	0.50	0.50	0.95	0.95	1.13	1.10	1.60	1.40	2.00	1.75	3	1.8
Mean	0.64	0.56	1.11	1.09	1.26	1.32	1.50	1.29	2.60	2.01	2.83	2.08

block 1 in mining levels two and three reaches 1.8 m^3 ($VB_1L_{2/3} = 1.13 \times 1.14 \times 1.4 \text{ m}$), which is nearly three times the volume of the final block volume (0.68 m^3) of block 2 and 3 ($VB_{2/3}L_{2/3} = 0.44 \times 1.1 \times 1.4 \text{ m}$). The block 4, resulting from the spacing of the orthogonal joint sets reaches a maximum volume of 2.46 m^3 ($VB_4L_{2/3} = 1.1 \times 1.6 \times 1.4 \text{ m}$). The volumes of the final blocks in mining levels four and five ($L_{4/5}$) are as followed: 8.06 m^3 ($VB_1L_{4/5} = 2.24 \times 2 \times 1.8 \text{ m}$), 3.23 m^3 ($VB_{2/3}L_{4/5} = 1.03 \times 1.75 \times 1.8 \text{ m}$) and 9.45 m^3 ($VB_4L_{4/5} = 1.75 \times 3 \times 1.8 \text{ m}$).

The computed median block volumes, defined by the joint spacing in the different mining levels can be compared with the data from the production volumes, given by the company in 2013 (Fig. 20). Only 11 blocks in mining level one, 38 blocks in mining level two and 140 blocks in mining level three were extracted. The mean block volumes are 1.76 m^3 , 1.97 m^3 , and 2.84 m^3 , respectively, for mining levels one, two, and three. Mining level three is standing out with around 81% of the volume and 74% of the extracted blocks. In this dataset, the amount of waste was not given, which is of course a very important information for the quality of extraction.

In general, the computed median block volumes from mining levels one to three, resulting from the joint spacing, are smaller than the mean block volumes given by the company (Table 4). The median block volumes of mining level one varying between 0.09 m^3 and 0.45 m^3 , from 0.68 m^3 to 2.46 m^3 in mining levels two and three and the maximum volumes can be reached within mining levels four and five, with volumes of 3.23 m^3 to 9.45 m^3 with respect to the increasing median joint spacings (Sousa et al. 2017). The acquired joint spacings and resulting final block volumes in mining level one indicating that the resulting block volumes are not suitable for the exploitation of dimension blocks. Only block 4 with the highest final block volume of 0.45 m^3 ($V(4)_1 = 0.5 \times 0.95 \times 0.95 \text{ m}$) is nearly suitable for minimum block volumes ($V_{\text{minimum}} = 0.4 \text{ m}^3 = 0.4 \times 1 \times 1 \text{ m}$) according to (Singewald 1992). All final block volumes in the lower excavation levels, except block two and three in mining levels two and three, fulfill the minimum requirements for block volumes and especially mining levels four and five are showing excellent quality of blocks. The assessment of the block volume is made assuming that all the joint sets are present in the quarry. This is not true, the joints are not always continuous therefore, in some areas only one or two joint sets are present consequently the extracted blocks will have higher volumes.

Two 3D-BlockExpert models, one in mining level five and one in mining level four were studied in the Granitos Ribeiro quarry (Fig. 21). The first modeled block is in the fifth mining level with edge lengths of 2.1 m in the X-direction, 7.8 m in Y-direction, 9 m in Z-direction, and a total volume of 147.42 m^3 . The 2.1 m in X-direction was defined by

Fig. 16 Horizontal joint spacing in different mining levels. Left picture with mining levels two to five using an image from the 3D model, which was computed by the images of a drone. Right picture is showing mining level one. Black lines indicating joint traces on the quarrying walls

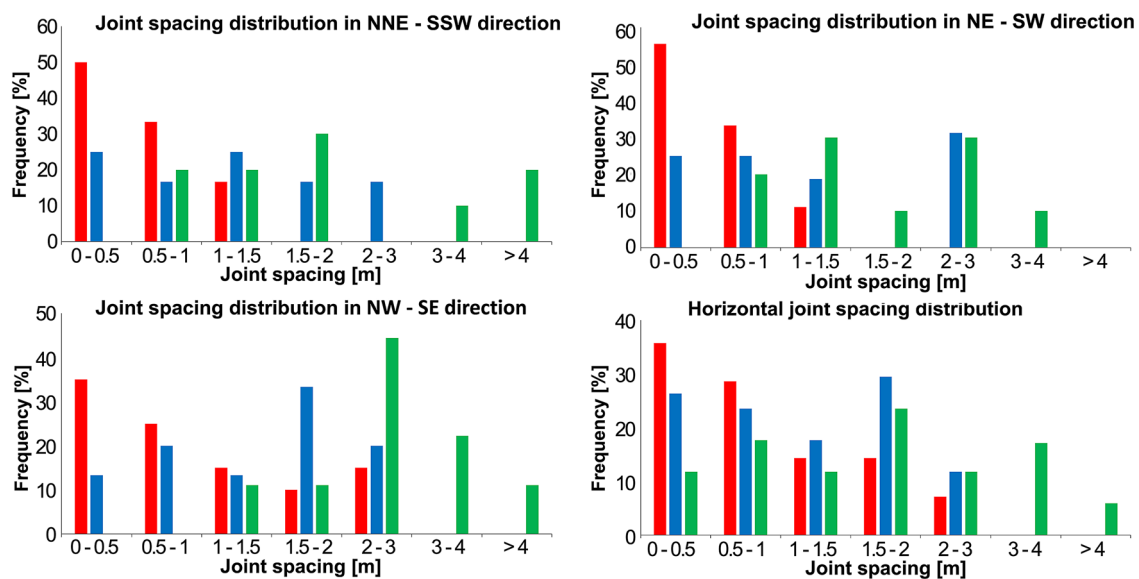
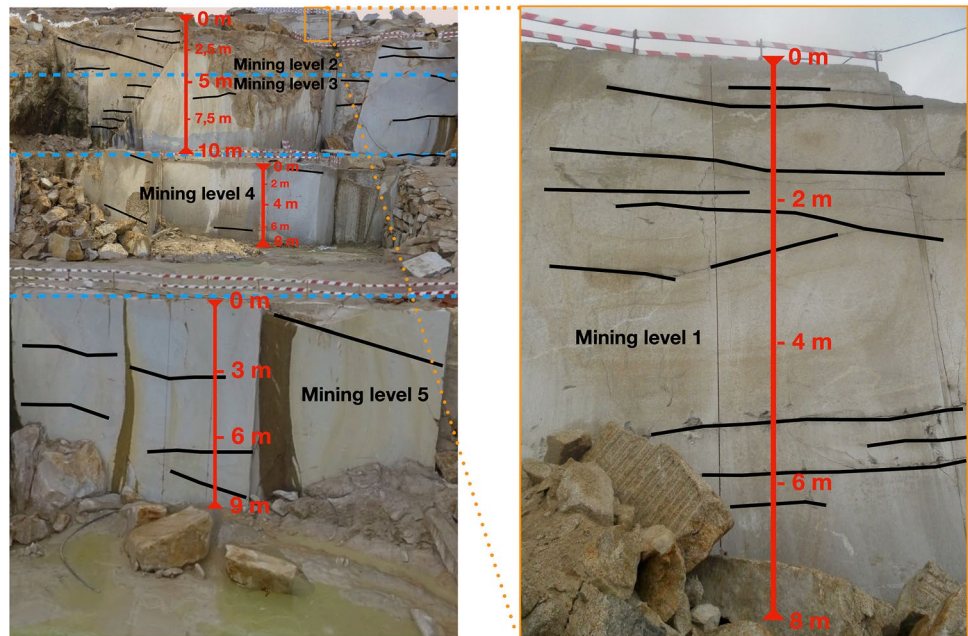


Fig. 17 Joint spacing distribution of the identified three main vertical and horizontal joint sets (red—mining level 1; blue—mining levels 2 and 3; green—mining levels 4 and 5)

the cutting pattern in the quarry. In total six joints were identified, which can be separated in three joint sets. One joint set is vertical and has a spacing of 5 m and is striking N–S. Another joint set is sub-vertical, has a spacing of around 2.5 m and is NE–SW orientated. The last joint set is sub-horizontal and has a spacing of 3 m. The joint planes cover up to 15% of the raw block volume. The wall in X-direction is due to the sawed nature of the quarry wall. The raw block was divided into 6 × 1.5 m slabs in Z-direction afterwards to identify in-situ blocks. The surface of the joints (black

color) represent waste and cannot be used for the extraction of dimensional stones. The raw block was separated in Z-direction into six slabs with a height of 1.5 m. In the final step, the size of the in-situ blocks were set with the typical sizes of 2 × 1.5 × 1.5 m, 2 × 0.75 × 1.5 m, 2 × 1 × 1.5 m, and 1 × 1 × 1.5 m. Proceeding from this assumption, 16 in-situ blocks with a total volume of 35.25 m³ can be extracted, which makes 24% of the total volume of the raw block.

The second raw block was studied in the fourth mining level and is in the same direction as the raw block before



Fig. 18 North facing view of all mining levels with the identified vertical main joint sets. The orange surfaces indicating the NW–SE joint set, the purple surfaces the NE–SW joint set and the green surfaces the NNE–SSW joint set

(Fig. 21). With its edge lengths of 9.7 m in X-direction, 8 m in Y-direction, and 7.7 m in Z-direction. The total volume (597.5 m³) is four times bigger than the previous raw block. The joint planes cover up to 10% of the raw block volume and are defined by a total of ten joints. In this block, more joint sets can be identified. The orthogonal joint sets, striking NE–SW and NW–SE (with a joint spacing of 2 m) are showing up. The N–E to NNE–SSW (with a joint spacing of 1 m) can be also recognized. Again, the raw block is divided by a sub-horizontal plane in the lower to the middle part of the block. In this 3D-BlockExpert model, the raw block was separated into five slabs, with a height of 1.5 m in Z-direction. The size of the in-situ blocks was chosen with following dimensions: 4 × 1.5 × 1.5 m, 2 × 1 × 1.5 m, and 1 × 1 × 1.5 m. In an ideal case, six blocks with a volume of each 9 m³, 24 blocks with a volume of each 3 m³ and 15 blocks with a volume of each 1.5 m³ can be extracted.

Fig. 19 Four modelled blocks and their maximum volume, resulting from the joint set orientation, the angle between the joint sets and median edge lengths of the joint spacings, from mining level one (Table 4). The angles of the two joints sets in block 4 are orthogonal. The gray frame around the block figures were chosen arbitrarily and are not rectangular

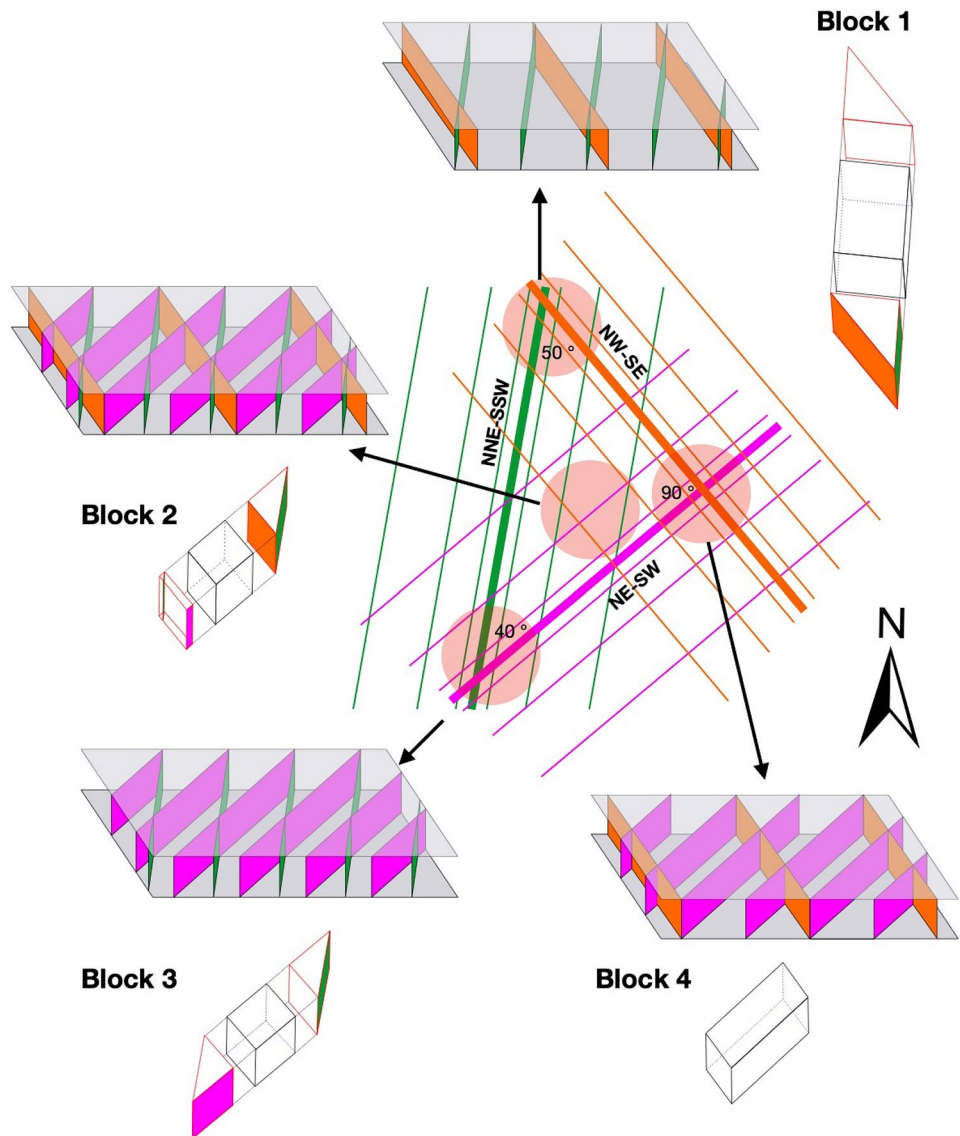
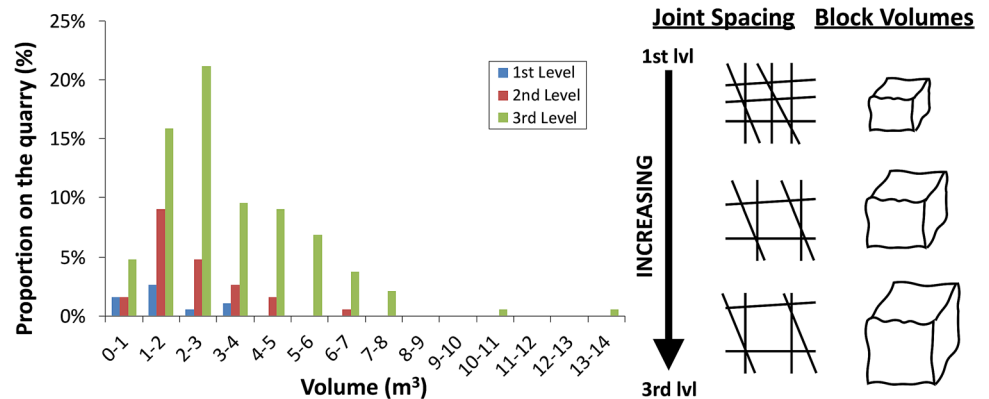


Table 4 Resulting block volumes in the observed mining levels, respecting the median spacing of the joint sets and the resulting geometry

Block	1. mining level				2. & 3. mining levels				4. & 5. mining levels			
	1	2	3	4	1	2	3	4	1	2	3	4
Final block volume (m ³)	0.39	0.09	0.09	0.45	1.8	0.68	0.68	2.46	8.06	3.23	3.23	9.45
Waste (m ³)	0.20	0.28	0.28	0	1.49	2.02	2.02	0	6.04	6.57	6.57	0
Total volume (m ³)	0.59	0.37	0.37	0.45	3.29	2.7	2.7	2.46	14.10	9.80	9.80	9.45
Lost volume (%)	33.8	76.6	76.6	0	45.2	74.9	74.9	0	42.85	67.03	67.03	0

Fig. 20 Extracted volumes in the Granitos Ribeiro quarry during production in 2013 (Sousa et al. 2017)

Overall, these blocks correspond to a total volume of 148.5 m³, which is about 25% of the total volume of the original raw block and comparable to the previous yield in the fifth mining level.

According to the Granitos Ribeiro owners, 10,380 m³ of granite was extracted in the year 2016 and a total of 2700 m³ were used for dimensional blocks. Therefore, the annual profit was around 26%, which is comparable to the calculated volumes with 3D-BlockExpert. This is true because exploitation works during 2016 happens in the deepest less fractured were the modelled blocks were located. However, such relationships must always consider the progress of the quarry. Large quarry like the Granitos Ribeiro quarry have areas with different fracturing pattern and joint density, consequently with variable yield. The quarry yield assessed from the modelling of a single raw block has only an indicative result.

Limestone quarries

In total, five limestone quarries were studied in several field surveys during April 2018 (Fig. 22). All of them are located in the Jurassic limestone massif, known as Maciço Calcário Estremenho (MCE). The company Solancis is extracting and processing dimension stones in several quarries and the following were selected: Codorneiro, Portela 8, Vale da Moita, Vale da Louceira and Cheira Pia do Zé Gomes. The quarries Vale de Moita and Vale da Louceira are located in the west flanks of the Candeeiros Hill, which is one of the elevated

morphostructures in the limestone massif (Carvalho et al. 2018). The Portela 8 quarry is located at the edge of the Candeeiros Hill. The quarry located most to the west is the Codorneiro quarry, which is situated next to the Alcobaca Depression. The last quarry, Cheira Pia do Zé Gomes is in the Santo António Plateau. The Mendiga Depression, a fault-related elongated depression separates the Candeeiros Hill from Santo António Plateau (Carvalho et al. 2018).

The jointing observed in the studied quarries show the WNW–ESE joint set as predominant, with differences among the quarries. These differences are related with the tectonic evolution of this area as point out by Carvalho (2013, 2018), mentioning the following main joint sets: NNE–SSW, WSW–ENE, WNW–ESE, NW–SE, and NNW–SSE. The joint spacing values are more frequent in the range 1–2 m, with low values higher than 4 m. The values of the joint spacing denote the possibility of extracting large blocks in some area of the quarries. These data were obtained in the ongoing extraction areas, the less fractured of the quarries. Therefore, the values of the joint spacing are higher than those mentioned by Carvalho (2013) who measured the more fractured areas.

Case study: Cheira Pia do Zé Gomes quarry

Ornamental stones are exploited in the Cheira Pia do Zé Gomes quarry, which belongs to one of six major exploitation sites in the MCE (Carvalho et al. 2018), the so called

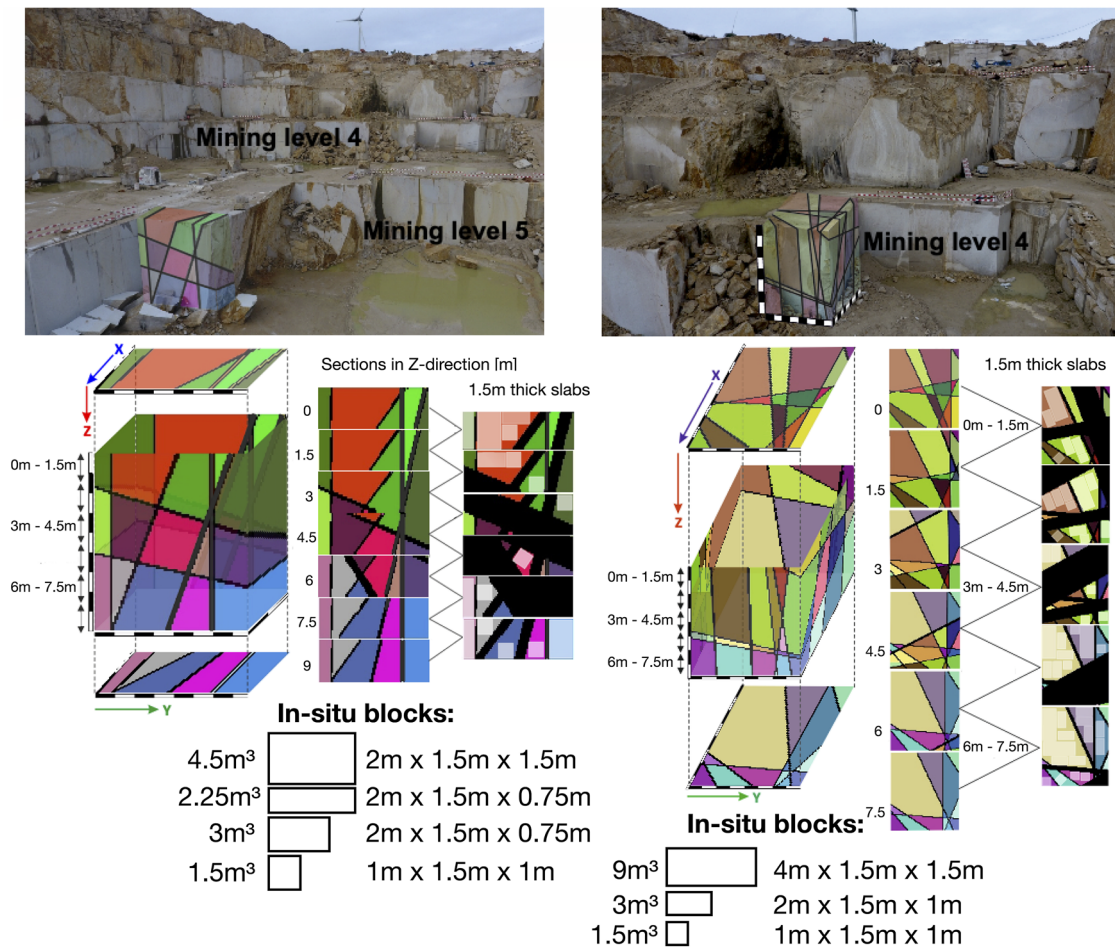


Fig. 21 In-situ block identification with the help of the software: 3D-BlockExpert. The first raw block (mining level 5) has a total volume of 147.42 m³ and a computed yield of 35.25 m³ (24% of total

volume). The second raw block (mining level 4) has a total volume of 597.5 m³ and a computed yield of 148.5 m³ (25% of total volume)

Pé da Pedreira (Fig. 22). The quarry is located 16 km NE of Rio Maior, near Alcanede. Locally the individual strata can be 3–6-m thick and the maximum thickness of the Pé da Pedreira unit can reach 40 m. The ornamental variety Moca Creme (Relvinha) is extracted by the Solancis company, which is a coarse-grained limestone with well-marked laminations (Carvalho et al. 2018). In general, the beige limestone is compact, with a density of 2.39 kg/m³ and an open porosity of 10.4% (Fig. 23). The varieties are showing an alignment of small size grains and fossils (Solancis 2013).

In the Cheira Pia do Zé Gomes quarry, two orthogonal joint system could be identified, which are sub-vertical to vertical and orientated in NNW–SSE and ENE–WSW direction (Figs. 24 and 25). The sub-horizontal bedding planes dipping with an angle of 22° to SSW. Similar results can be found in the work from Carvalho et al. 2014 showing the NNW–SSE and ENE–WSW striking joint sets in the Pé da Pedreira unit. These studied joints can be related to the major families of faults in the MCE, which are NNE–SSW,

NW–SE and NE–SW orientated. The faults were active during the opening phase of the Atlantic ocean (extension) and reactivated during the Alpine compression (strike-slip) (Carvalho 2018).

The joint spacing was measured for both mining levels and the following results representing the median spacing of the entire quarry by measurements made in the field and aerial survey. The vertical joints in the Cheira Pia do Zé Gomes quarry have a median spacing of 1.25 m in NNW–SSE direction and varying from 0.7 to 1.6 m (Table 5). The spacing of the vertical joints in ENE–WSW direction have a median of 1 m, reaching a maximum of 3.3 m. The median horizontal joint spacing is 1.8 m and varying between 0.7 m and 3.3 m (Fig. 26). In general, the NNW–SSE joint set is showing a high-joint spacing distribution in the range of 0.5–1 m (Fig. 26). Around 90% of the ENE–WSW joint set is distributed in the range of 0.5–1.5 m. About 30% of the horizontal bedding planes are distributed in range of 2–3 m.

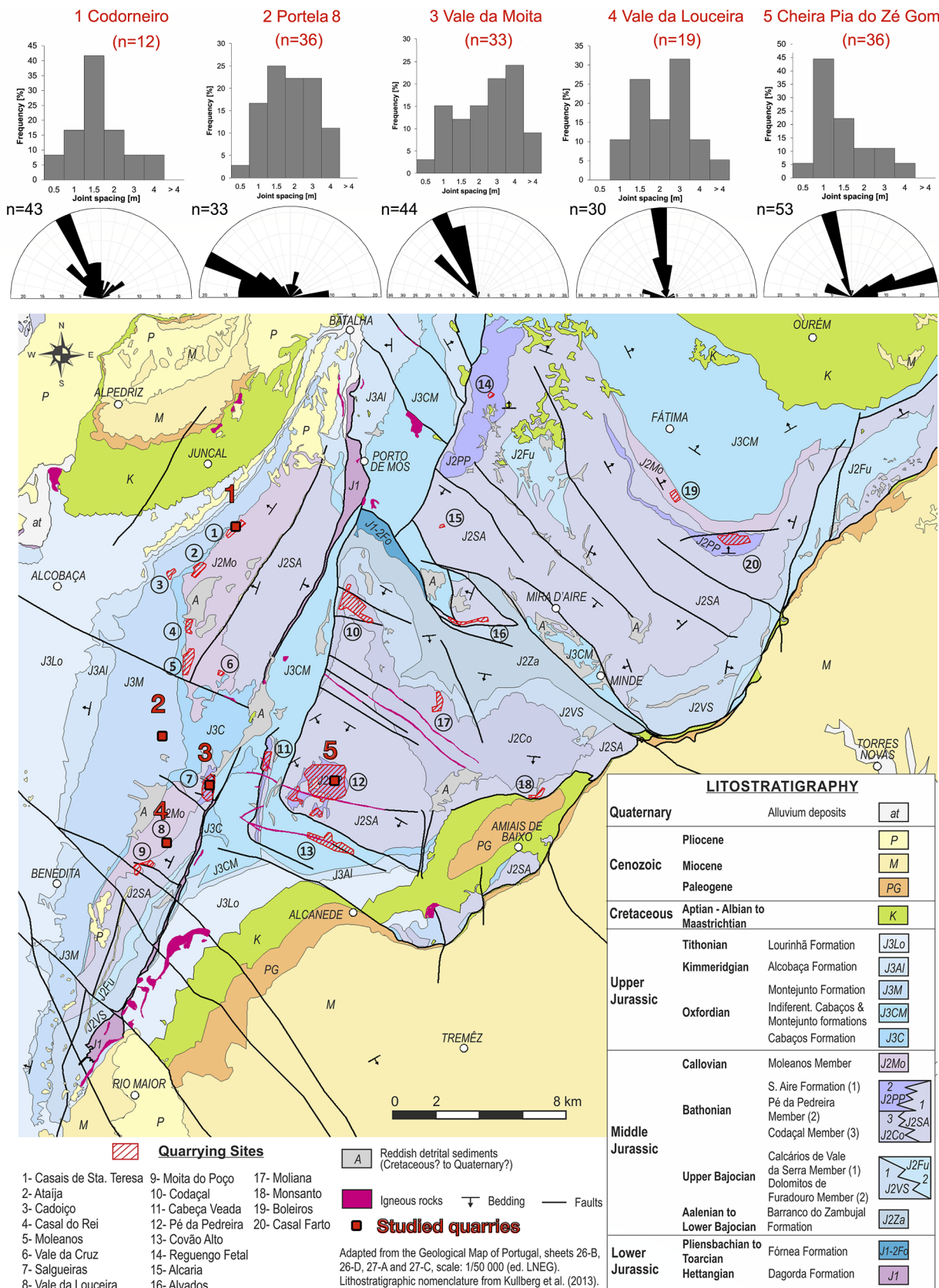
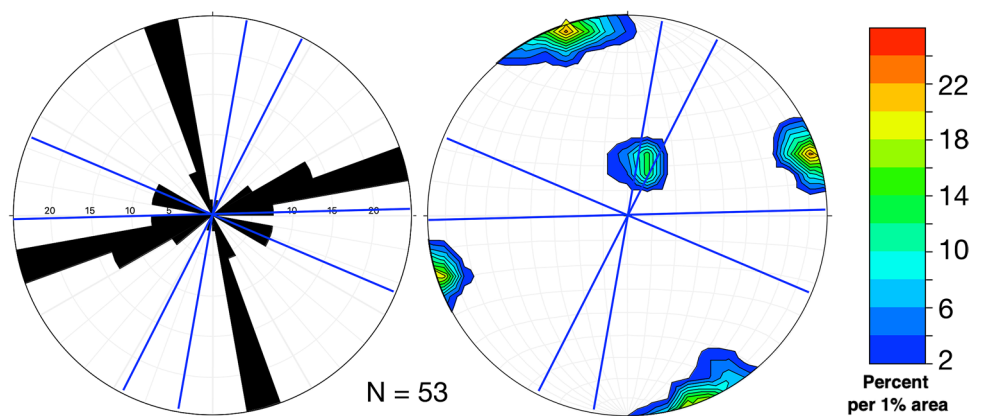


Fig. 22 Lithostratigraphic map of the MCE with locations (red numbers: 1–5), joint spacings and rose diagrams of the joints in the studied quarries (map modified after Carvalho et al. 2018)



Fig. 23 Some of limestone varieties extracted in the Cheira Pia do Zé Gomes and Vale da Moita quarries

Fig. 24 Rose diagram of the two identified vertical fracture directions and stereographic projection of the density distribution of pole points for measured joints in Cheira Pia do Zé Gomes quarry. Blue lines indicating the strike direction of the sawed quarry faces (Schmidt net, lower hemisphere)



The joint space data obtained by aerial survey are higher than the field data. The median spacing of the NNW–SSE striking joint set is with 3.13 m, 2.5 times higher than the data measured by hand in the field. The second joint spacing also has increased from 1 to 2.34 m. The horizontal joint spacing measured by aerial surveys slightly increased from 1.8 to 1.99 m. In this case, the aerial data obtained from aerial photography cannot give a clear depict of the fracturing pattern and erroneous conclusions and decisions will be achieved is such data were used. Closed and tight vertical joints are hardly identified in aerial photos and fracturing data obtained with such techniques must be always checked before drawing definite conclusions. The horizontal joints are more easily recognized in the photos.

The two investigated spacings of the vertical joint sets and the additional horizontal spacings (Figs. 26 and 27) were used to compute median block volumes. The vertical NNW–SSE and ENE–WSW joint sets are orthogonal. In total four directions of sawed quarry faces were found, which have following directions: N10°E, N28°E, N68°W, and N88°E (Fig. 25). The N10°E striking quarry faces can be found only in the first mining level. Nearly orthogonal to the previous quarry face a second cutting direction can be found, which is only located in a smaller area in the N of the quarry. The last two quarry faces can be found in the second mining level.

A schematic representation of the fracture systems and bedding plane in Fig. 28 helps to understand the location and the geometry of the in-situ blocks. The maximum block

Fig. 25 Orthophoto and digital surface model (DSM) with the mining levels (L1, L2), mapping of the joint sets and cutting pattern in the Cheira Pia do Zé Gomes quarry

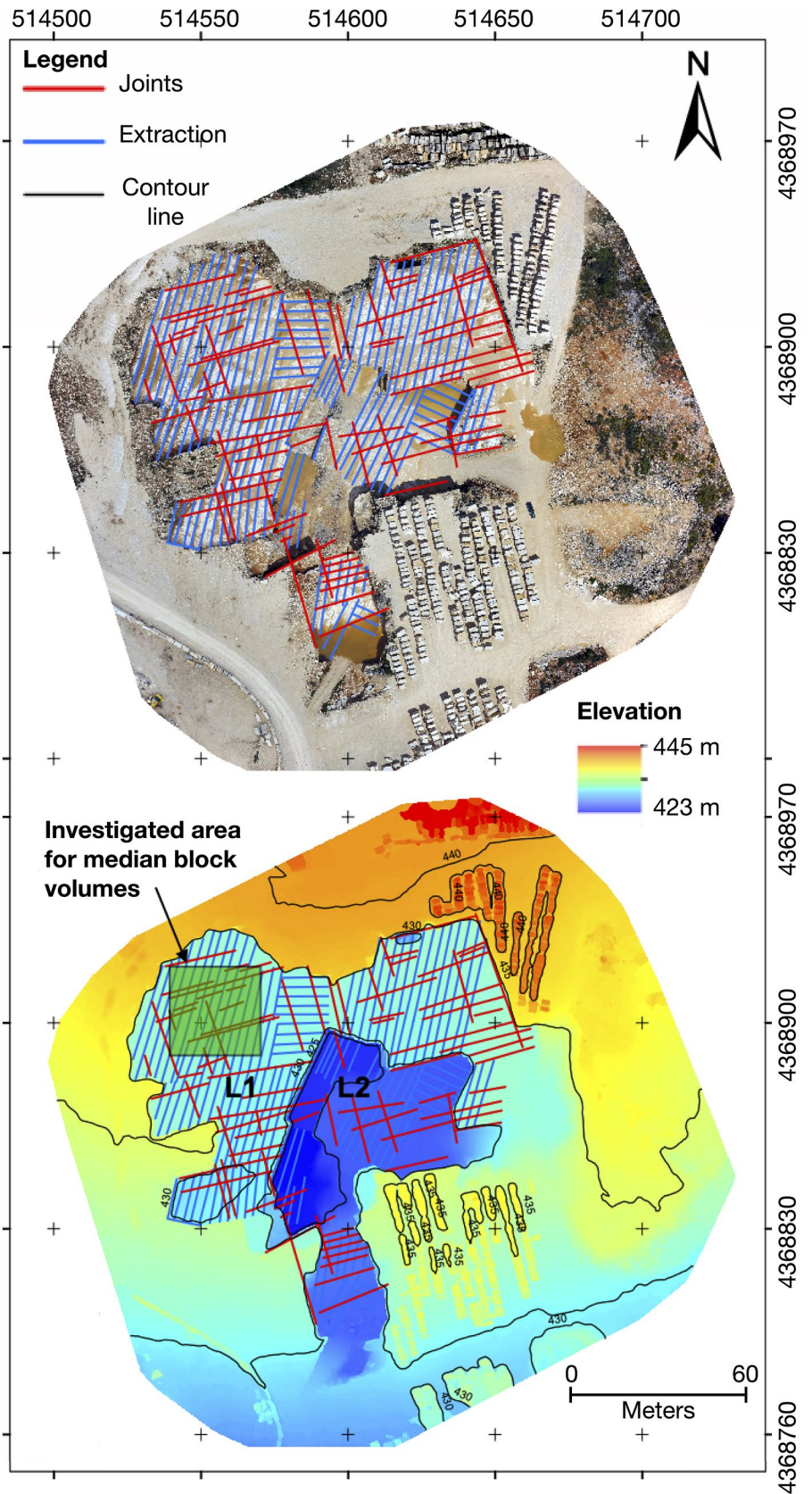


Table 5 Median and mean joint spacing in the Cheira Pia do Zé Gomes quarry from field data and aerial photography

Joint set	Measured by compass			Measured with 3D model		
	NNW–SSE	ENE–WSW	Horizontal	NNW–SSE	ENE–WSW	Horizontal
Median	1.25	1.00	1.80	3.13	2.34	1.99
Mean	1.19	1.31	1.97	4.24	2.51	2.07
n	10	16	10	18	27	14

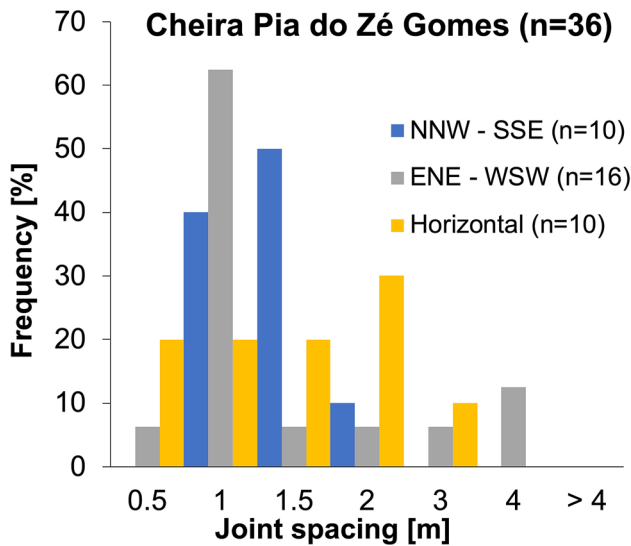


Fig. 26 Joint spacing distribution of the identified two main vertical joint sets and the horizontal bedding plane in the Cheira Pia do Zé Gomes quarry

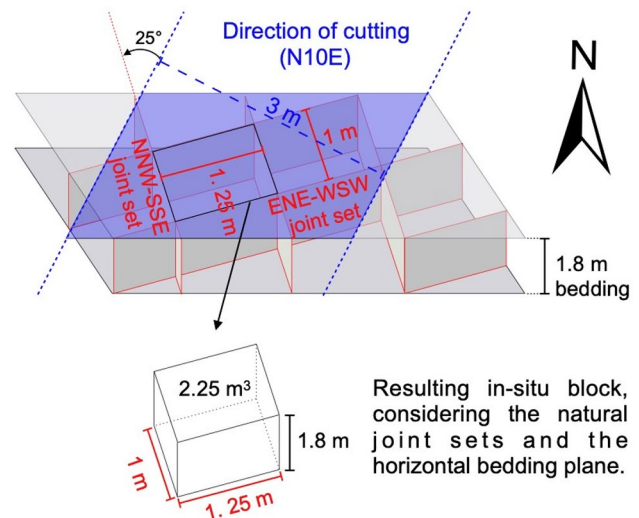


Fig. 28 Schematic sketch of the natural vertical joint sets and bedding plane, respecting the median edge lengths of the joint spacings. The dotted blue lines indicating the orientation of the cutting direction (N10°E)

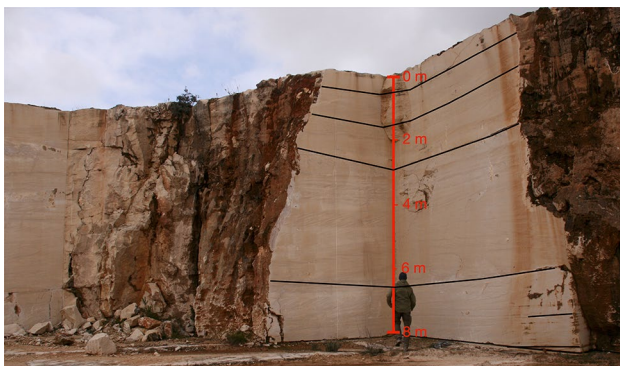


Fig. 27 Horizontal joint spacing in the first mining level, located in the NW part of the Cheira Pia do Zé Gomes quarry

(median joint spacings obtained in the field) has a possible volume of 2.25 m^3 ($VB = 1.25 \times 1 \times 1.8 \text{ m}$), considering the edge lengths of the horizontal bedding plane (1.8 m) and the vertical joints, NNW–SSE (1.25 m) and ENE–WSW (1 m). Using the data from the aerial survey, a volume of 14.58 m^3 was computed, considering the edge lengths of the horizontal bedding plane (1.99 m) and the vertical joints,

NNW–SSE (3.13 m) and ENE–WSW (2.34 m). The dotted blue lines indicating the orientation of the cutting direction in the first mining level, located in the north western part of the quarry. The extracted slabs are in average 3 m thick and will be mined in N10°E direction and parallel to the sedimentary lamination. The blue parallelogram has a surface area of 5.44 m^2 and a total volume of 9.8 m^3 . The schematic sketch is showing that with the current cutting pattern only two raw blocks ($2 \times 2.25 \text{ m}^3$), resulting from the natural fractures and bedding plane, can be extracted. This means that a volume of around 54% will be lost and only 46% can be used as a raw block.

To minimize non-economic blocks and increase quarry production, the cutting direction must be changed, using natural fractures as limits of the final blocks (Yarahmadi et al. 2018). The cutting direction should be aligned to the NNW–SSE (N15°W) striking joint set, because the median joint spacing is slightly bigger (1.25 m) than the joint spacing of the ENE–WSW striking joint set. This means, the cutting pattern must be rotated by approximately 25°, from N10°E to N15°W (Fig. 28), by taking the two main joint sets into consideration. With this approach and adjusting the thickness of the extracted slabs to the median spacing

of the NNW–SSE striking joint sets, a median block with the computed volume of 2.25 m³ can be extracted without any major loss of volume in the investigated area of the first mining level (Fig. 25). This approach can be used for different areas in the quarry, if the fracturing pattern changes.

With the help of the 3D-Model, the dimension of 20 already extracted blocks in the south and central part of the quarry were measured, with following average edge lengths: 2.5 m (length) × 1.21 m (width) × 1.05 m (height). The resulting mean block has a volume of 3.18 m³, which has a higher volume of 0.93 m³ than the computed median block volume (2.25 m³) from above. If we compare these dimensions from the extracted blocks with the mean joint spacings (Table 5), with 1.31 m (ENE–WSW) × 1.19 m (NNW–SSE) × 1.97 m (horizontal bedding) and a total volume of 3.07 m³, then the block volumes are nearly similar.

Case study: Vale da Moita quarry

The Vale da Moita quarry is located 15 km NNE of Rio Maior and belongs to the Candeeiros Hill Formation, where outcrops of the Pé da Pedreira Member also can be found. The fine to medium-grained and biolithoclastic limestone is exploited at the Portela das Salgueiras site (Carvalho et al. 2014). The Pé da Pedreira Member in this area has a total thickness of 100 m. The limestones are light-cream, cut parallel to the sedimentary lamination and the ornamental variety is known as Semi Rijo Salgueiras (Carvalho et al. 2014). The Solancis company extracting eight varieties in the Vale da Moital quarry: Branco Artico, Branco do Mar, Branco Imperial, Branco Moon, Branco Oriental, Branco Snow, Branco Real and Creme Real (Fig. 23). In general, the limestones are of compact appearance, with a density of 2.2–2.3 kg/m³ and an open porosity of 14–18%. The varieties are showing fine to medium size brownish grains and fossils (Solancis 2013).

Two joint sets in Vale da Moita quarry were identified by measurements in the field. The more dominant joint set is

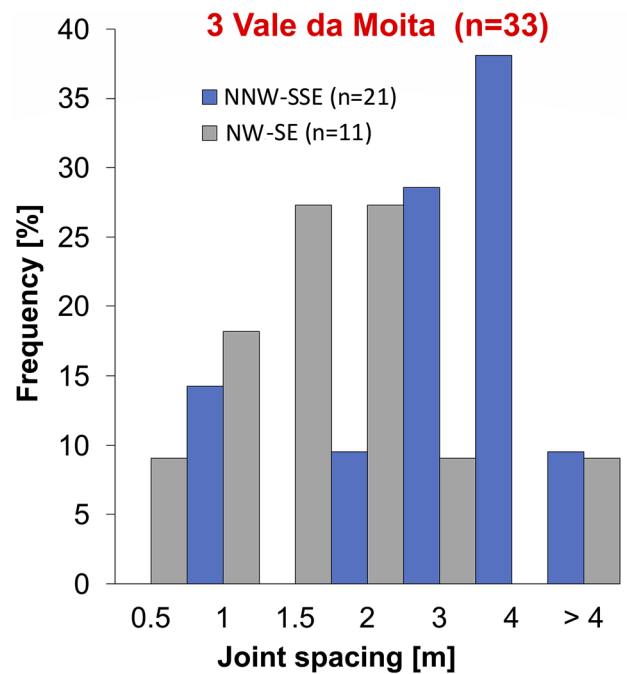


Fig. 30 Joint spacing distribution of the identified main vertical joint sets in the Vale da Moita quarry

striking NNW–SSE and the second one in NW–SE direction, with an acute angle of at least 20–25° (Fig. 29). Both joint sets are sub-vertical to vertical. The stratification is dipping with an angle of 14° to the ENE. The quarry is located near the Rio Maior-Porto de Mós Fault.

The joint spacing was measured in all mining levels by compass and by studying the orthophoto, which is a result of the drone images. The following results representing the median spacing of the vertical joint sets through the entire quarry. The vertical joints set striking in NNW–SSE direction have a median spacing of 3 m, varying from 0.65 to 7.4 m and are showing a high-joint distribution in the range of 3–4 m (Fig. 30). The median spacing of the NW–SE joints

Fig. 29 Rose diagram and stereographic projection of the density distribution of pole points for measured joints and bedding planes in the Vale da Moita quarry. Purple lines indicating strike direction of sawed quarry faces (Schmidt net, lower hemisphere)

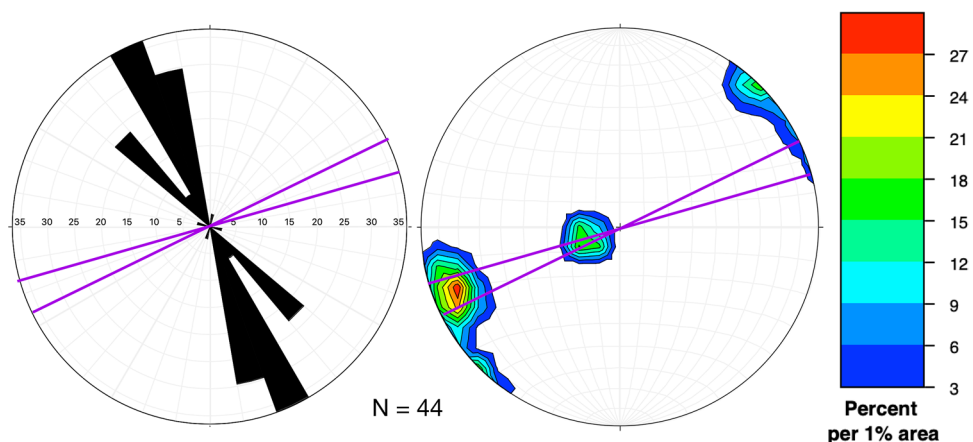
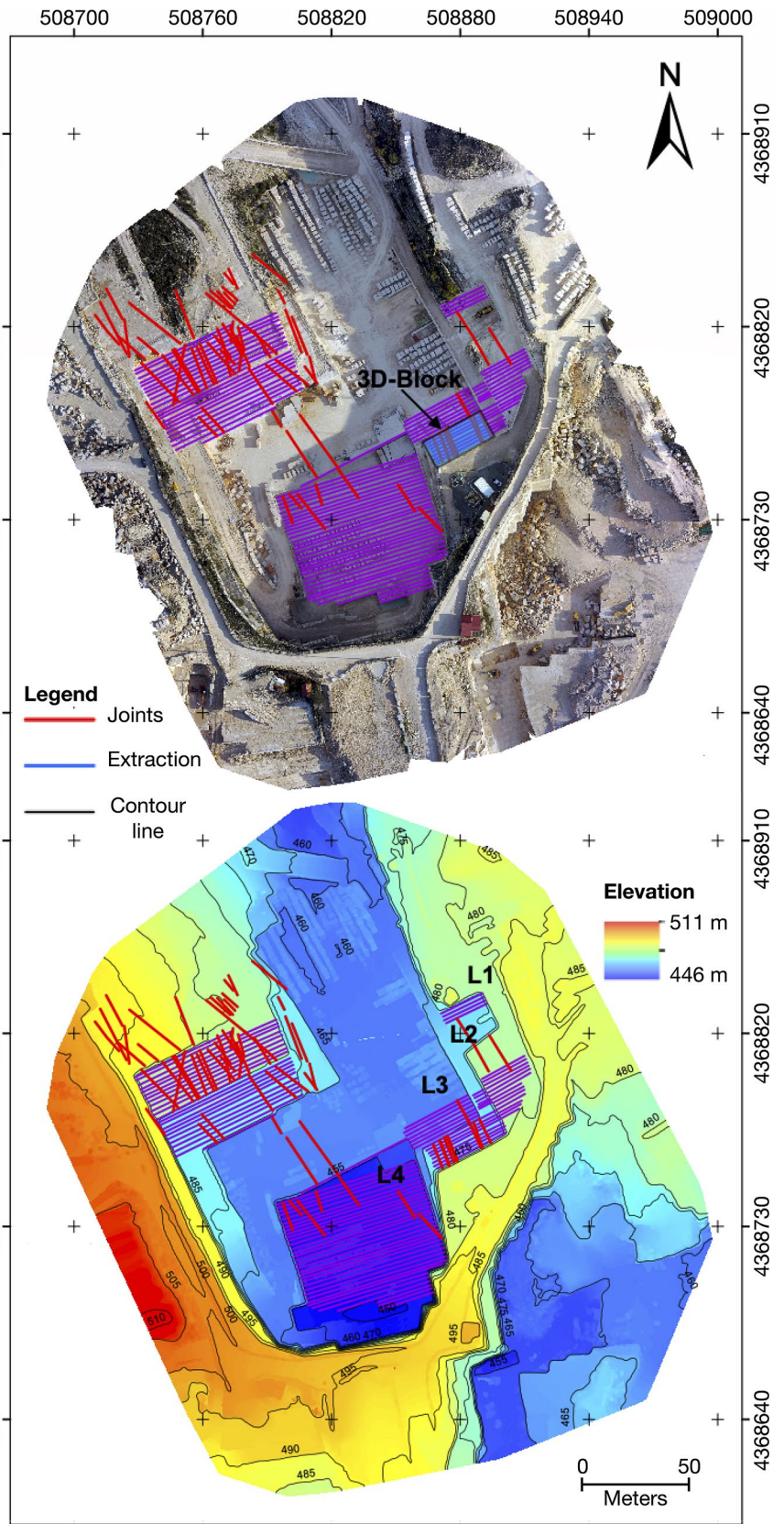


Fig. 31 Orthophoto and digital surface model (DSM), with the mining levels (L1–L4), location of the 3D-BlockExpert Model, mapping of the joint set and cutting pattern in the Vale da Moita quarry



is 1.5 m, varying between 0.5 and 5 m and showing a high-joint spacing distribution in range of 1–2 m. The stratification is not a critical issue in the Vale da Moita limestones and, therefore, the horizontal spacings were not measured. The quarry phases are not oriented along the stratification.

In Fig. 31 it can be seen that a change in the direction of the extracted walls was implemented. The extracted walls in mining levels L1 to L3 are striking N63°E. In mining level L4, the extraction was rotated by 10° to N73°E, which is orthogonal to the main NNW–SSE joint set. A higher distribution of joints can be found within an area located in the NW of the first mining level (L1). The change in the cut direction was probably implemented to increase the extraction of the blocks. This highlights the importance

of a permanent evaluation of the fracturing pattern during the quarry evolution. Only this way will be possible a swift change in the extraction procedures and maximize the extraction.

To identify in-situ blocks in the Vale da Moita quarry, 3D-BockExpert was used in the eastern part of the quarry (Fig. 32). The modeled block is in the second mining level with edge lengths of 8 m in the X-direction, 30.8 m in Y-direction, 7.9 m in Z-direction and a total volume of 1946.6 m³. The 8 m in X-direction was defined by reaching the extraction wall of the second mining level. In total, 12 joints were identified, which are all sub-vertical, striking in NNW–SSE direction and dipping to the ENE. Except for one joint (joint number 6 at 20 m in Y-direction) all joints

Sub-vertical joint sets with resulting in-situ block volumes

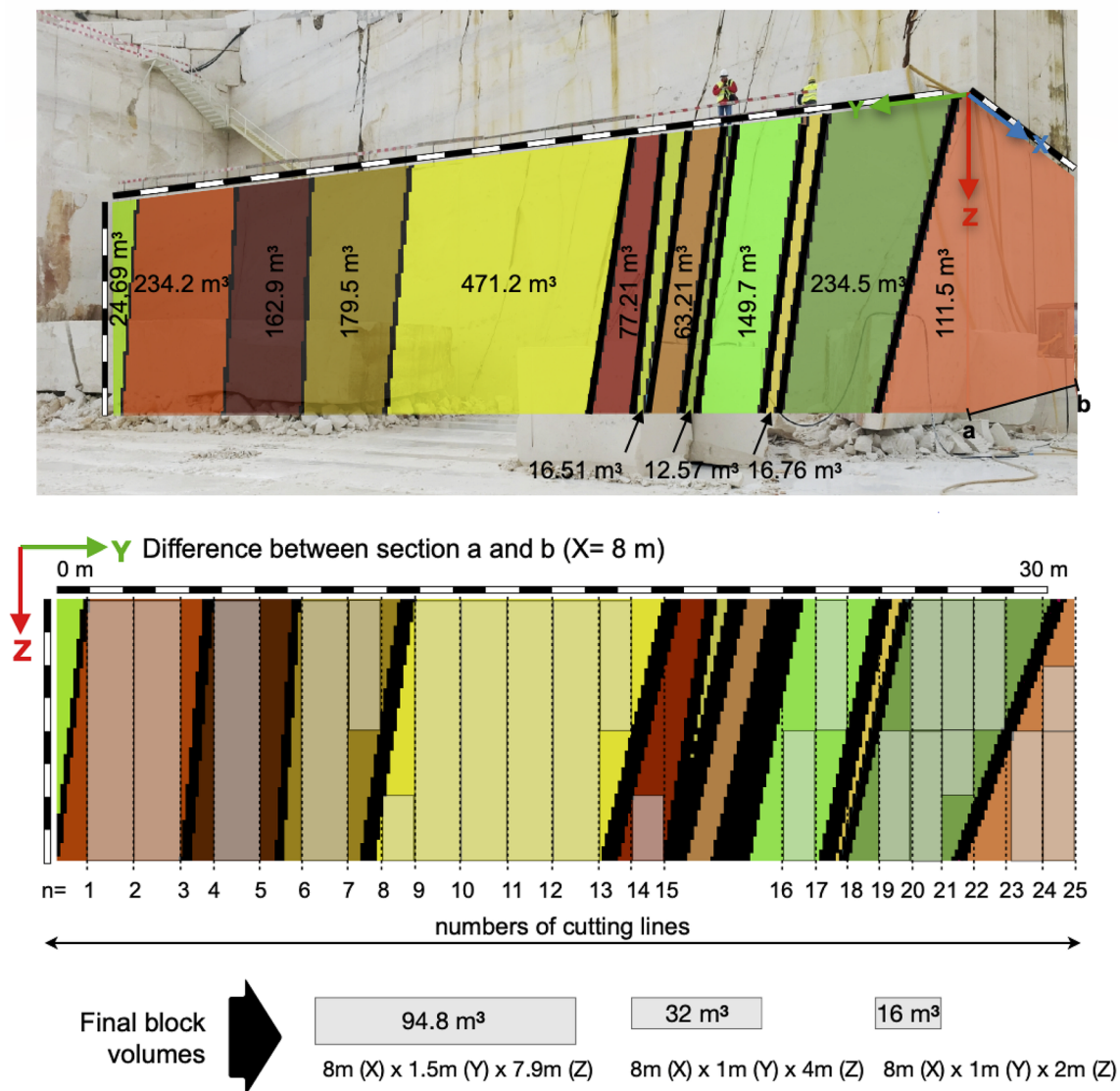


Fig. 32 In-situ block identification with the help of the software: 3D-BockExpert in the Vale da Moita quarry. The raw block from mining level two has a total volume of 1946.6 m³ and is divided by 12 sub-vertical joints into 13 in-situ blocks

are parallel oriented. The NNW–SSE striking vertical joints of the raw block have a median spacing of 2.5 m. The high spacing, ranging from 2.5 to 7.4 m, causing relatively big block volumes in the first 18 m (in Y-direction). The following 5 m, the spacings are narrower, in range of 0.5 to 1.3 m. The vertical joints dividing the raw block with a volume of 1946.6 m³ into 13 separate in-situ blocks. There are no orthogonal joints or horizontal bedding planes, which could divide the raw block and, therefore, the raw block volume was projected 8 m in X-direction (Fig. 31). The resulting three smallest blocks have a volume of 12.57 m³, 16.51 m³, and 16.76 m³, which is together 2.36% of the total volume. There are three more blocks with a volume smaller than 100 m³: 24.69 m³ (1.27%), 63.21 m³ (3.25%), and 77.21 m³ (3.97%). The next bigger blocks have a volume of 111.5 m³ (5.73%), 149.7 m³ (7.69%), 162.9 m³ (8.37%), 179.5 m³ (9.22%), 234.2 m³ (12.03%), and 234.5 m³ (12.05%). The last and biggest block has a volume of 471.2 m³, which is 24.21% of the raw block (1946.6 m³). The joint planes cover a volume of 192.05 m³ and, therefore, 9.87% of the total block volume.

Three sizes for possible in-situ blocks were chosen, resulting from the X-direction of the quarrying walls thickness (8 m), the thickness of the Z-direction (7.9/4/2 m), and a chosen thickness of 1.5 or 1 m in Y-direction, given us following block volumes: 94.8 m³ (8 m (X) × 1.5 m (Y) × 7.9 m (Z)), 32 m³ (8 m (X) × 1 m (Y) × 4 m (Z)), and 16 m³ (8 m (X) × 1 m (Y) × 2 m (Z)). Continuing with this assumption, 8 in-situ blocks (each 94.8 m³) with a volume of 758.4 m³, 11 blocks (each 32 m³) with a volume of 352 m³, and 4 blocks (each 16 m³) with a volume of 64 m³ can be extracted, which means 60.33% of the total raw block volume can be extracted. Overall, these in-situ blocks correspond to a total volume of 1174.4 m³. Considering that already 9.87% of the 1946.6 m³ are covered by the joint planes, leaving a maximum quarrying waste of 29.8%. The results show a high yield in this area of the quarry, which will be lower where the fracturing density increases.

Reducing the number of cuttings and the controlled positioning of the cutting lines was applied in this case study, which was only possible with the knowledge of the location of the joints and the resulting in-situ blocks. In this case, 25 vertical cuttings were made, to obtain the predicted final blocks, mentioned above. Even the remaining blocks can be considered as reasonable smaller blocks for dimensional stones, which means the amount of waste (29.8%) can be reduced furthermore.

Marble quarries

The marble quarries are located in several mining areas of the Estremoz Anticline, as following: Mármoreos Galvão, Bentel and Geopedra quarries near the Estremoz mining

area, the Marmetal quarry in Borba mining area, and finally in south-eastern the António Galego, Granoguli and Cochicho quarries (Fig. 33).

The Estremoz Anticline is affected by the Late Variscan fragile deformation, being identified two sets of arrays, sub-vertical NNE–SSW and ENE–WSW trending conjugated faults and sub-vertical NNW–SSE and NE–SW trending faults (Lopes 2003; Lopes and Martins 2015; Menningen et al 2018). Tectonic overprint (multiple) in the marble quarries can cause lower yields (Mosch 2008). The jointing identified in the studied quarries fall in those families (Fig. 33). However, the jointing in the quarries can be very different from the regional faults according to the local geological setting (Lopes 2003). The joint spacing data show values lower than 4 m, with prevail values in the range 0–1.5 m. The proximity of transversal main faults and dikes near the studied quarries can justify these low values (Carvalho et al 2008).

The Estremoz Marble has high quality, with excellent mechanical–physical properties and an appealing aesthetic. These marbles are fine- to coarse-grained and colored from white to grey with many intermediate varieties. Spots and veins randomly distributed are common and distinctive of these marbles.

Case study: Cochicho Quarry (Pardais Region)

The deepest marble quarry (150 m deep) is located in the Pardais mining area, which is situated in the most south-eastern part of the Estremoz Anticline (Fig. 34). The Cochicho quarry belongs to one of the smaller exploration areas in the Estremoz Anticline, the Pardais area with 229 ha of surface area (Carvalho et al. 2008). The quarrying area is influenced by NE–SW striking transversal faults, longitudinal NW–SE to NNW–SSE oriented shear zone and altered dolerite dikes (Carvalho et al. 2008).

Half of the 21 quarries in the Pardais area are active and still extracting white- and cream-colored fine- to medium-grained marbles. Within these white-colored marbles, grey to dark grey and fine to medium-grained marbles occurring (Carvalho et al. 2008). The whitish varieties with reddish and brownish veins and spots are common. In Fig. 35 some examples of these varieties are presented.

During the fieldwork in 2017 (Klein 2018), 96 natural fracture planes in the mining levels between 68 and 112 m under ground level were measured. Additionally, the data of 17 joint spacings were obtained. Due to the active extraction of blocks, several mining levels could not be accessed and studied.

The density distribution of pole points for the measured joints identifying three groups of joints (Fig. 36) with one dominant joint set striking in NE–SW direction and dipping with an angle of 20–30° to SE. The second joint set is showing a preferred NNW–SSE strike direction, dipping with an

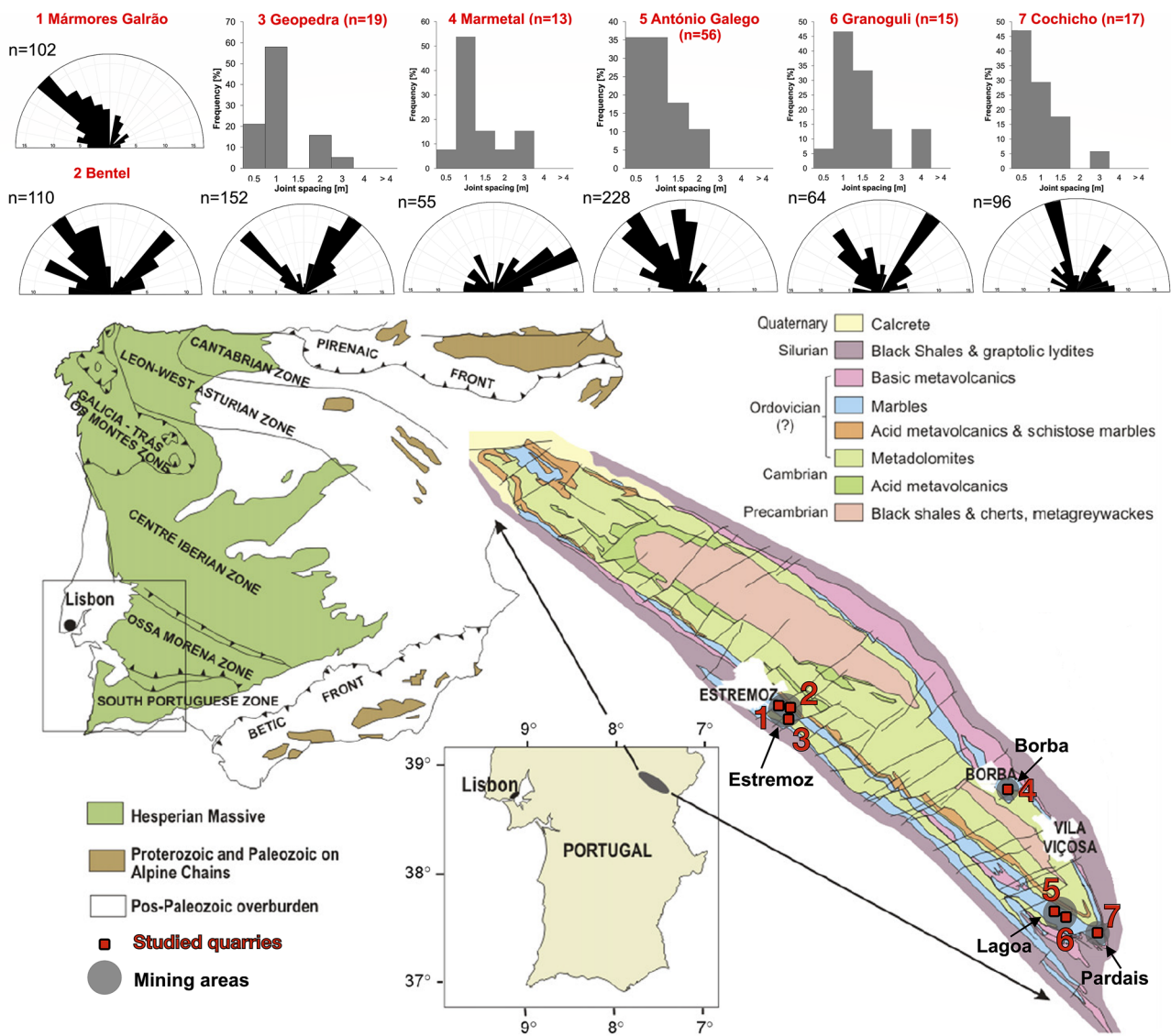


Fig. 33 Lithostratigraphic map and location of the Estremoz Anticline, with indication of the quarry locations (red numbers: 1–7): 1—Mármores Galrão, 2—Bentel, 3—Geopedra, 4—Marmetal, 5—

António Galego, 6—Granoguli, and 7—Cochicho (measured joint spacings and rose diagrams of the identified joints provided by Klein 2018; map modified from Carvalho et al. 2008)

angle of 40° up to 85° to ENE. The last set is nearly vertical and striking in ENE–WSW direction.

Comparing the obtained data from Klein 2018 with the joint data from Carvalho et al. 2008 (Fig. 37) for the entire Pardais mining area, similar orientations of the joint sets are noticeable. Both vertical oriented joints can be related with the measurements from Carvalho et al. 2008. Only the sub-vertical, NE–SW striking joints are more dominant developed within the Cochicho quarry.

The joint spacing was measured for the sub-horizontal N35°E striking joint set, the joints striking in N16°W direction, which are dipping with an angle of 42° and 84° to ENE and the vertical joint set striking to N80°E (Fig. 38). The sub-horizontal joints striking to N35°E and dipping with

an angle of 20° to SE, have a median spacing of 0.98 m and varying from 0.45 m to 1.5 m. The joints striking to N16°W and dipping with an angle of 42° to ENE, have a median spacing of 0.76 m and varying from 0.35 to 1.5 m. The same joint set, striking in N16°W direction, but dipping with an angle of 84° to ENE have a median spacing of 0.63 m and varying from 0.3 to 2.5 m. The last joint set, which is vertical and striking to N80°E, has a median spacing of 0.5 m and varying from 0.3 to 1.3 m. All joint sets are showing a high-joint spacing distribution between 0 and 0.5 m. Around 75% of the N80°E striking joint set is distributed in 0–0.5 m range. The biggest joint spacing, which was only measured one time, is 2.5 m. No joint spacing distribution between 1.5 and 2 m was identified. Only a small amount of joint spacing

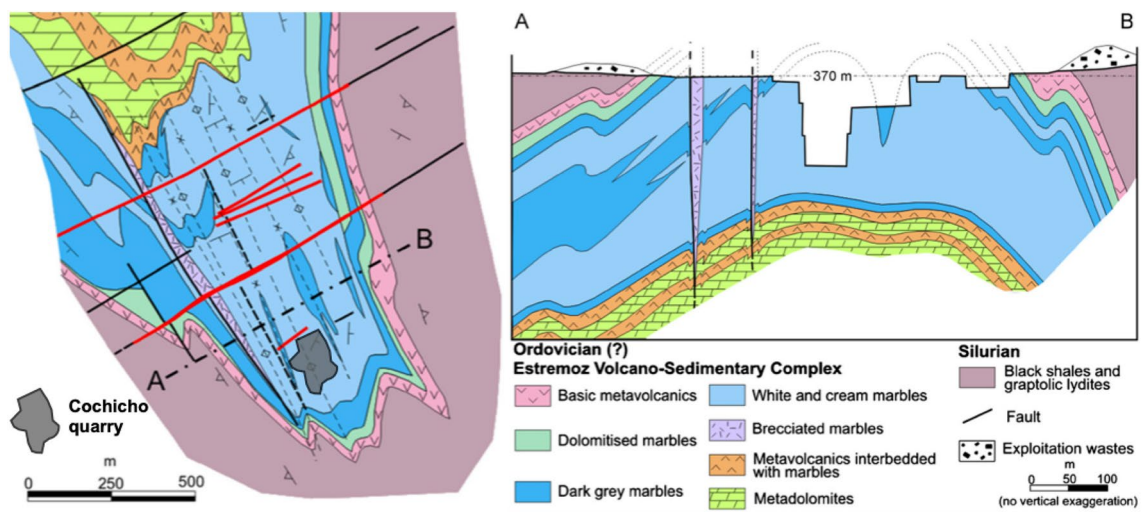


Fig. 34 Geological map and profile of the Pardais region (between point A and B) with the location of the Cochicho quarry (modified after Carvalho et al. 2008)

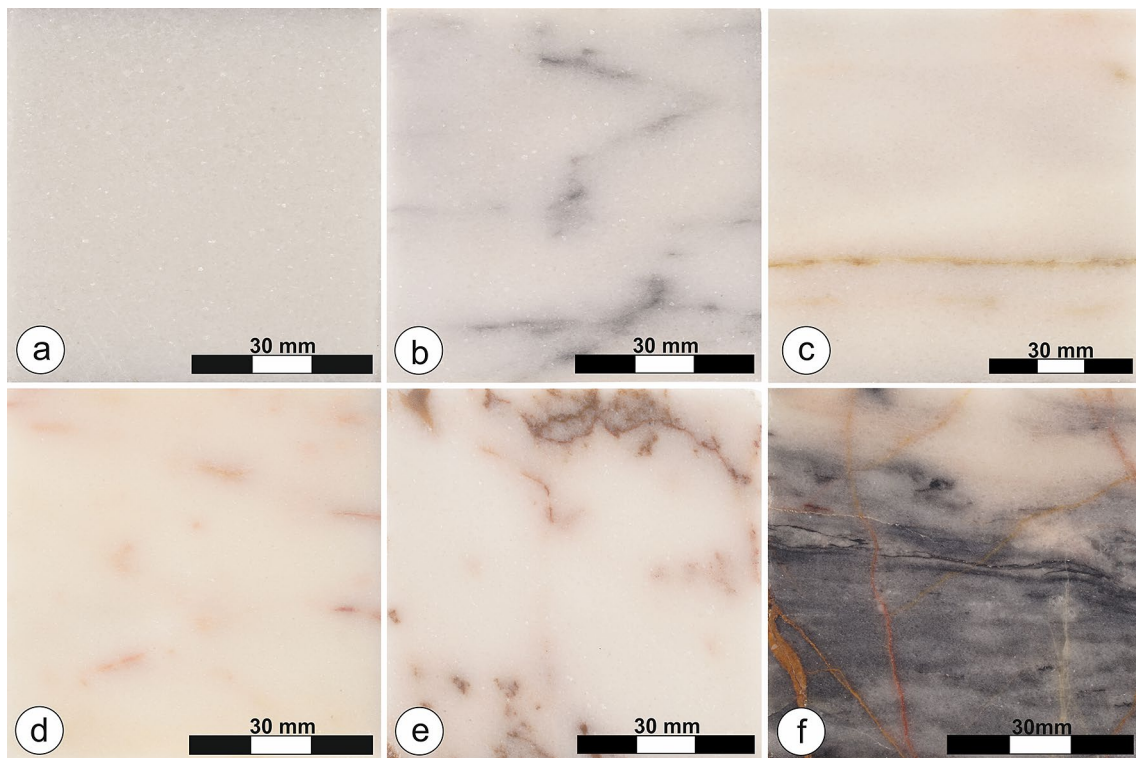


Fig. 35 Macroscopic images of the marble varieties from the Estremoz Anticline: **a** Branco, **b** Branco Vergado, **c** Branco Estremoz, **d** Branco Anilado, **e** Creme Vergado, and **f** Marinela

measurements for each joint set ($n=4-5$) were done, causing the results presented in this study to be quite unreliable.

To identify in-situ blocks in the Cochicho quarry, 3D-BockExpert was applied in the 21st and 22nd mining levels (Fig. 39). The first modeled block is located 107 m

under ground level with edge lengths of 3.1 m in X-direction, 10.1 m in Y-direction, 5.1 m in Z-direction, and a total volume of 162.8 m^3 (Fig. 40).

The resulting three smallest blocks have a volume of 0.82 m^3 , 1.27 m^3 , and 1.39 m^3 , which correspond to 2.14%

Fig. 36 Rose diagram of the identified sub-vertical to vertical and horizontal fracture directions and projection of the density distribution of pole points for measured joints in the Cochicho quarry. Purple lines indicating the strike direction of sawed quarry face in the mining levels 107 m to 112 m under ground level (data from Klein 2018; Schmidt net, lower hemisphere)

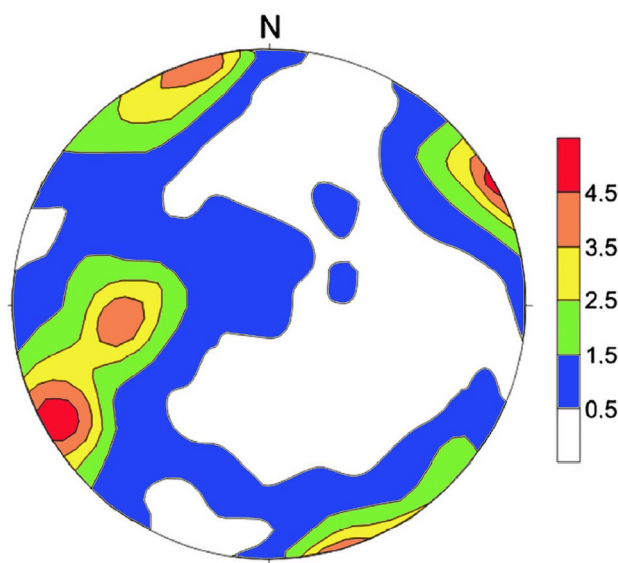
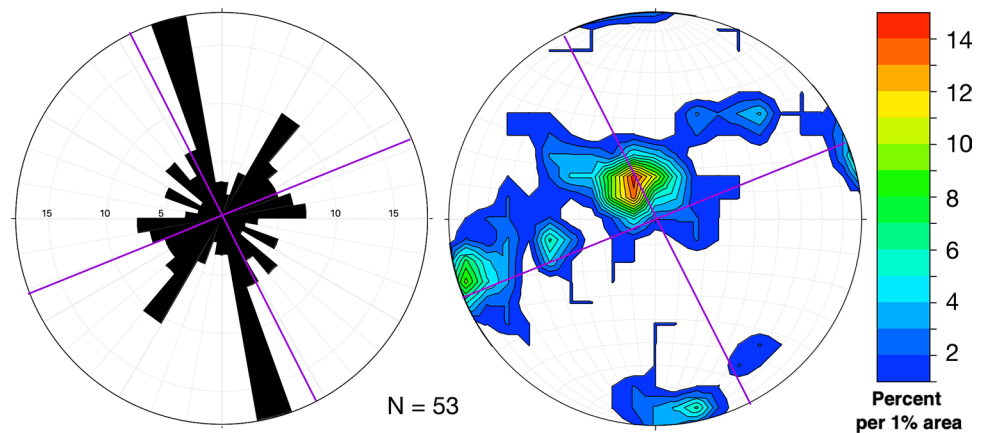


Fig. 37 Stereogram representing the data of the Pardais region (modified after Carvalho et al. 2008; Schmidt net, lower hemisphere)

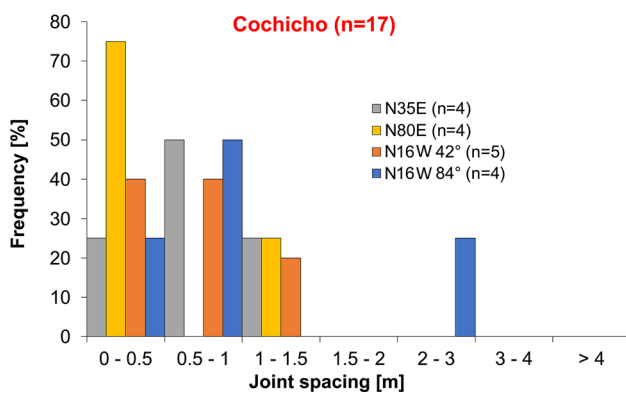


Fig. 38 Joint spacing distribution of the identified main sub-horizontal N35°E striking joint set, the joints striking in N16°W direction and the vertical joint set striking to N80°E (data from Klein 2018)

of the total volume. Seven blocks with a total volume of 50.08 m³, have following block volumes: 2.01 m³, 2.04 m³, 2.94 m³, 5.43 m³, 7.91 m³, 13.78 m³, and 15.98, which is 30.76%. The three biggest blocks: 21.22 m³ (13.29%), 34.46 m³ (21.58%), and 37.38 m³ (23.41%) have a volume of 93.06 m³, which is 57.61% of the raw block (162.8 m³).

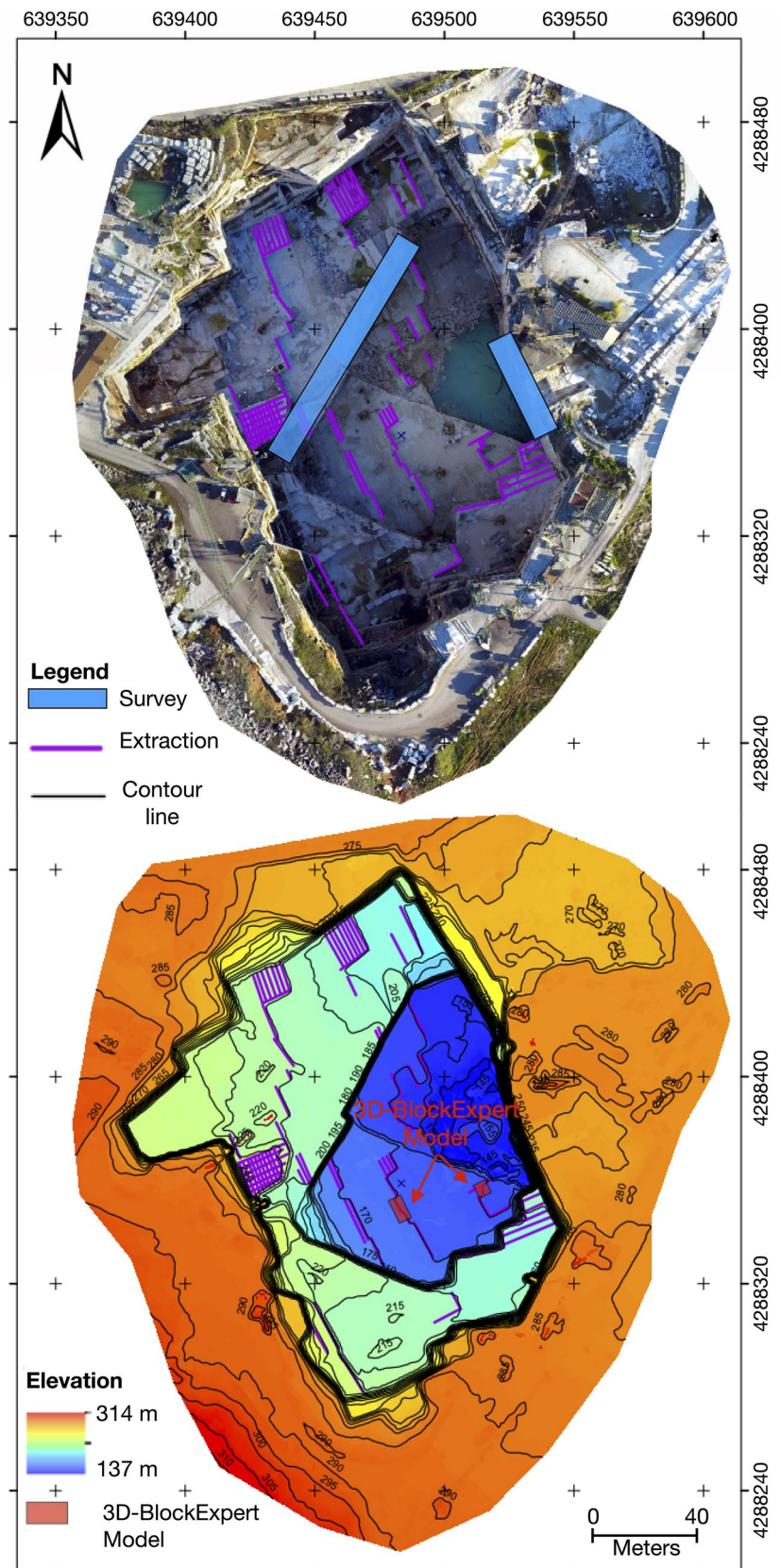
In total, six sizes for possible in-situ blocks were chosen, resulting from the X-direction of the slab thickness (1.5/1.6 m), the thickness of the Y-direction (varying from 1 to 4 m) and a chosen thickness of 0.5 to 2 m in Z-direction. Based on this assumption, following block volumes were computed: 0.75 m³ (1.5 m (X) × 1 m (Y) × 0.5 m (Z)), 0.8 m³ (1.6 m (X) × 1 m (Y) × 0.5 m (Z)), 1.6 m³ (1.6 m (X) × 1 m (Y) × 1 m (Z)), 1.875 m³ (1.5 m (X) × 2.5 m (Y) × 0.5 m (Z)), 3.2 m³ (1.6 m (X) × 2 m (Y) × 1 m (Z)), and 12.8 m³ (1.6 m (X) × 4 m (Y) × 2 m (Z)).

From the raw block (162.8 m³), eight computed in-situ blocks can be extracted. In total three in-situ blocks (each 0.75 m³) with a volume of 2.25 m³ and one block with a volume of 1.875 m³ can be extracted from the first slab, which is 1.5 m wide. From the second slab, one block with a volume of 0.8 m³, one block with a volume of 1.6 m³, one block with a volume of 3.2 m³, and one block with a volume of 12.8 m³ can be extracted (Klein 2018). Counted together, the computed in-situ blocks have a volume of 22.53 m³, which correspond to 13.8% of the total volume of the raw block.

The second modeled block is located 112 m under ground level with edge lengths of 3 m in the X-direction, 3 m in Y-direction, 5 m in Z-direction, and a total volume of 45 m³ (Fig. 41). Five joints, which cover up 5.11% (2.3 m³) of the total volume, divide the raw block into six separated blocks. Again, the raw block was prepared to get cut in 1.5 m thick slabs, parallel to the YZ-surface (Klein 2018).

The resulting six blocks have following volumes: 2.8 m³ (6.2%), 4.3 m³ (9.5%), 5.1 m³ (11.4%), 7.7 m³ (17.2%), 9.2 m³ (17.2%) and the biggest block with a volume of 13.5 m³ (30%).

Fig. 39 Orthophoto and digital surface model (DSM), with locations of the 3D-BlockExpert models, survey windows and mapping of the cutting pattern in the Cochicho quarry. Unfortunately, no joint sets could be mapped by this approach, due to the covered surfaces of the mining levels



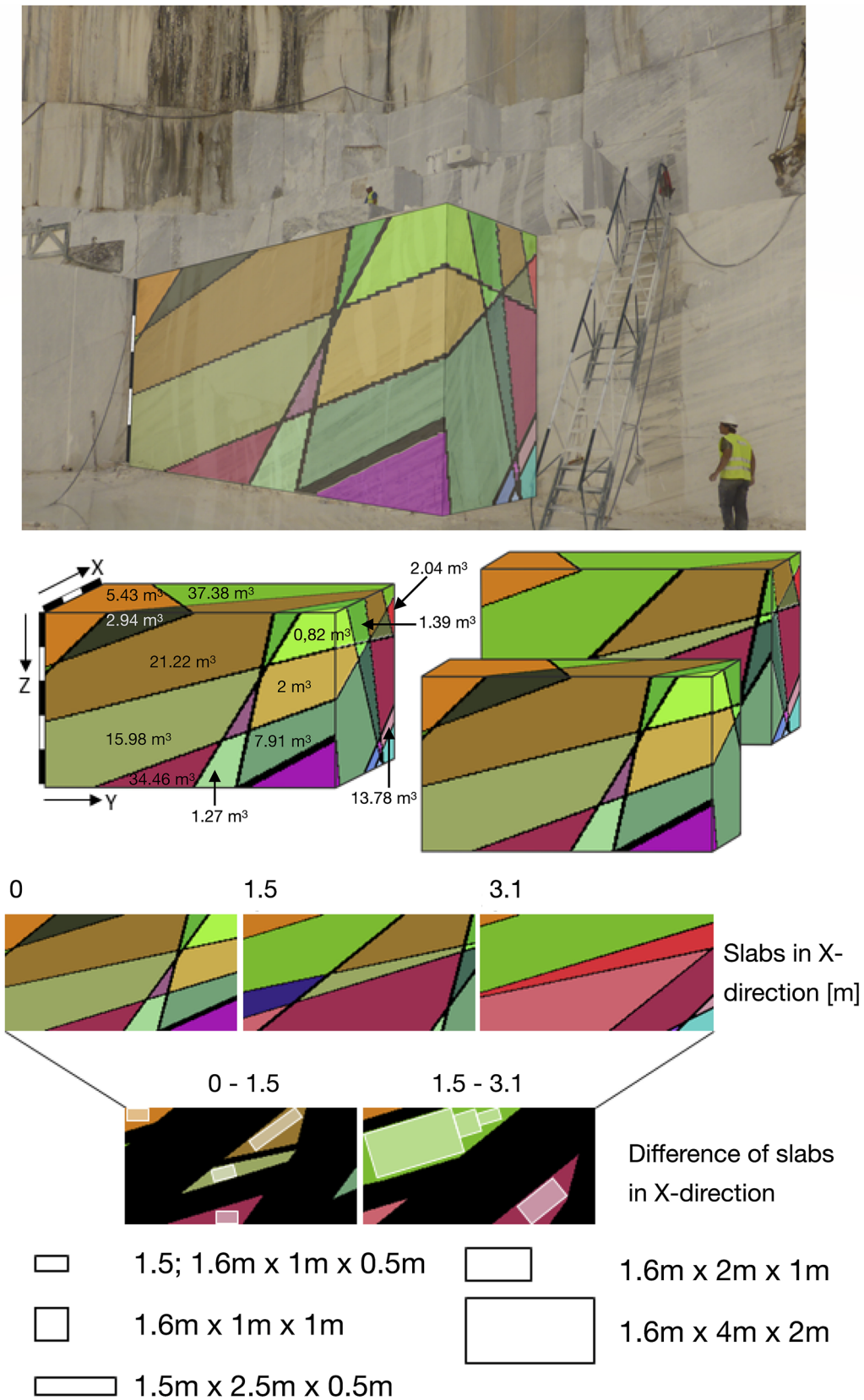


Fig. 40 In-situ block identification with the help of the software: 3D-BlockExpert in the Cochicho quarry. The raw block from the 21st mining level has a total volume of 162.8 m³ and a computed yield of 22.53 m³ (13.8% of total volume) (modified after Klein 2018)

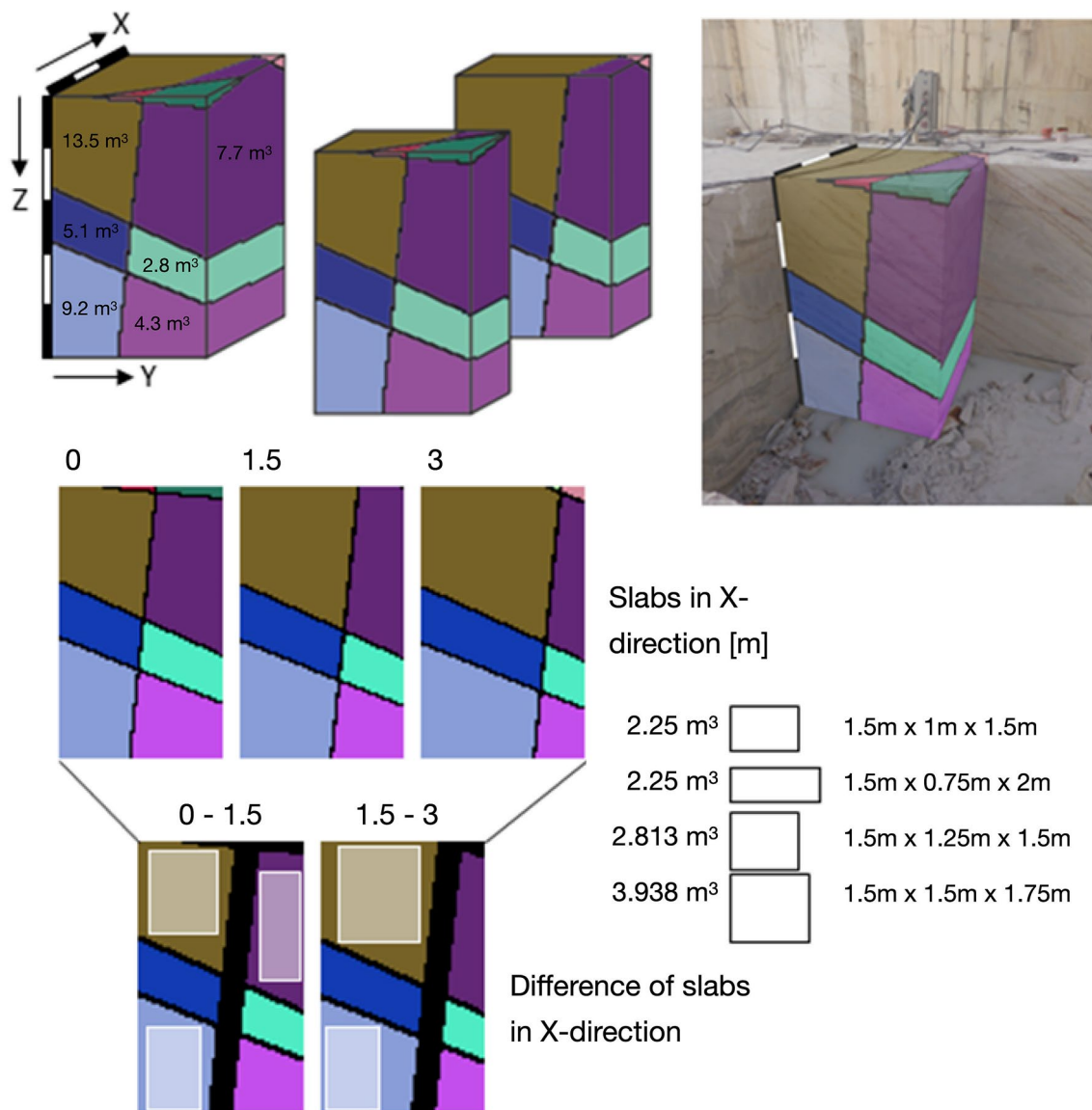


Fig. 41 In-situ block identification with the help of the software: 3D-BlockExpert in the Cochicho quarry. The raw block from the 22nd mining level with a total volume of 45 m³ and a computed yield of 13.5 m³ (30% of total volume) (modified after Klein 2018)

In total, four sizes for possible in-situ blocks were chosen, resulting from the X-direction of the slab thickness (1.5 m), the thickness of the Y-direction (varying from 0.75 to 1.5 m) and a chosen thickness of 1.5 to 2 m in Z-direction. Based on this assumption, following block volumes were computed: 2.25 m³ (1.5 m (X) × 1 m (Y) × 1.5 m (Z)), 2.25 m³ (1.5 m (X) × 0.75 m (Y) × 2 m (Z)), 2.813 m³ (1.5 m (X) × 1.25 m (Y) × 1.5 m (Z)), and 3.938 m³ (1.5 m (X) × 1.5 m (Y) × 1.75 m (Z)).

At the end, five computed in-situ blocks were identified within the raw block. Two in-situ blocks (each 2.25 m³) with a volume of 4.5 m³ and one block with a volume of 2.813 m³ can be extracted from the first slab. A smaller volume of in-situ blocks was identified in the second slab. Here, only

one block with a volume of 2.25 m³ and one block with a volume of 3.938 m³ can be extracted. In total, the computed in-situ blocks correspond to a volume of 13.5 m³, which is 30% of the total volume of the raw block.

A typical yield in the Pardais region was calculated with 20% of the extracted volume (Carvalho et al. 2008). The first modeled block, which is situated in the 21st mining level and 107 m under the ground level, only indicates a yield of 14%, which is below the stated number of Carvalho et al. (2008). One of the reasons, for the lower yield, are the joints with the acute angle to the direction of the extraction. Another possible reason is the slight offset of the measured extraction walls in this area, which are not totally parallel to the NNW–SSE striking joints (Fig. 39). Already a small

adjustment of 10°, could improve the extraction of in-situ blocks.

The second raw block, which is situated in the 22nd mining level and 112 m under the ground level, is showing a yield which is two times higher than the previous raw block from the 21st mining level. The higher yield can be explained by the orientation of the joint surfaces, which are orthogonal to the YZ-surface and, therefore, not that limiting for the chosen orientation of the extraction walls and in-situ blocks (Klein 2018). The raw blocks in the Cochicho quarry are extracted parallel to the NW–SE striking shear zone by wire saws, which correspond to the YZ-surface of the 3D-BlockExpert models. Orthogonal to the NW–SE striking shear zone and parallel to the XZ-surface, faults and dolerite discontinuities take place. Additionally, both vertical joint sets striking parallel to the shear zone and dolerite discontinuities. The direction of mining in the Cochicho quarry is aligned to the natural joint planes and only need small corrections. The second raw block is already showing a higher yield of 30%, resulting from a heterogenic distribution and orientation of the joints.

Like already mentioned above, the Cochicho quarry is the deepest marble quarry in this region and the quarry walls can be up to 150 m high. Structural data can be only obtained at the footwalls of the quarry, like it was the case with the surveys of Klein 2018, or even by rope climbing (Salvini et al. 2017). Both approaches make the surveys unsafe and the data often incomplete to understand the entire area. Data for discontinuities that intersect a defined scan line were collected by Klein 2018 in accessible areas, using traditional scan line mapping techniques (Salvini et al. 2017). Unfortunately, information about the orientation and location of the scanlines are missing and only the result of the measured joint sets of the entire quarry can be presented (Fig. 39). Therefore, a photogrammetric survey was carried out, using UAV technology to obtain high resolution 3D point clouds and DSMs, a helpful tool if integrated with traditional geological surveys to derive important parameters, such as fracture orientation, intensity, density, and size (Salvini et al. 2017). Both orthophotos were computed with the software Pix4D and the function “Orthoplane”, which allows the user to choose any wall of the 3D point cloud to receive a high resolution orthophoto of the desired quarry wall.

In total, four survey windows were applied in the 3D point cloud, to generate detailed orthoplanes of chosen quarrying walls: two at the NW facing wall and two at the NE facing wall. The NW facing wall (Fig. 42), where the survey windows 1 and 2 are located, is situated in the lower part of the Cochicho quarry and includes five extraction levels. The chosen wall is around 30 m deep and 85 m wide. The second quarry wall is facing NE (Fig. 43), which is parallel to the NW–SE striking extraction walls and include survey windows 3 and 4. This wall is special, because it is showing

nearly the entire depth of the Cochicho quarry. The computed orthoplane is 124 m deep, 61 m wide and including 21 extraction levels. In the first four extraction levels, the previous mined slabs could be identified. In the lower parts, this observation was not possible, which could be explained with a change of mining direction.

The size of the survey windows (32 × 6 m) was fit to the average distance between the extraction levels (6 m) in the quarry and a chosen length of 32 m. In the next step, all observed and visible discontinuities within the survey windows were counted and measured to calculate the P_{10} , P_{20} , and P_{21} values (Salvini et al. 2017).

A difficulty, which was also described by Salvini et al. (2017), was to assign a set of discontinuities to the correct set identified by the field survey, which was done by Klein 2018. Because only line traces are visible, the inclination of the discontinuity set could not be defined. Therefore, the sets were labeled with D1–D4, D1 and D2 in first wall, D3 and D4 in second wall. Table 6 shows the calculated values of P_{10} , P_{20} , and P_{21} from survey windows 1 to 4.

Furthermore, information about the distance between the extraction levels and the thickness of the slabs could be measured. The height of the extraction level varies between 5.8 and 6.3 m. The thickness of the extracted slabs is showing a mean of 1.66 m and varying from 1.36 to 2.2 m.

Slate quarries

To understand the natural fracture patterns and the resulting in-situ block geometry of the slates in the quarries near Vila Nova de Foz Côa (Northern Portugal), data in the Cupastone and Solicel quarry (Fig. 44) were collected by conventional methods and aerial photography. The slate schists of Foz Côa are of gray-dark to black color, when deeply fractured oxides precipitate and the schist is showing a brownish coloration (Lourenço et al. 2009).

The schists are exploited in an area, called Pedreiras do Poio, which is located inside the Vale do Côa Archaeological Park, a World Heritage classified site by UNESCO since 1998. The quarries are located 5 km west of the Vilarica Fault (NNE–SSW strike), conditioning the geomorphology of the area and forming the Longroiva graben, which continuous north through the Vale da Vila, near Vila Nova de Foz-Côa (Fig. 44). The Vilarica Fault divides the region into two great blocks, resulting in a horizontal displacement of 5.5 km. The western block is extremely eroded after it ascended about 300–400 m after the Vilafranquian. The studied quarries are in the eastern block, which is less eroded and still preserves the Ordovician. The sedimentary sequences in the quarries representing the opening and closing of a primitive ocean (Sousa et al. 2015).

The studied areas, quarries Solicel and Cupastone, are located at the edges of a WNW–ESE-elongated hill, with

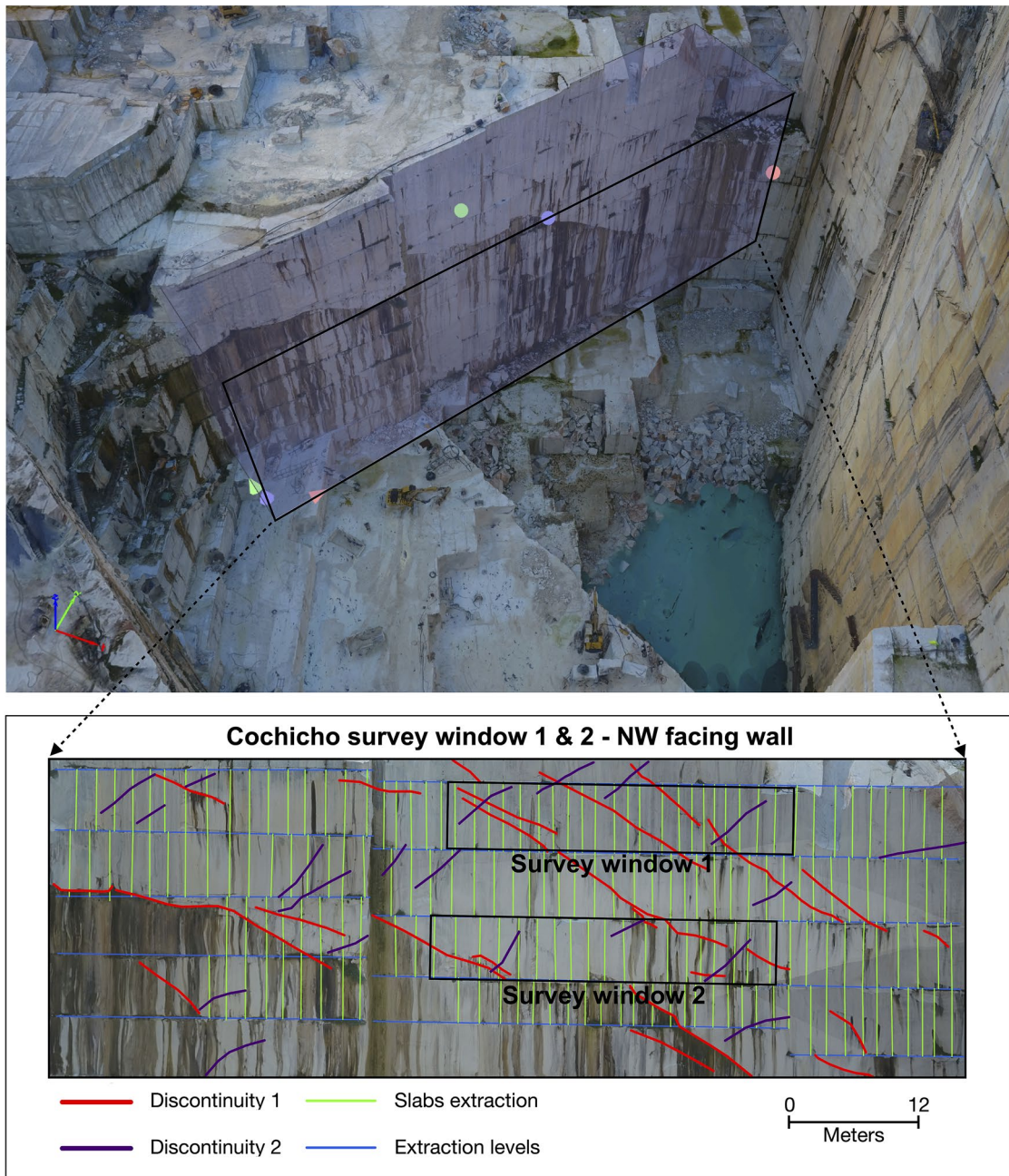


Fig. 42 The top picture is showing the 3D model with the location of the orthoplane of the NW facing wall of the Cochicho quarry. In the lower part, the survey windows 1 and 2 were used to map the discon-

tinuity sets D1 and D2. The blue lines indicating the extraction levels and orthogonal to them the green lines the extracted slabs (see Fig. 38 to locate in the quarry)

the highest area resulting from the continuity of the Foz-Côa plateau, which lies at the NW of the quarries. This plateau, with an approximate height of 360 m, is cut by two predominantly WNW–ESE rivers, that run to the Côa River at a height of 125 m. The exploited mining levels are part of the geological unit known as Desejosa Formation, which is part of the Dúrico-Beirão SuperGroup (Lourenço et al. 2009).

The extracted rocks are exploited through the bedding planes, which can reach a thickness up to 3 m.

The Solicel Company is extracting two varieties of ornamental stones, called Black Schist (Xisto Negro) and Oxidised Schist (Xisto Oxidado) in their quarry (Fig. 45). There are benches of striped shales composed of thin dark beds and light gray component, which alternate successively. This stone is very anisotropic, it shows a flexural

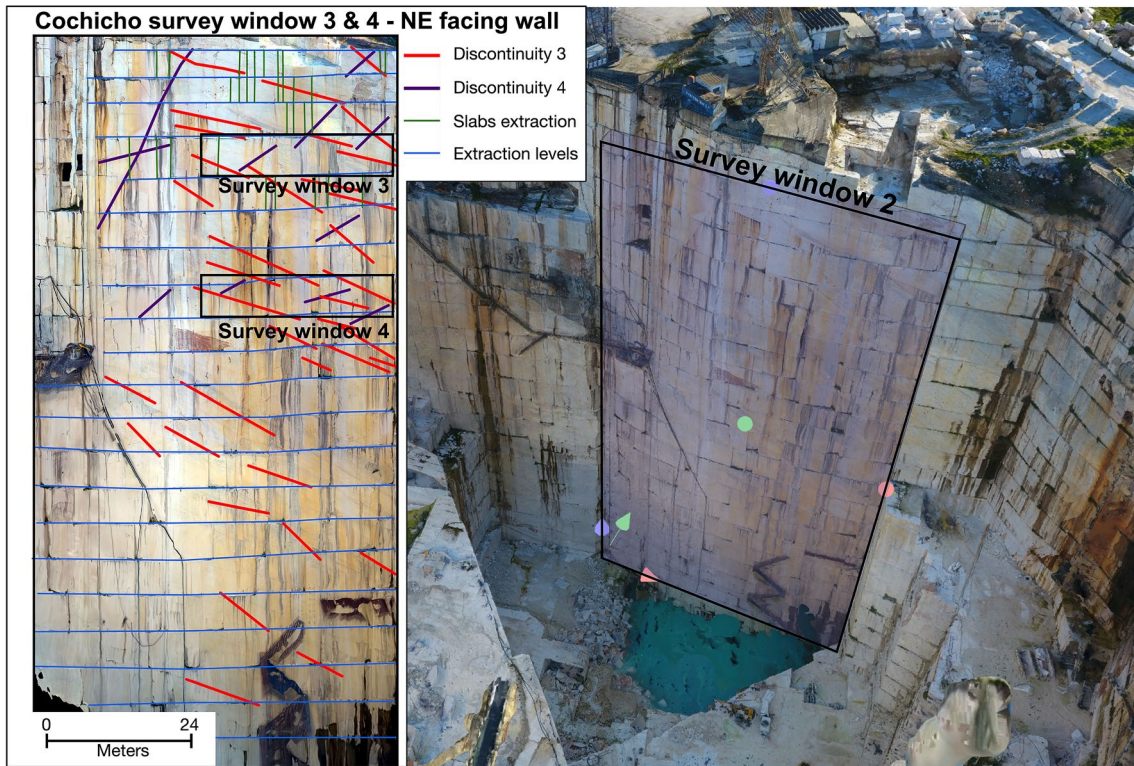


Fig. 43 The right picture is showing the 3D model with the location of the orthoplane of the NE facing quarry wall, which is parallel to the direction of the extracted raw blocks. In the left part, the survey

windows 3 and 4 were used to map the discontinuity sets D3 and D4. The blue lines indicating the extraction levels and the green lines the extracted slabs (see Fig. 39 to locate in the quarry)

Table 6 Calculated values of P_{10} , P_{20} , and P_{21} in survey windows 1 to 4

Set	Window 1			Window 2		
	P_{10} (m^{-1})	P_{20} (m^{-2})	P_{21} (m/m^2)	P_{10} (m^{-1})	P_{20} (m^{-2})	P_{21} (m/m^2)
D1	0.156	0.026	0.044	0.188	0.031	0.024
D2	0.125	0.021	0.022	0.094	0.016	0.021
Set	Window 3			Window 4		
	P_{10} (m^{-1})	P_{20} (m^{-2})	P_{21} (m/m^2)	P_{10} (m^{-1})	P_{20} (m^{-2})	P_{21} (m/m^2)
D3	0.188	0.031	0.026	0.156	0.026	0.044
D4	0.094	0.016	0.023	0.094	0.016	0.028

strength value three times higher in the longitudinal direction than in the transverse one (Morales Demarco 2013). The rock columns made of this local schist were used in vineyards in the Douro Valley region, forming the characteristic landscape of narrow terraces. Today, the demand of this material changed, due to the use of cheaper materials in the already diminishing demand of new vineyard areas. Nowadays the production is oriented on facades, interior surfaces and pavements (Lourenço et al. 2009; Sousa et al. 2015).

The jointing is very similar in the studied quarries and follow the previous studies in the area (Gomes 1987; Búrcio 2004; Lourenço et al. 2009, 2012; Sousa et al. 2015). The

regional faults NNE–SSW to NE–SW and NW–SE (Fig. 44) seems control the jointing in the quarries.

Case study: Solicel quarry

In the Solicel quarry three sub-vertical to vertical joint sets could be identified. The most dominant joint sets are striking in $N20^{\circ} - 40^{\circ}E$ and $N40^{\circ} - 60^{\circ}E$ direction. One orthogonal joint set is striking in $N50^{\circ} - 70^{\circ}W$ direction (Fig. 46). The sub-horizontal bedding planes dipping with an angle of 16° to SSW.

In the upper part of the Solicel quarry, where the weathered slate is extracted, also three joint sets were found. The

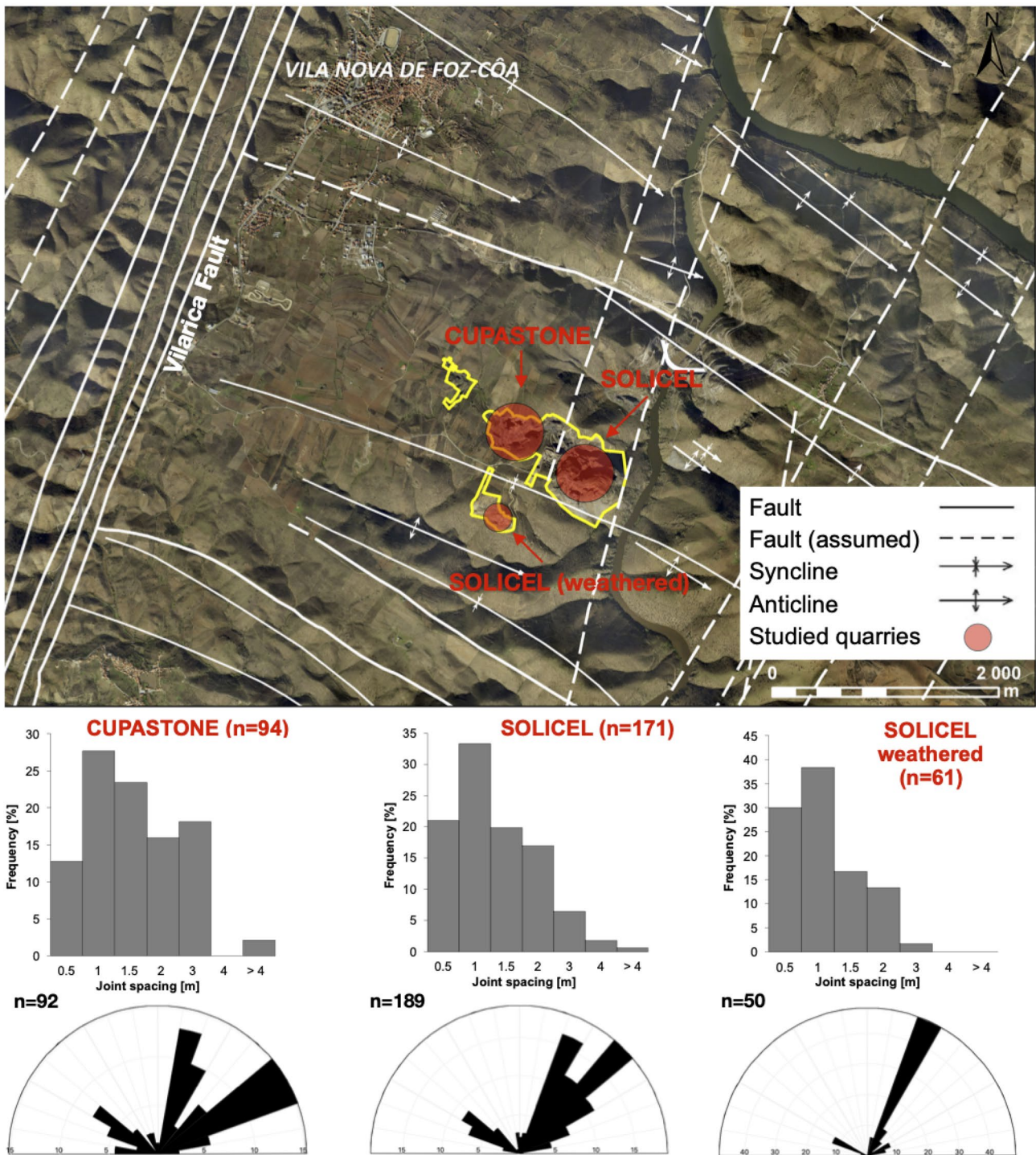


Fig. 44 Aerial photography with locations of the Solicel and Cupastone quarries. The main geological structures are marked within the map. Joint spacing distribution and Rose diagram of the identified

fracture directions of the studied slate quarries (map was modified after Lourenço et al. 2009)

dominant joint set is striking in N20°– 30°E direction. Two less dominant joint sets are striking in N60°– 70°E and N60°– 70°W direction (Fig. 47). A difference in the strike direction of the sawed quarry face was noticed.

While the quarry faces in the lower part of the quarry have a strike direction of N61°W, the strike direction in the upper part of the quarry is around N69°W.

Fig. 45 Black Schist (Xisto Negro) from the Solicel quarry, with typical thin dark beds and light gray component (left). Typical natural and rugged surface (right)

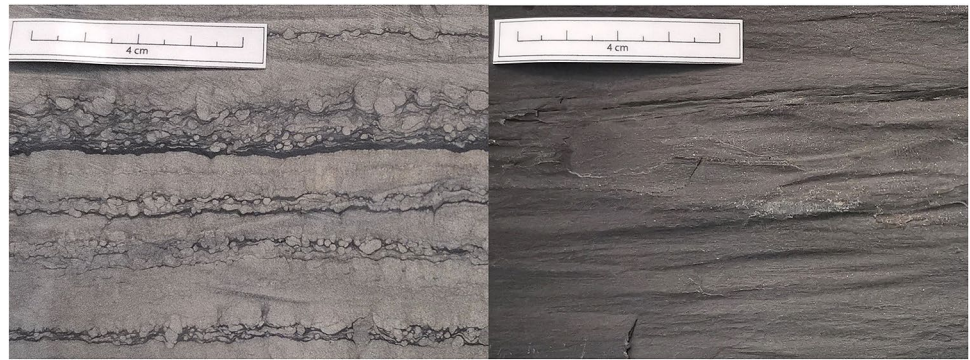


Fig. 46 Rose diagram of the three identified vertical fracture directions and stereographic projection of the density distribution of pole points for measured joints in the Solicel quarry. Blue line is indicating the strike direction of the sawed quarry face (Schmidt net, lower hemisphere)

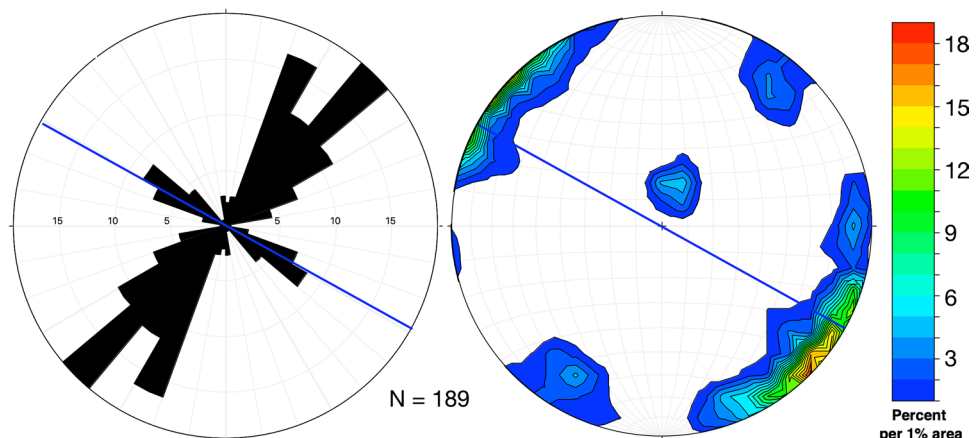
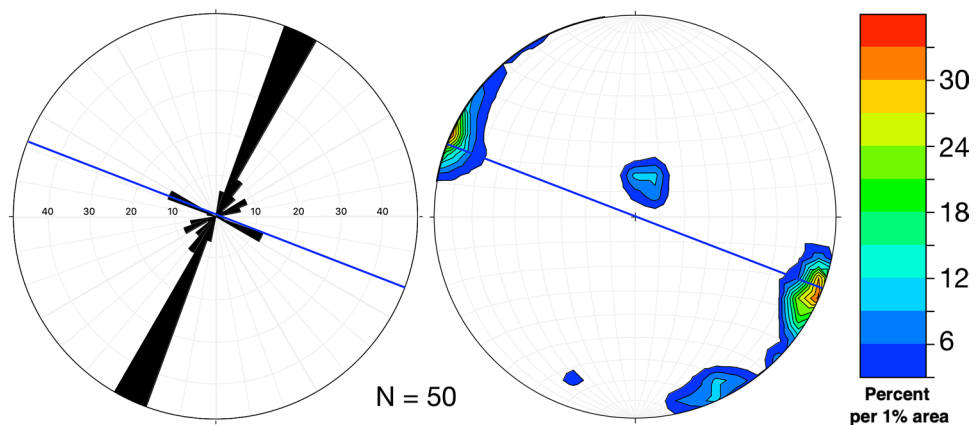


Fig. 47 Rose diagram of the three identified vertical fracture directions and stereographic projection of the density distribution of pole points for measured joints in the upper part of the Solicel quarry for the weathered slate. Blue line is indicating the strike direction of the sawed quarry face (Schmidt net, lower hemisphere)



Similar results can be found in the work from Lourenço et al. 2009 mentioning that, the fracturing is mostly noticeable on the thicker benches, occurring in two families: $N20^{\circ}-30^{\circ}E$ and $N40^{\circ}-60^{\circ}E$ (Fig. 48) (Gomes 1987). The benches are sub-horizontal and typically incline about 10° south. In some places and because of tectonic activity, the benches even tilt about 45° to SE.

The quarry zone is located on a plunging synclinal in the ESE, with sub-horizontal stratification dipping to the south and striking in $N54^{\circ}E$ direction (Lourenço et al.

2009). The primary schistosity ($S1$) is parallel to the stratification ($S0$), which allow easy separation of the rock. The cleavage planes ($S2$) in the slates are sub-vertical and formed later than the rock. The fractures are perpendicular to $S0/S1$ and $S2$, making it possible to obtain parallelepiped blocks (Lourenço et al. 2009).

The studied joints in the Solicel quarry are located 5 km west of the major Vilarica Fault which is striking in NNE–SSW direction. The distance to the main faults and the distance to the axial planes of the first-order folds

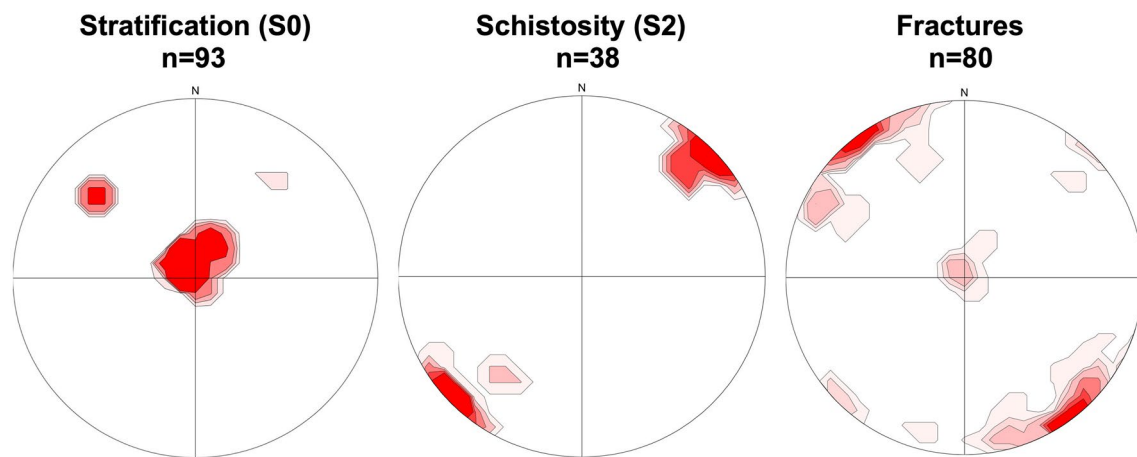


Fig. 48 Stereographic projection of the density distribution of pole points for measured stratification (contours at: 0, 1, 3, 5, 10), schistosity (contours at: 0, 1, 5, 10, 15, 20), and fractures (contours at: 0, 1, 3,

5, 10, 15, 20) in the Pedreiras do Poio mining area (data from Gomes 1987; Schmidt net, lower hemisphere)

influencing the quality of the dimensional stone extraction. The immediate vicinity to the main fractures is causing a dense joint pattern in the rocks. The quarries should be localized in the wide hinge zones of the major synclines (Búrcio 2004).

The joint spacing was measured along two scan lines (Fig. 49) in the lower and most active part of the Solicel quarry. The following result representing the median spacing of the above-mentioned part of the quarry by measurements made in the field (Fig. 50). The sub-vertical joints in the Solicel quarry striking to $N20^{\circ}-40^{\circ}E$, have a median spacing of 0.75 m and varying from 0.2 to 3.5 m. The orthogonal joint set with its $N50^{\circ}-70^{\circ}W$ direction has a spacing of 1 m, varying from 0.4 to 2.1 m. The sub-vertical joint set striking to $N40^{\circ}-60^{\circ}E$ has a median spacing of 1.1 m and varying from 0.2 to 5.1 m. The median horizontal spacing is 1.3 m and varies between 0.3 and 3.1 m. In general, the sub-vertical joint sets are showing a high-joint spacing distribution in the range 0.5–1 m. Less than 5% of the spacings are greater than 3 m.

The joint spacing in the upper part of the Solicel quarry (Fig. 51), where the weathered slate is extracted near the surface, was measured along the quarry walls. The sub-vertical to vertical joints striking in $N20^{\circ}-30^{\circ}E$ direction have median spacing of 0.6 m and varying from 0.2 to 1.9 m. The sub-vertical joint set striking to $N60^{\circ}-70^{\circ}E$ has a median spacing of 1.28 m and varying from 0.2 to 2 m. The orthogonal joint set, which is striking in $N60^{\circ}-70^{\circ}W$ direction has a spacing of 1 m, varying from 0.3 to 2.3 m.

The median horizontal spacing is 1.3 m and is varying between 0.3 and 3.3 m. In general, the sub-vertical joint sets are showing a high-joint spacing distribution in the range 0.5–1 m. Only the horizontal joints are showing a joint spacing distribution of 70% in the range 0.5–1 m.

The data for the joint spacing obtained by aerial survey are showing slightly higher values than the field data (Table 7), except of the $N60^{\circ}-70^{\circ}W$ striking joint set. The median spacing of the $N20^{\circ}-30^{\circ}E$ striking joint set is with 0.90 m higher than the data measured by hand in the field. The joint spacing of the $N60^{\circ}-70^{\circ}E$ striking joint set also has increased by 0.5 m to a median spacing value of 1.78 m. The median horizontal spacing is 1.42 m and similar with the spacing obtained by compass. Only the spacing of the $N60^{\circ}-70^{\circ}W$ shows a lower value of 0.88 m, which is 12% less than the field measurements. The differences seem to be related with fracturing pattern rather than the errors related with this methodology. When the visibility of the joint traces is low the fracturing density is underestimated, but this was not the case. The selected areas for field measurements and aerial survey do not match completely, therefore, differences are expected to occur.

To identify the fractures in the lower part of the quarry and to make a comparison with the conventional methods, a helpful plugin was used in CloudCompare to perform planar facet extraction. With function FACETS planes from unstructured 3D point clouds can be extracted and their dip and dip direction calculated (Millis et al. 2019). To get information about the fractures, especially in the higher located rock slopes, a 3D point cloud was generated by drone images from the field survey in April 2018. This allows us to map discontinuities throughout the quarry and even in areas which are nearly impossible to reach.

After applying the FACETS function in CloudCompare, color-coded planes will be generated, corresponding to a certain range of dip and dip directions of surfaces in the unstructured 3D point cloud, which can be set in a previous stage (Millis et al. 2019). The results of the dip and dip directions can be visualized in stereoplots, but to avoid

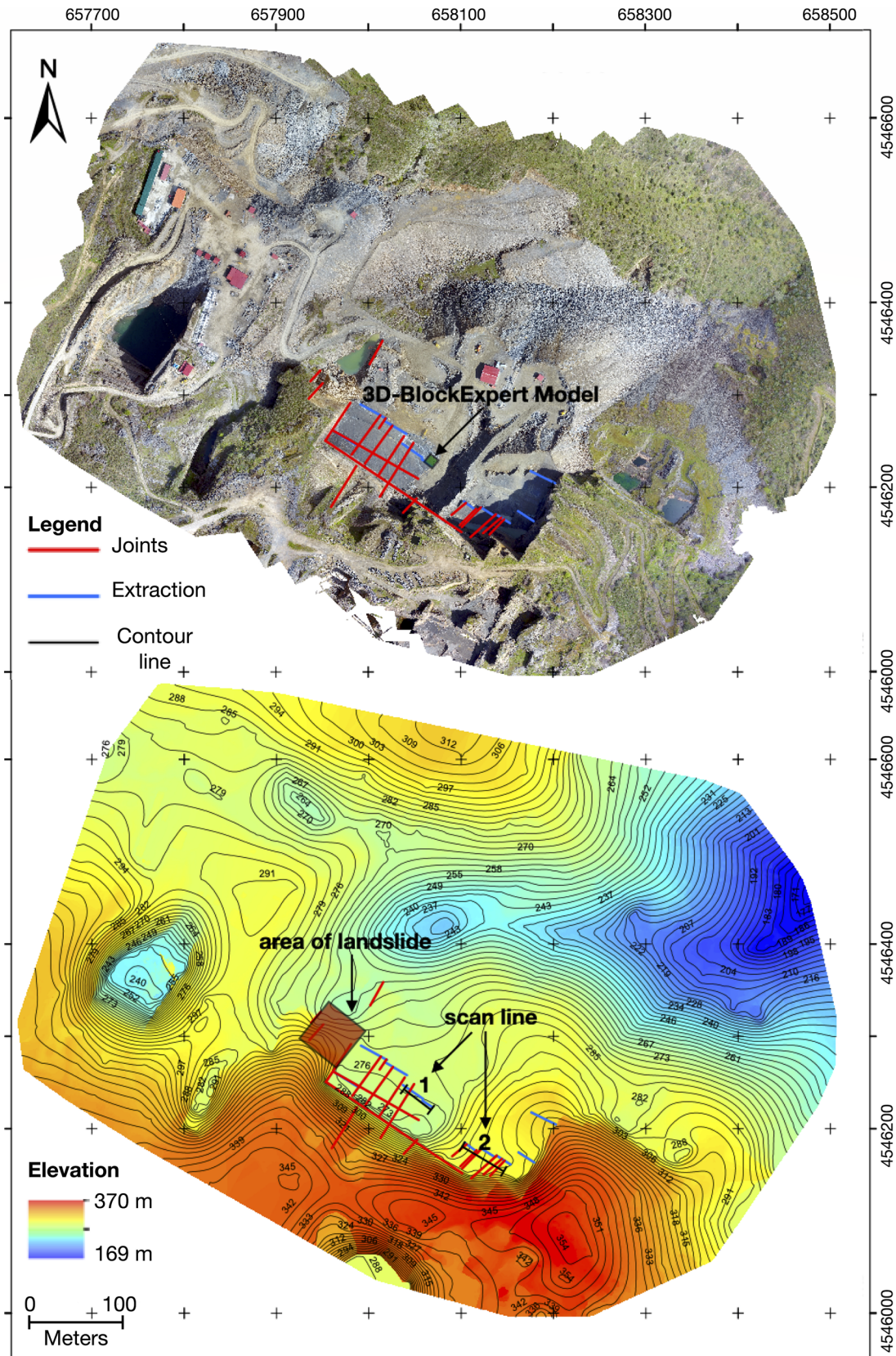


Fig. 49 Orthophoto and digital surface model (DSM), with location of the scan lines, 3D-BlockExpert Model, mapping of the joint sets and cutting pattern in the lower part of the Solicel quarry

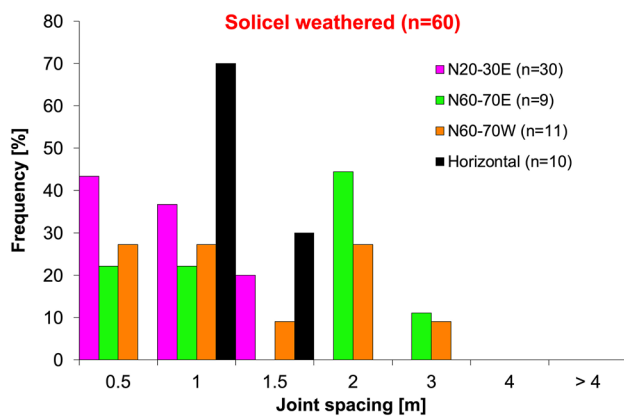


Fig. 50 Joint spacing distribution of the identified main sub-vertical joint sets and the horizontal bedding plane in the lower part of the Solicel quarry

diffusion of the discontinuity sets and drift in the estimated set orientation, the high density of data must be filtered (Millis et al. 2019).

In the first part of Fig. 52, a large-scale study of the entire quarry was done and two stereoplots, corresponding to two nearly orthogonal joint sets in the Solicel quarry, were generated. These sets of facets were chosen, since they are covering more than 80% of the walls located in the quarry. The first picture is showing the computed 3D point cloud with violet facets striking to $N47^{\circ}E$ (mean values calculated by FACETS) and the orange facets striking to $N59^{\circ}W$ (mean values calculated by FACETS). The violet facets correspond also with the green facets and the orange facets with the blue ones. This coloration is caused by the vertical joints, which are striking in the same direction but dipping to the opposite quadrant. FACETS is grouping similar facets with the same coloration. The calculated striking of the joint sets from FACETS match the data from the field (Fig. 46), which were measured by compass.

In total two small-scale approaches with FACETS were done, following scan line 1 and 2 (Fig. 49). In the second part of Fig. 52, an active quarrying wall was selected, which was studied also with the 3D-BlockExpert software. In this area, also the green and orange facets are present and corresponding to the mean values of the large-scale survey, except of some small differences. The green facets striking to $N52^{\circ}E$ (mean values calculated by FACETS) and the orange facets striking to $N56^{\circ}W$ (mean values calculated by FACETS).

Another small-scale survey with FACETS was done in the higher part of the quarry, following scan line 2 (Fig. 49). The upper part of Fig. 53 is showing the same computed facets of the large-scale survey as in Fig. 52 and serves as an overview of the scan line 2 location.

In the second part of Fig. 53, another active quarrying wall was selected. In this area, the violet/green and orange facets are present and corresponding to the mean values of the large-scale survey, except of some small differences. The violet facets striking to $N34^{\circ}E$ and the orange facets striking to $N56^{\circ}W$. Both joint sets of the second scan line are orthogonal. The orange facets of the first and second scan line are showing a constant strike direction of $N56^{\circ}W$. A change in striking direction was only noticed in the NE–SW striking joints, supporting the assumption of two separate joint sets in NE–SW and NNE–SSW direction (Fig. 46). Due to the small survey areas, a high degree of accuracy in the generated results can be expected (Millis et al. 2019). The study of both scanlines shows the importance of window sampling in different parts of the quarry, to identify a change in joint direction and, therefore, the change of in-situ block locations.

The measured spacings of the sub-vertical joint sets and the additional horizontal spacing were used to compute median block volumes for both scan lines. The mean values of the small-scale surveys for dip and dip direction, calculated by the FACETS plugin (Figs. 52 and 53), were used to calculate the block volumes. The quarrying direction follows the schistosity (S2) with $N60^{\circ}W$. The almost vertical joint sets in the first scan line striking to $N56^{\circ}W$ and $N52^{\circ}E$. Both joint sets are not orthogonal and have an angle of 72° . The maximum block (median joint spacings obtained in the field) has a possible volume of 1.08 m^3 ($VB_1L_1 = 0.83 \times 1 \times 1.3 \text{ m}$), considering the joint set orientation and median edge lengths of the sub-horizontal bedding plane (1.3 m), the $N56^{\circ}W$ (1 m) and $N52^{\circ}E$ (1.1 m) orientated vertical joint sets. This means that a volume of 0.42 m^3 will be lost, which correspond to 28.09% of the total volume (1.50 m^3).

Using the calculated strike direction and spacing of the joint sets from the scan line 2, a volume of 0.975 m^3 ($VB_2L_2 = 0.75 \times 1 \times 1.3 \text{ m}$) was computed, considering the median edge lengths of the sub-horizontal bedding plane (1.3 m), and the orthogonal joint sets striking to $N56^{\circ}W$ (1 m) and $N34^{\circ}E$ (0.75 m). In this case no waste will be produced, due to the orthogonal joint sets.

The dimension of 14 extracted blocks were measured during the field work with following average edge lengths: 3.05 m (length) \times 1.23 m (width) \times 0.79 m (height). The resulting median block has a volume of 2.95 m^3 , which is three times bigger than the computed median block volume (0.975 m^3) from above. This result is biased because only the largest blocks are held in quarry.

To identify in-situ blocks in the Solicel quarry, 3D-BlockExpert was used at the scan line 1 (Fig. 49). The modeled block is in the lower part of the Solicel quarry with edge lengths of 12 m in X-direction, 14 m in Y-direction, 4.9 m in Z-direction and a total volume of 823.2 m^3 (Fig. 54). In

Fig. 51 Orthophoto and digital surface model (DSM), with location of the 3D-BlockExpert Model and mapping of the joint sets and cutting pattern in the upper part of the Solicel quarry

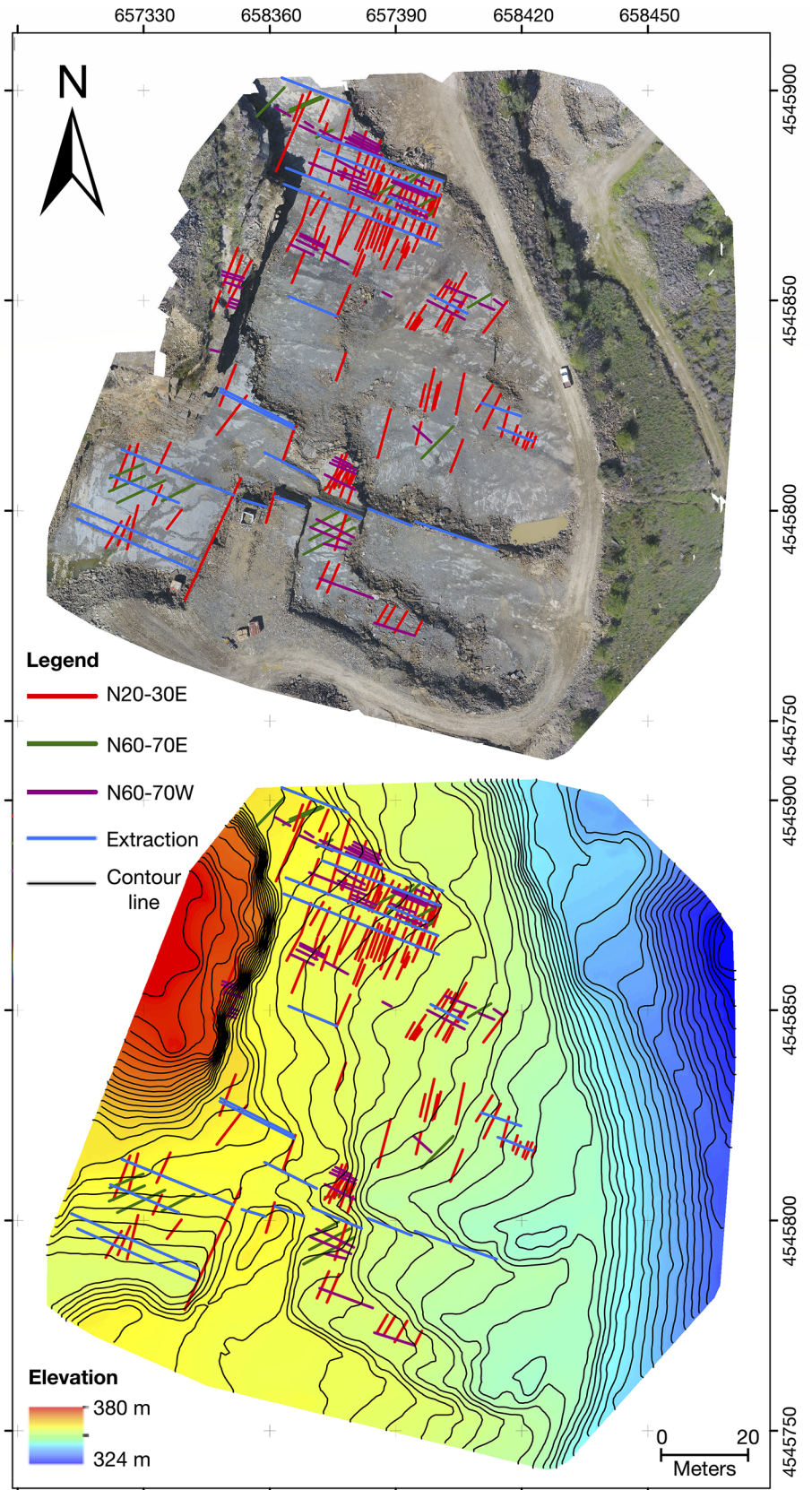


Table 7 Median and mean joint spacing of the investigated joint sets and horizontal planes divided into data obtained in the field and by aerial photography in the upper Solicel quarry

Joint set	Measured by compass				Measured with 3D-Model			
	N20°–30°E	N60°–70°E	N60°–70°W	Horizontal	N20°–30°E	N60°–70°E	N60°–70°W	Horizontal
Median	0.60	1.28	1.00	1.30	0.90	1.78	0.88	1.42
Mean	0.72	1.37	1.05	1.27	0.98	1.90	1.02	1.50
n	30	9	11	10	22	12	10	8

total 15 sub-vertical to vertical joints and 2 sub-horizontal bedding planes were identified.

The median spacing of the N52°E striking sub-vertical to vertical joints is 1 m (value measured from the spacings in the 3D-BlockExpert model (Fig. 54), which is the same value as the spacings for the entire quarry. The median spacing of the N56W striking joints is 2.1 m and is 2.1 times higher than the median spacing in the entire quarry.

The horizontal bedding plane is dividing the raw block in Z-direction with a volume of 823.2 m³ into three separate raw blocks (Fig. 54). Ten blocks with the biggest volume, defined by the natural fracture systems, are shown in Fig. 54. Nine of ten of the biggest blocks are located between section b and c. These ten blocks volumes ranging from 11.61 to 32.62 m³. The biggest block has a volume of 32.62 m³, which is nearly 4% of the total volume. Between section a and b, one of the bigger blocks is located, with a volume of 13.51 m³, which is 1.64% of the total volume. These ten blocks have a volume of 193.2 m³, which is 23.5% of the total volume. The joint planes cover up 112.2 m³, which represent 13.63% of the total block volume.

The raw block was separated in Z-direction along the bedding plane into 3 slabs, with a thickness of 1 m (difference of section a and b), 2.8 m (difference of section b and c) and 0.9 m (difference of section c and d), and edge lengths of 12 m in X-direction and 14 m in Y-direction. This allows us, a view inside the three slabs to identify the in-situ blocks. The high-joint density of the NE striking joint sets, especially in an area which is 2 m wide, five joints (at 9–11 m in Y-direction) causing very small in-situ blocks. In between section b and c, these NE striking joints covering a large area of the raw slab, making it impossible to extract useable dimension stones (Fig. 54). The sub-vertical joints have a big influence of the final volume of the in-situ blocks, like it is the case again in between section b and c. This slab is 2.8 m thick and there are three sub-vertical joints striking in NW direction (around 3 m and from 10 m in X-direction), which were marked with orange lines in Fig. 54. Especially the two sub-vertical NE striking joint sets, with a narrow joint spacing of only 1.3 m, leaving nearly no volume for in-situ blocks. In the other two thinner slabs, these joints are present and their propagation through the entire raw block can be followed. In the thinner slab (between section C and D), the

quantity of the in-situ blocks is higher, but the dimension is limited by the height (Z-direction) of the slab.

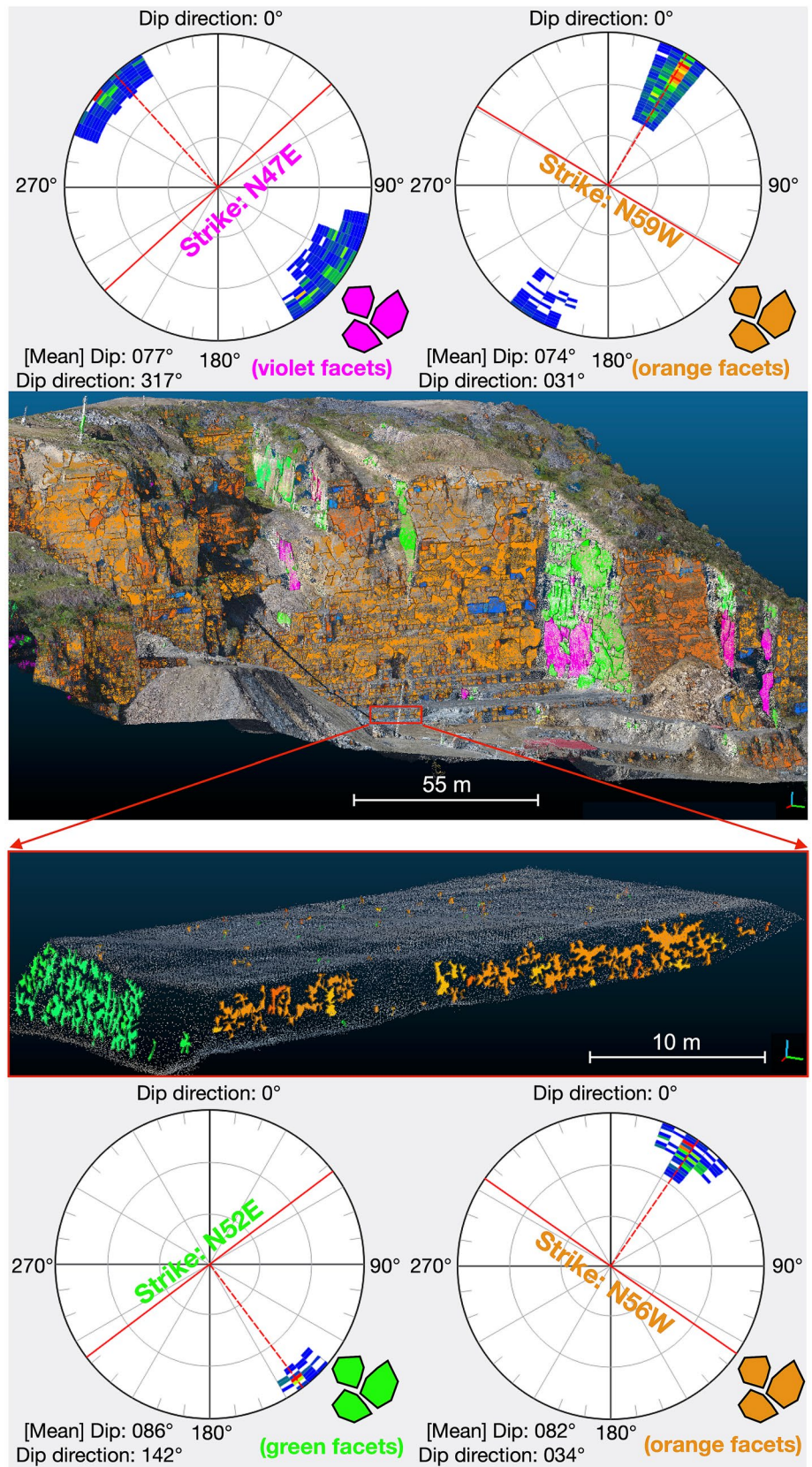
Possible final block sizes were chosen with 4 m, 3 m and 2 m in X-direction, 1 m in Y-direction resulting from the joint spacing of the N52°E striking joint set and the thickness of the Z-direction (1 m, 2.8 m or 0.9 m). The in-situ blocks have following volumes between sections a and b: 4 m³, 3 m³, and 2 m³. The smallest in-situ block volumes will be extracted between sections c and d with volumes of 3.6 m³, 2.7 m³, and 1.8 m³. The largest block volumes of the in-situ block can be found between section b and c, with 11.2 m³, 8.4 m³ and 5.6 m³ (Fig. 54).

Proceeding from this assumption, 7 final in-situ blocks (4 m³) with a volume of 28 m³, 1 final in-situ blocks (3 m³) with a volume of 3 m³, and 13 blocks (2 m³) with a volume of 26 m³ can be extracted between sections a and b, which means a total volume of 57 m³ will be extracted (Fig. 54). Between sections b and c, in total four final in-situ blocks (11.2 m³) with a volume of 44.8 m³, four final in-situ blocks (8.4 m³) with a volume of 33.6 m³, and ten blocks (5.6 m³) with a volume of 56 m³ can be extracted, which is a total block volume of 134.4 m³. Between the last sections of c and d, a total block volume of 72 m³ can be extracted, with following final in-situ blocks: 7 final in-situ blocks (3.6 m³) with a volume of 25.2 m³, 4 final in-situ blocks (2.7 m³) with a volume of 10.8 m³ and 20 blocks (1.8 m³) with a volume of 36 m³. Overall, these in-situ blocks correspond to a total volume of 263.4 m³, which is about 32% of the total volume of the original raw block (823.2 m³). This value is higher than the usually mentioned for the yield in slate quarries (Walsh 1999; Morales Demarco 2013). The raw block modelled is located in a low fractured area of the quarry, therefore, the global yield of the quarry will be lower.

Landslides and rockfall instability

Rockfall is the most common cause (over 20%) of accidents and fatalities in an active quarry (Alejano et al. 2012). The process of rockfall is mainly driven by slope inclination and involves the detachment of rock fragments, rolling, sliding and deposition (Robiati et al. 2019). The safety of the workers in the quarries must be guaranteed while they became increasingly deeper during exploitation. Data of

Fig. 52 Identified fracture surfaces from a 3D point cloud dataset. Upper part is showing the entire quarry and a large-scale FACETS survey with corresponding stereoplots of the calculated fracture systems and calculated mean dip and dip directions. The location of the first small-scale survey of the active quarrying area is shown within the red rectangle. The mean striking direction of the corresponding facets is shown in the stereoplots



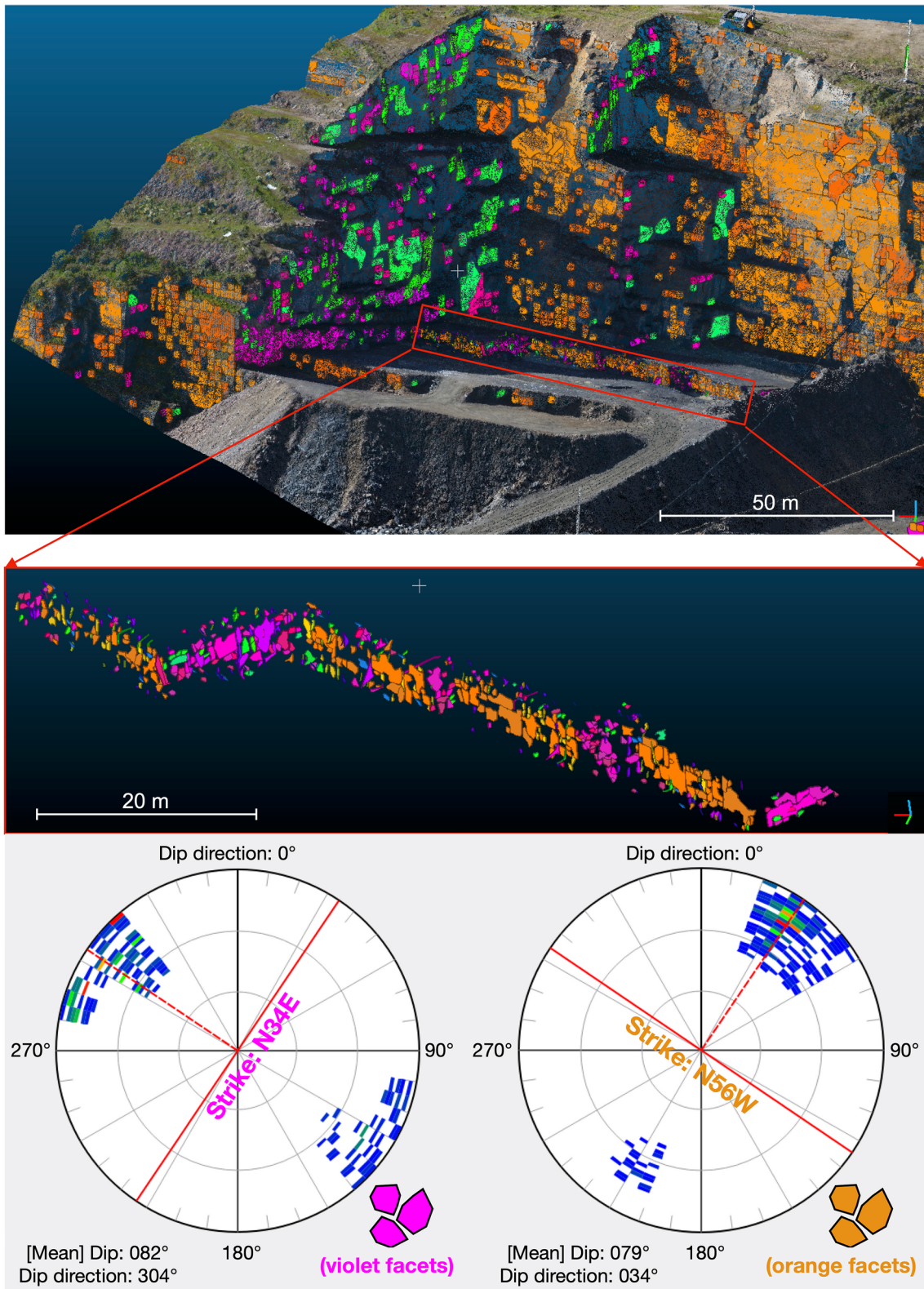
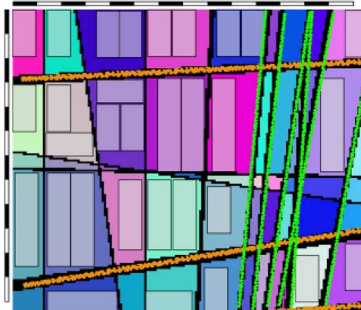
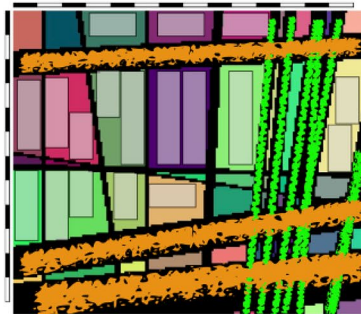
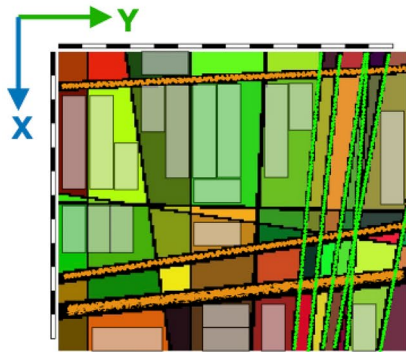
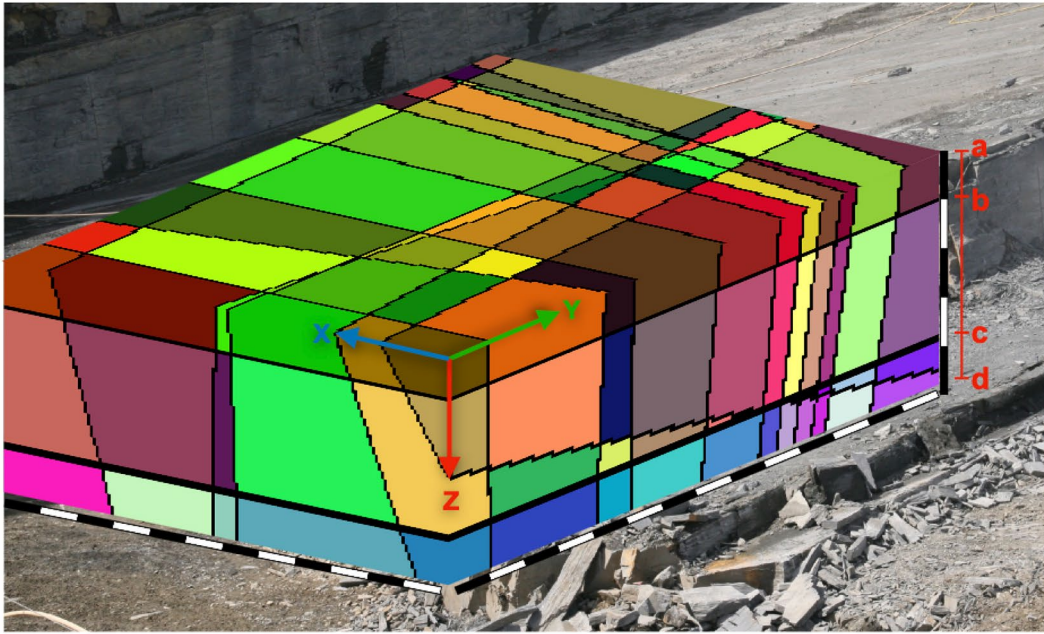


Fig. 53 Identified fracture surfaces from the same 3D point cloud dataset of Fig. 52. Upper part is showing the entire quarry from a different angle of view and the same facets from the large-scale survey.

The location of the second small-scale survey of the upper active quarrying area is shown within the red rectangle. The mean striking direction of the corresponding facets is shown in the stereoplots



◀**Fig. 54** In-situ block identification with the help of the software 3D-BlockExpert in the Solicel quarry. The raw block from the lower mining level with a volume of 823.3 m³ has a yield of 263.4 m³ (32% of total volume). Orange lines pointing out NW striking joints and the green lines the NE striking joints and the space they are covering

photogrammetric surveys can help to study landslides and rockfall instability. The resulting high-resolution point clouds can be analysed with tools like FACETS to characterize the distribution of discontinuities in a rock slope, like joints, faults and stratification.

In Fig. 55, the FACETS application uses the point cloud to identify the dip and dip direction a fault in a quarry. The same point cloud was also used to determine the stratification in the same quarry. The mean striking direction and the calculated mean dip and dip directions of the corresponding facets is shown in the stereoplots.

Two examples for landslides and rockfall instability can be found within Fig. 56. The blue facets representing critical planes dipping with 69° to the SSW which can cause rockfall in the Mármoreos Galvão quarry (Estremoz region, Portugal). The second example in the Solicel quarry is showing a previous rockfall that happened just some weeks before the field survey in April 2018. This rockfall was caused by undercutting of the slope and causing instability.

The previous examples were intended to inspire and have not been carried out further in detail. They are only to show how new technologies can improve in the characterization of fracturing. For detailed studies please see Alejano et al. (2012) and Robiati et al. (2019).

Final comments

In this research, several examples of combining both field measurements and fracturing modelling in quarries of building stones were presented and discussed. We selected quarries in four different rocks: granite, marble, limestone, and slates. The development of the quarries is conditioned by the rock structure, fracturing pattern, and weathering profile. Remarkable differences were found in the studied quarries, notorious even in the quarries of same rock type.

Fracturing assessment is of critical importance during the evaluation process of the building stones resources. A detailed field survey of the joint sets is very important to this evaluation. However, large areas to map and/or inaccessible walls and quarry fronts needs to be also mapped. Unmanned aerial vehicles help in this task by capturing imagery that enables orthophotos, digital surface models and 3D models. Also, the fracturing modelling is a powerful tool helping in the process of the quarry yield evaluation.

In this section, instead of conclusions from research already presented for individual cases, a general discussion

is proposed. The study of the fracturing in building stone quarries is a stimulating task by incorporating new techniques and technologies, but always based in field work. A general discussion is presented, by mention the observations in studied quarries, the complexity related with the natural fracturing and structural issues and the new possibilities from new approaches. To combine the field work and geological knowledge with new technical opportunities is a challenge we need to win.

Fracturing in the studied quarries follows the regional fracturing pattern. This is true for all rock types, but small differences can be found from quarry to quarry. Quarries have large areas and the field measurements are sometimes difficult and only a small portion of the quarry is mapped. In the mapped areas not all the joint sets are visible, and the fracturing information is affected by this bias. On the other hand, the degree of development of the quarry has an impact on the accessibility of the joints. Large and deep quarries allow the evolution of the fracturing with depth to be assessed, particularly the increase in spacing in sub-horizontal joints and the decrease in fracture density. These controlling factors should be considered when a comparison between the fracturing in quarries is made.

The results of joint spacing are generally consistent with those of previous investigations in the rocks and quarries studied. However, the above considerations regarding the differences in the joint pattern also apply to the values of the joint spacing. Measurements were made on the front faces of the quarries, where the joint spacing is greater than in the other parts of the quarries. The more fractured areas of the massif are not exploited or are rapidly abandoned, so that joint spacings calculated from information obtained in a single quarry are always the best values for the entire outcrop. Given the above limitations, the results of joint spacing evaluations should not be used to draw general conclusions, and some caution should be exercised.

Assuming a uniform distribution of the joint sets in the quarries and considering the mean values of joint spacing, it is possible to identify the in-situ blocks and their volume. This is a statistical approach that can be used to compare the yield values in multiple quarries. In fact, all quarries show changes in the fracturing pattern and joint density. A yield variation can be expected in any quarry and larger range happens when several quarries are associate. When lithological and structural questions are taking into consideration, these differences reach extreme values. Some examples are the extreme fracturing and weathering of the syn-tectonic granites when compared with sound and less fractured post-tectonic, the limestone quarries located in very different sedimentary and stratigraphic levels, the marble and slate quarries located in folded and thrust areas or in unfolded areas.

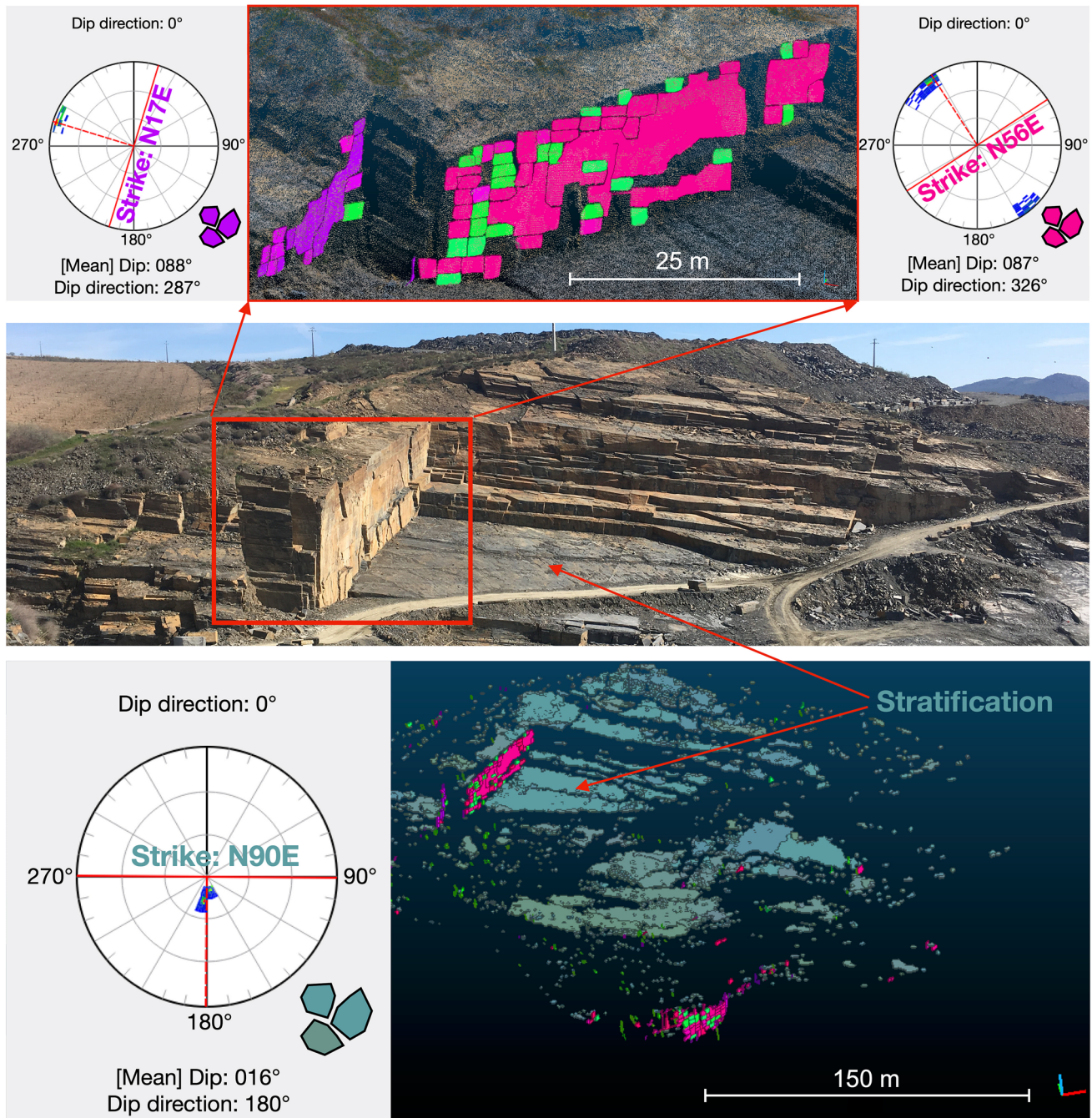


Fig. 55 The identification of joints, faults, and stratification during the quarry development is possible with the plugin FACETS

Despite the above limitations the statistical approach to yield assessment is a powerful tool to guide the mining activity in a quarry, by defining the best approach to maximize the extraction of commercial blocks. In different parts of the quarry not all the joint sets are visible and/or the joint spacing is much higher than the mean values. In those cases, the yield and volume of the blocks will be higher, and every person can be successful with such excellent natural conditions. When choosing between different quarrying areas and

options, reliable data are key to successful quarry development. Quarry activity cannot happen only where yield is higher, an overall evolution of the quarry fronts is crucial to maintain the production level trough time.

Modelling the joints in a quarry front with software programs like 3D-BlockExpert helps in quarry management. It is possible to model the trend of joint surfaces, to calculate the shape and volume of the in-situ blocks and the quarry yield. Besides the fracturing characterization and expected

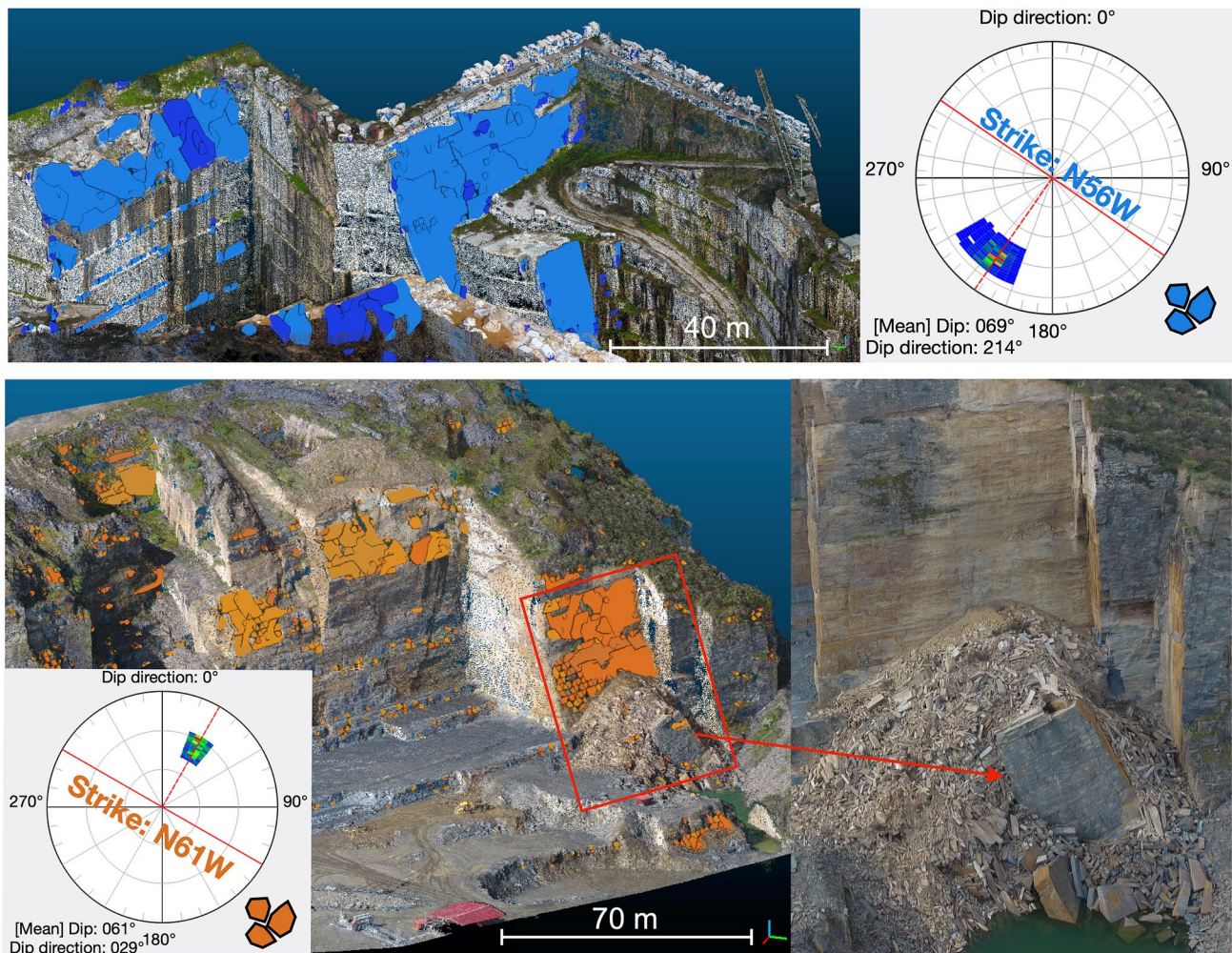


Fig. 56 The plugin FACETS was used in CloudCompare to identify dip and dip direction of critical slopes which, can cause rockfall in the Mármores Galvão quarry (upper point cloud) and Solicel quarry (lower point cloud)

quarry yield, the effect of changing the cutting direction of the block can also be assessed. A small shift in the cutting angle improves the number and volume of final blocks. Another important tool of this software (3D-BlockExpert) is the prediction of the possible blocks that will be cut from the initial raw block or quarry front. Considering the fracturing pattern in a specific quarry area, it is possible to maximize the final blocks by changing the distance between the cuts. Sometimes, large blocks are destroyed avoiding higher quarry yield. Usually, such operations are performed automatically on a quarry front, using previous defined dimensions without checking whether the best option has been applied. Of course, such an option requires continuous monitoring of the quarry front, the collection of jointing data, modelling and finally investigation of the best option. These procedures are time consuming, and technical personnel capable of performing such tasks are needed, but the

effort can be worthwhile. A modest increase of 10% in commercial blocks will pay the investment.

Yield values were determined for the modelled quarry fronts that correspond to the best values found in the literature and are consistent with the real values reported by quarry technicians. The values of yield obtained in the fronts of studied quarries range from 14 to 60%. As mentioned above, these values represent only a local picture of fracture formation in a narrow area of the quarries. They do not give a false picture of quarry yield but show how fracture pattern and fracture density affect the ability to deliver commercial blocks. The results are consistent with reality and give confidence for increased use of these modelling software in quarry operations.

Unmanned aerial vehicles are helpful in the characterization of the quarry fronts, namely in the identification of the joints in accessible walls and allowing a general view of the quarry. When evaluating a small portion of the

quarries, it is possible to identify the main joint sets and faulted/folded areas that are not visible. Furthermore, post-processing of point clouds from aerial photography allows the creation of digital surface models, orthophotos and 3D models that can be used to manage the development of the quarry (occupied area, extracted volume, waste volume and quarry yield). Since these techniques can be adapted to the requirements of each quarry, a new field of application opens up.

Information from aerial surveys can be used in many cases to increase the detail of information from field measurements and to improve knowledge of fracturing. The distance between sub-horizontal joints and stratigraphic levels can be determined without difficulty from an orthoplane of quarry walls. Inaccessible areas where traditional field surveys methods are not applicable can be considered here and now, strengthening fracture characterization, improving knowledge of exploitation constraints, and helping to increase yield.

The orthophotos of clean outcrops showing joint traces provide information about joint sets and joint spacings. However, surfaces must be clean, and visibility is a limiting factor—waste covers joint traces and closed joints are difficult to identify. In addition, evaluation based only on aerial photographs may yield different values than the results of field measurements. The joint pattern and spacing changes in a quarry, and differences between values from field measurements and aerial photographs can be expected to occur when different areas have been evaluated.

The comparison of the main joint sets and the cutting can be easily done in an orthophoto, or a 3D model. The maximization of the yield is achieved when the joints are used to define the extracted blocks. This means that one cutting direction is defined by the most important joint set and the other cut direction will be perpendicular to first one. In some cases, a slight difference is evident between the joint strike and the cut directions. Probably, the cutting direction was initially determined considering the joint strike, which changed in the quarry, or the cutting direction was determined incorrectly. A small angle between the cutting direction and the main joint set can result in large losses. Aerial photos can be used to control the extraction by adapting the cut direction to the fracturing. A permanent evaluation of the joint pattern during the extraction is mandatory, and changing the angle can improve the quarry yield.

The identification of the main joint sets or faults planes is also possible by applying special plugins to the point clouds. Such capabilities can be useful for obtaining a quick overview of the joint pattern in large areas, identifying variations in the joint pattern, confirming the joint pattern in an active quarry front, and distinguishing structural planes such as stratification. Potential slide planes can be identified to avoid

deepening of the quarry without previous stabilization or other safety measures.

3D models are suitable for evaluating the volume quarried and waste dumped in a given period. Such information can be used for various purposes, such as to calculating quarry yield by the relation between the volume quarried and the volume of blocks extracted, or for monitoring the evolution of resources. Land planning management can benefit from such information, as an update of occupied land and quarry development is always done on an annual or multi-annual basis.

The combination of all these techniques is essential in today's building stone industry. With the development of extraction and processing techniques, the quantity of material extracted from the quarries increases each year. Quarries must be able to follow the demand of raw material by maximizing the yield and improving the extraction techniques. Basic geological information such as joint set striking and spacing and their changes in the quarry area are key factors to improve the quarry yield. Combining traditional field techniques with information provided by drone imagery, 3D models and fracture modelling is the forthcoming evolution in the quarry management.

There is no single methodology, as all quarries are different, and the solutions must be suitable for the existing problems. Instead of presenting a general methodology, we focused on giving a picture of the possibilities to take into account the new technical developments. We strongly believe that the future for the natural stone industry starts now. These new techniques can be unfamiliar today, but their popularization and friendly use are contributing to their increasing application. In the coming decades, more and more of these tools will help improve quarry evaluation and management.

Despite these new developments, basic fieldwork and knowledge of the geological background should not be ignored. They are always the basis for quarry management and can never be replaced by the information provided by these new techniques. On the contrary, maximizing these new technologies and techniques requires a deeper knowledge of geological information. Only in this way can the best option for new studies be identified to augment the existing information. Nice figures without valid information are only nice figures.

The examples given in this text are just a few of the situations where the combined methods improve geological knowledge and help in the quarry management. This new approach can be applied to single quarry, a cluster or to a pristine area. It is the problem to be solved that determines the best methodology to apply. Other applications are possible, and this will be our next focus.

Acknowledgements This research is included in the project POCI-01-0247-FEDER-024535, INOVSTONE 4.0—TECNOLOGIAS AVANÇADAS E SOFTWARE PARA A PEDRA NATURAL. The study on the Estremoz marbles has been supported by the PPP-project from the DAAD (Az. 57213019) what we grateful acknowledge. Acknowledges are due to all the companies mentioned in text who give permission to study the quarries. Luís Sousa thanks the support of the Centro de Geociências (CGeo), projects UIDB/00073/2020 and UIDP/00073/2020 financed by Fundação para a Ciência e a Tecnologia. We are also grateful to Johanna Menningen, Calvin Klein, Amanda Ricardo, Sebastian Oriolo and Dmitri Nikolayev for the help with the fieldwork. S.S. also thanks the 3D-BlockExpert-TEAM: Dr. Dmitry Nikolayev, Dr. Stefan Mosch and Dr. Andreas Hoffmann.

Funding Open Access funding enabled and organized by Projekt DEAL.

Open Access This article is licensed under a Creative Commons Attribution 4.0 International License, which permits use, sharing, adaptation, distribution and reproduction in any medium or format, as long as you give appropriate credit to the original author(s) and the source, provide a link to the Creative Commons licence, and indicate if changes were made. The images or other third party material in this article are included in the article's Creative Commons licence, unless indicated otherwise in a credit line to the material. If material is not included in the article's Creative Commons licence and your intended use is not permitted by statutory regulation or exceeds the permitted use, you will need to obtain permission directly from the copyright holder. To view a copy of this licence, visit <http://creativecommons.org/licenses/by/4.0/>.

References

- Akara MEM, Reeves DM, Parashar R (2020) Enhancing fracture-network characterization and discrete-fracture-network simulation with high-resolution surveys using unmanned aerial vehicles. *Hydrogeol J*. <https://doi.org/10.1007/s10040-020-02178-y>
- Alejano L, Veiga M, Gómez-Márquez I, Dellerio H (2012) Application of rockfall risk assessment techniques in two aggregate quarries. Paper presented at the 12th ISRM Congress, Beijing, China, October 2011. Paper Number: ISRM- Allmendinger 12CONGRESS-2011-338, pp. 1861–1864
- Allmendinger RW, Cardozo N, Fisher DM (2011) Structural geology algorithms. Cambridge University Press, Cambridge (ISBN 978-1-107-01200-4)
- Alves TM, Manuppella G, Gawthorpe RL, Hunt DW, Monteiro JH (2003) The depositional evolution of diapir- and fault-bounded rift basins: examples from the Lusitanian Basin of West Iberia. *Sed Geol* 162(3):273–303. [https://doi.org/10.1016/S0037-0738\(03\)00155-6](https://doi.org/10.1016/S0037-0738(03)00155-6)
- Annavarapu S, Kemeny J, Dessureault S (2012) Joint spacing distributions from oriented core data. *Int J Rock Mech Min Sci* 52:40–45. <https://doi.org/10.1016/j.ijrmms.2012.02.003>
- Azerêdo AC (1998) Geometry and facies dynamics of Middle Jurassic carbonate ramp sandbodies, West-Central Portugal. *Geol Soc Lond Spec Publ* 149(1):281–314
- Azerêdo AC (2007) Formalização da litostratigrafia do Jurássico Inferior e Médio do Maciço Calcário Estremenho (Bacia Lusitânica). *Comunicações Geológicas* 94:29–51
- Bogdanowitsch M (2020) Characterization of selected dimensional stone quarries in Portugal: airborne photogrammetric surveys, optimization of block extraction and technical properties. MSc. thesis, Universidade Georg-August, Göttingen
- Bruzzi AFG, Alameda-Hernández P, Klen AM, Pereira TM, Lana MS (2020) Probability density function of rock mass discontinuity distances. *Geotech Geol Eng*. <https://doi.org/10.1007/s10706-020-01634-6>
- Búrcio MDM (2004) Controle Estrutural da Localização de Pedreiras de Esteios de Xisto para Vinha em Vila Nova de Foz Côa. Thesis, Universidade de Évora, Évora, MSc
- Carvalho JMF (2013) Tectónica e caracterização da fraturação do Maciço Calcário Estremenho, Bacia Lusitaniana. Contributo para a prospeção de rochas ornamentais e ordenamento da atividade extrativa. PhD thesis, University of Lisboa
- Carvalho JMF (2018) Jointing patterns and tectonic evolution of the Maciço Calcário Estremenho, Lusitanian Basin, Portugal. *J Struct Geol* 110:155–171
- Carvalho JMF, Lisboa JV (2018) Ornamental stone potential areas for land use planning: a case study in a limestone massif from Portugal. *Environ Earth Sci* 77(5):273. <https://doi.org/10.1007/s12665-018-7382-x>
- Carvalho J, Henriques P, Falé P, Luís G (2008) Decision criteria for the exploration of ornamental-stone deposits: application to the marbles of the Portuguese Estremoz Anticline. *Int J Rock Mech Min Sci*. <https://doi.org/10.1016/j.ijrmms.2008.01.005>
- Carvalho JMF, Lisboa JV, Moura AC, Carvalho C, Sousa LMO, Leite MM (2013) Evaluation of the Portuguese ornamental stone resources. *Key Eng Mat* 548:3–9
- Carvalho JMF, Sampaio J, Machado S, Mídões C, Prazeres C, Sardinha R (2014). Caracterização e valorização da área de intervenção de Pé da Pedreira. Cluster da Pedra Natural
- Carvalho J, Lopes C, Mateus A, Martins L, Goulão M (2018) Planning the future exploitation of ornamental stones in Portugal using a weighed multi-dimensional approach. *Resour Policy* 59:298–317. <https://doi.org/10.1016/j.resourpol.2018.08.001>
- Casal Moura A (2000) Granitos e rochas similares de Portugal. Instituto Geológico e Mineiro, Porto
- Dewez TBJ, Girardeau-Montaut D, Allanic C, Rohmer J (2016) FACETS: a cloudcompare plugin to extract geological palnes from unstructured 3D point clouds. *Int Archives Photogr Remote Sens Spatial Inform Sci XLI-B5*:799–804. <https://doi.org/10.5194/isprsarchives-XLI-B5-799-2016>
- Dershowitz WS, Einstein HH (1988) Characterizing rock joint geometry with joint system models. *Rock Mech Rock Eng* 21:21–51
- Duarte J, Gonçalves G, Cunha M, Figueiredo F (2020) Photogrammetry in structural characterization of limestones massifs (In Portuguese). *Comunicações Geológicas* 107. Especial I:73–77
- Egels Y, Kasser M (2001) Digital photogrammetry. CRC Press, ISBN, p 9780748409457
- Ehlen J (1999) Fracture characteristics in weathered granites. *Geomorphology* 31(1–4):29–45
- Ferrari F, Ziegler M, Apuani T, Loew S (2019) Geostatistical analyses of exfoliation and tectonic joint set spacing in alpine granites (Aar Valley, Switzerland). *Bull Eng Geol Environ* 78:1645–1668. <https://doi.org/10.1007/s10064-018-1251-4>
- Figarska-Warchoł B, Stańczak G (2019) Using digital photographs and orthophotomaps of a quarry to assess the geometry and density of discontinuities in a sandstone deposit. *Arch Min Sci* 64(3):509–532. <https://doi.org/10.24425/ams.2019.129366>
- Gomes LMF (1987) Estudo das Pedreiras do Poio: Vila Nova de Foz Côa. Trabalho realizado no âmbito da cadeira de Projecto de Engenharia I. Curso de Engenharia Geológica. Coimbra
- ISRM (1978) Suggested methods for the quantitative description of discontinuities in rock masses: International Society for Rock Mechanics Commission on Standards of Laboratory and Field Tests. *Int J Rock Mech Min Sci Geodyn Abstr* 1978:319–368

- ISRM (1981) Basic geotechnical description of rock masses. *Int Soc Rock Mech* 18:85–110
- Klein C (2018) Lagerstättenkundliche und gesteintechnische Charakterisierung der Marmore der Estremoz-Antiklinale. Bachelorthesis. Goettingen
- Kullberg JC, Rocha RB, Soares AF, Rey J, Terrinha P, Azerêdo AC, Callapez P, Duarte LV, Kullberg MC, Martins L, Miranda JR, Alves C, Mata J, Madeira J, Mateus O, Moreira M, Nogueira CR (2013) A Bacia Lusitaniana: Estratigrafia, Paleogeografia e Tectónica. In: Dias R, Araújo A, Terrinha P, Kullberg JC (eds) *Geologia de Portugal, vol II. – Geologia Meso-Cenozóica de Portugal*. Escolar Editora, Lisboa, pp 195–348
- Lazar A, Vižintin G, Beguš T, Vulić M (2020) The use of precise survey techniques to find the connection between discontinuities and surface morphologic features in the Laže Quarry in Slovenia. *Minerals* 10:326. <https://doi.org/10.3390/min10040326>
- Lopes JLG (2003) Contribuição para o Conhecimento Tectonoestratigráfico do Nordeste Alentejano. Transversal Terena-Elvas. Implicações Económicas no Aproveitamento de Rochas Ornamentais Existentes na Região (Mármore e Granitos). PhD thesis, University of Évora
- Lopes L, Martins R (2015) Global heritage stone: Estremoz Marbles, Portugal. *Geol Soc Lond Spec Publ* 407(1):57–74. <https://doi.org/10.1144/SP407.10>
- Lopes L, Silva JB (2006) Constrangimentos geológicos na exploração de mármore no anticlinal de Estremoz. Presented at the VII Congresso Nacional de Geologia. Pólo de Estremoz, Universidade de Évora, Sociedade Geológica de Portugal, pp 1027–1030
- Lourenço J, Mateus A, Coke C, Ribeiro A (2002) A zona de falha Penacova-Régua-Verín na região de Telões (Vila Pouca de aguiar), alguns elementos determinantes da sua evolução em tempos tardi-variscos. *Comum Inst Geol e Mineiro* 89:105–122
- Lourenço JMM, Sousa LMO, Gomes LMF, Oliveira AS (2009) Os xistos de Foz-Côa (Norte de Portugal): novas oportunidades de desenvolvimento. *Proyecto RUMYS, III Reunión – Taller Internacional de Rutas Minerales en Iberoamerica, México*
- Lourenço JMM, Sousa LMO, Oliveira AS (2012) O xisto de Vila Nova de Foz-Côa. In Lourenço JMM, Sousa LMO, Oliveira AS (Eds.), *Rota da Pedra, Cap. 5*, pp. 29–35. Vila Real, Universidade de Trás-os-Montes e Alto Douro. ISBN: 978-972-704-374-3
- Medinac F (2019) Advances in pit wall mapping and slope assessment using unmanned aerial vehicle technology. Master Thesis. Toronto
- Menningen J, Siegesmund S, Lopes L, Martins R, Sousa L (2018) The Estremoz marbles: an updated summary on the geological, mineralogical and rock physical characteristics. *Environ Earth Sci* 77:191. <https://doi.org/10.1007/s12665-018-7328-3>
- Millis S, Wong D, Chan K (2019) Digital mapping of discontinuities. Conference Paper
- Montani C (2017) XXVIII report marble and stones in the world 2016. Ed. Aldus, Carrara, Italy
- Montani C (2018) XXIX report marble and stones in the world 2017. Ed. Aldus, Carrara, Italy
- Montani C (2019) XXX report marble and stones in the world 2018. Ed. Aldus, Carrara, Italy
- Morais AIF (2003) Inventariação, caracterização e valorização das pedreiras do granito Amarelo Real. MSc thesis, University of Trás-os-Montes e Alto Douro
- Morales Demarco M, Oyhançabal P, Stein K-J, Siegesmund S (2013) Dolomitic slates from Uruguay: petrophysical and petromechanical characterization and deposit evaluation. *Environ Earth Sci* 69:1361–1395. <https://doi.org/10.1007/s12665-012-1921-7>
- Morales Demarco M (2012). Mineralogical, petrophysical and economical characterization of the dimensional stones of Uruguay. Implications for deposit exploration. PhD thesis, University of Gottingen
- Mosch S (2008) Optimierung der Exploration, Gewinnung und Materialcharakterisierung von Naturwerksteinen. Dissertation. Goettingen
- Mosch S, Nikolayew D, Ewiak O, Siegesmund S (2011) Optimized extraction of dimension stone blocks. *Environ Earth Sci* 63(7–8):1911–1924. <https://doi.org/10.1007/s12665-010-0825-7>
- Mustafa S, Khan MA, Khan MR, Sousa LMO, Hameed F, Mughal M, Niaz A (2016) Building stone evaluation—a case study of the sub-Himalayas, Muzaffarabad region, Azad Kashmir, Pakistan. *Eng Geol* 209:56–69. <https://doi.org/10.1016/j.enggeo.2016.05.007>
- Nefeslioglu HA, Gokceoglu C, Sonmez H (2006) Indirect determination of weighted joint density (wJd) by empirical and fuzzy models: Supren (Eskisehir, Turkey) marbles. *Eng Geol* 85(3–4):251–269. <https://doi.org/10.1016/j.enggeo.2006.02.004>
- Nikolayev D, Siegesmund S, Mosch S, Hoffmann A (2007) Modell-based prediction of unfractured rock masses. *Zeitschrift Der Deutschen Gesellschaft Für Geowissenschaften* 158(3):483–490. <https://doi.org/10.1127/1860-1804/2007/0158-0483>
- Pagano M, Palma B, Ruocco A, Parise M (2020) Discontinuity characterization of rock masses through terrestrial laser scanner and unmanned aerial vehicle techniques aimed at slope stability assessment. *Appl Sci* 10:2960. <https://doi.org/10.3390/app10082960>
- Palmström A (2001) Measurement and characterization of rock mass jointing. In: Sharma VM, Saxena KR (Eds) *In-situ characterization of rocks*. Balkema Publishers, pp 49–97
- Pereira MF, Solá AR, Chichorro M, Lopes L, Gerdes A, Silva JB (2012) North-Gondwana assembly, break-up and paleogeography: U-Pb isotope evidence from detrital and igneous zircons of Ediacaran and Cambrian rocks of SW Iberia. *Gondwana Res* 22(3–4):866–881. <https://doi.org/10.1016/j.gr.2012.02.010>
- Priest SD (1993) *Discontinuity analysis for rock engineering*. Chapman and Hall, London
- Rasmussen LL (2020) UnBlocks^{gen}: a python library for 3D rock mass generation and analysis. *SoftwareX* 12, 100577. https://github.com/ElsevierSoftwareX/SOFTX_2020_237
- Robiati C, Eyre M, Vanneschi C, Francioni M, Venn A, Coggan J (2019) Application of remote sensing data for evaluation of rockfall potential within a quarry slope. *ISPRS Int J Geo Inf* 8(9):367. <https://doi.org/10.3390/ijgi8090367>
- Salvini R, Mastrococco G, Seddaiu M, Rossi D, Vanneschi C (2017) The use of an unmanned aerial vehicle for fracture mapping within a marble quarry (Carrara, Italy): photogrammetry and discrete fracture network modelling. *Geom Nat Hazards Risk* 8(1):34–52. <https://doi.org/10.1080/19475705.2016.1199053>
- Santos I, Sousa L, Lourenço J (2018) Granite resource evaluation: example of an extraction area in the north of Portugal. *Environ Earth Sci* 77(17):608. <https://doi.org/10.1007/s12665-018-7780-0>
- Santos I (2017) Ordenamento das zonas extrativas de granito no concelho de Vila Pouca de Aguiar: um estudo na área de Reserva da Serra da Falperra. MSc thesis, University of Trás-os-Montes e Alto Douro
- Schneider C (2009) Optimierung im Abbau von Naturwerkstein auf der Basis von Kluftanalysen. Diplomarbeit, Goettingen
- Schneider C, Siegesmund S, Stein KJ, St. Löbens (2022) Joint analysis as an important tool for an optimizing block extraction of natural stones. *Environ Earth Sci*. <https://doi.org/10.21203/rs.3.rs-583642/v1>
- Shang J, West LJ, Hencher SR, Zhao Z (2018) Geological discontinuity persistence: implications and quantification. *Eng Geol* 241:41–54. <https://doi.org/10.1016/j.enggeo.2018.05.010>
- Siegesmund S, Török A (2014) Building stones. In: Siegesmund S, Snehlage R (eds) *Stone in architecture: properties, durability*, 5th edn. Springer, Berlin, pp 11–95

- Siegesmund S, Sousa L, López-Doncel RA (2018) Editorial to the topical collection in Environmental Earth Sciences “Stone in the architectural heritage: from quarry to monuments—environment, exploitation, properties and durability.” *Environ Earth Sci* 77:730. <https://doi.org/10.1007/s12665-018-7755-1>
- Singewald C (1992) *Naturstein—exploration und Gewinnung*. 260 S. Köln, Bad Bentheim (Rudolf Müller)
- Solancis (2013) SOLANCIS Portuguese limestone: ITLabs. <http://www.solancis.com/>. Accessed 26 Dec 2019
- Sousa LMO (2000) Estudo da fracturação e das características físico-mecânicas de granitos da região de Trás-os-Montes com vista a sua utilização como rocha ornamental. PhD thesis. Universidade de Trás-os-Montes e Alto Douro
- Sousa LMO (2007a) Granite fracture index to check suitability of granite outcrops for quarrying. *Eng Geol* 92(3–4):146–159. <https://doi.org/10.1016/j.enggeo.2007.04.001>
- Sousa LMO (2007b) Granito Amarelo Real: características gerais e contribuição para o ordenamento da exploração na serra da Falperra. *Boletim De Minas* 41(2):161–174
- Sousa LMO (2010) Evaluation of joints in granitic outcrops for dimension stone exploitation. *Q J Eng GeolHydrogeol* 43(1):85–94. <https://doi.org/10.1144/1470-9236/08-076>
- Sousa LMO (2014) Petrophysical properties and durability of granites employed as building stone: a comprehensive evaluation. *Bull Eng Geol Env* 73(2):569–588. <https://doi.org/10.1007/s10064-013-0553-9>
- Sousa L (2019) Behaviour of hard stones submitted to different foot traffic. *Environ Earth Sci* 78:680. <https://doi.org/10.1007/s12665-019-8693-2>
- Sousa LMO, Suárez del Río LM, Calleja L, Ruiz de Argandoña V, Rey AR (2005) Influence of microfractures and porosity on the physico-mechanics properties and weathering of ornamental granites. *Eng Geol* 77:153–168
- Sousa L, Búrcio M, Lourenço J, Oliveira A (2015) Historic black shale quarries of Foz-Côa, Northern Portugal. In: Douet J (Eds), *TERUEL LIFE+ European quarry landscapes—collected essays from the first meeting of the European Quarry Landscapes Network*, pp. 67–71. Ayuntamiento de Teruel. ISBN: 978-84-88220-26-4
- Sousa LMO, Oliveira AS, Alves IMC (2016) Influence of fracture system on the exploitation of building stones: the case of the Mondim de Basto granite (north Portugal). *Environ Earth Sci* 75(1):39. <https://doi.org/10.1007/s12665-015-4824-6>
- Sousa LMO, Barabasch J, Stein K-J, Siegesmund S (2017) Characterization and quality assessment of granitic building stone deposits: a case study of two different Portuguese granites. *Eng Geol* 221:29–40. <https://doi.org/10.1016/j.enggeo.2017.01.030>
- Sousa L, Siegesmund S, Wedekind W (2018) Salt weathering in granitoids: an overview on the controlling factors. *Environ Earth Sci* 77:502. <https://doi.org/10.1007/s12665-018-7669-y>
- Sousa L, Lourenço J, Pereira D (2019) Suitable re-use of abandoned quarries for restoration and conservation of the old city of Salamanca—world heritage site. *Sustainability* 11(16):4352. <https://doi.org/10.3390/su11164352>
- Sousa L, Pita P, Carvalho J, Lourenço J (2020) Granitos ornamentais do norte de Portugal - características, potencialidades e constrangimentos. *Boletim de Minas* 54 - Edição Especial - Rochas Ornamentais - 2019-2020, pp 7–25
- Szeliski R (2011) *Computer vision*. Springer, London (ISBN 978-1-84882-934-3)
- Taelman D, Elburg M, Smet I, Paeppe P, Lopes L, Vanhaecke F, Vermeulen F (2013) Roman marble from Lusitania: petrographic and geochemical characterisation. *J Archaeol Sci* 40(5):2227–2236. <https://doi.org/10.1016/j.jas.2012.12.030>
- Török A, Bögöly G, Somogyi A, Lovas T (2020) Application of UAV in topographic modelling and structural geological mapping of quarries and their surroundings—delineation of fault-bordered raw material reserves. *Sensors* 20:489. <https://doi.org/10.3390/s20020489>
- Walsh JA (1999) Methods of evaluating slate and their application to the Scottish slate quarries. PhD thesis, University of Glasgow. <http://theses.gla.ac.uk/4391/>
- Wang S, Ahmed Z, Hashmi MZ, Pengyu W (2019a) Cliff face rock slope stability analysis based on unmanned aerial vehicle (UAV) photogrammetry. *Geomech Geophys Geo-Energy Geo-Resour*. <https://doi.org/10.1007/s40948-019-00107-2>
- Wang S, Ahmed Z, Hashmi MZ, Pengyu W (2019b) Cliff face rock slope stability analysis based on unmanned arial vehicle (UAV) photogrammetry. *Geomech Geophys Geo-Energy Geo-Resour*. <https://doi.org/10.1007/s40948-019-00107-2>
- Yarahmadi R, Bagherpour R, Sousa LMO, Taherian G (2015) How to determine the appropriate methods for identifying the geometry of in situ rock blocks in dimension stones. *Environ Earth Sci* 74(9):6779–6790. <https://doi.org/10.1007/s12665-015-4672-4>
- Yarahmadi R, Bagherpour R, Tabaei M, Sousa LMO (2017) Investigation of intact rock geomechanical parameters’ effects on commercial blocks’ productivity within stone reserves: a case history of some quarries in Isfahan. *Iran J Afr Earth Sci* 134:383–388. <https://doi.org/10.1016/j.jafrearsci.2017.07.013>
- Yarahmadi R, Bagherpour R, Taherian S-G, Sousa LMO (2018) Discontinuity modelling and rock block geometry identification to optimize production in dimension stone quarries. *Eng Geol* 232:22–33. <https://doi.org/10.1016/j.enggeo.2017.11.006>
- Yarahmadi R, Bagherpour R, Khademian A, Sousa LMO, Almasi SN, Esfahani MM (2019a) Determining the optimum cutting direction in granite quarries through experimental studies: a case study of a granite quarry. *Bull Eng Geol Env* 78(1):459–467. <https://doi.org/10.1007/s10064-017-1158-5>
- Yarahmadi R, Bagherpour R, Taherian S-G, Sousa LMO (2019b) A new quality factor for the building stone industry: a case study of stone blocks, slabs, and tiles. *Bull Eng Geol Env* 78(1):533–542. <https://doi.org/10.1007/s10064-017-1040-5>

Publisher's Note Springer Nature remains neutral with regard to jurisdictional claims in published maps and institutional affiliations.